

Utah State University

DigitalCommons@USU

All Graduate Theses and Dissertations

Graduate Studies

12-2008

The Effect of Climate Change on the Hydrology of a Mountainous Catchment in the Western United States: A Case Study at Reynolds Creek, Idaho

Anurag Nayak
Utah State University

Follow this and additional works at: <https://digitalcommons.usu.edu/etd>

 Part of the [Civil Engineering Commons](#)

Recommended Citation

Nayak, Anurag, "The Effect of Climate Change on the Hydrology of a Mountainous Catchment in the Western United States: A Case Study at Reynolds Creek, Idaho" (2008). *All Graduate Theses and Dissertations*. 82.

<https://digitalcommons.usu.edu/etd/82>

This Dissertation is brought to you for free and open access by the Graduate Studies at DigitalCommons@USU. It has been accepted for inclusion in All Graduate Theses and Dissertations by an authorized administrator of DigitalCommons@USU. For more information, please contact digitalcommons@usu.edu.



THE EFFECT OF CLIMATE CHANGE ON THE HYDROLOGY OF A MOUNTAINOUS
CATCHMENT IN THE WESTERN UNITED STATES: A CASE
STUDY AT REYNOLDS CREEK, IDAHO

by

Anurag Nayak

A dissertation submitted in partial fulfillment
of the requirements for the degree

of

DOCTOR OF PHILOSOPHY

in

Irrigation Engineering

Approved:

Dr. David G. Chandler
Major Professor

Dr. Daniel G. Marks
Committee Member

Dr. Christopher M. U. Neale
Committee Member

Dr. Gary P. Merkley
Committee Member

Dr. David G. Tarboton
Committee Member

Dr. Lawrence E. Hipps
Committee Member

Dr. Byron R. Burnham
Dean of Graduate Studies

UTAH STATE UNIVERSITY
Logan, Utah

2008

Copyright © Anurag Nayak 2008

All Rights Reserved

ABSTRACT

The Effect of Climate Change on the Hydrology of a Mountainous Catchment in the
Western US: A Case Study at Reynolds Creek, Idaho

by

Anurag Nayak, Doctor of Philosophy

Utah State University, 2008

Major Professor: Dr. David G. Chandler
Department: Biological and Irrigation Engineering

This research is focused on understanding the sensitivity of a hydrologic regime at the Reynolds Creek Experimental Watershed (RCEW), a snowmelt dominated semi-arid mountain basin located in southwest Idaho, to climate warming.

Climate data, collected during 1962 to 2006 at many locations in the RCEW, was carefully checked, preprocessed, and corrected for errors and noise signals introduced by the instrument malfunctioning and extreme weather conditions. An Automated Precipitation Correction Program (APCP) was developed to remove mechanical errors from the weighing-recording bucket type precipitation gauge measurements. APCP produces comparable results to the manual techniques but a degree faster (few minutes against 2-3 days) and is not influenced by operator biases.

Long-term climate data collected over a range of elevations of RCEW were analyzed for temporal trends. Significant increase in temperatures, with minimum temperature rising at a faster rate than maximum temperature, was observed at all

elevations. Though trends in annual precipitation and streamflow were not significant, streamflow shows a seasonal shift to larger winter and early spring flows, and reduced late-spring and summer flows. These analyses indicate more precipitation as rain than snow, decrease in snow water equivalent (SWE), reduction in number of soil freeze days, and earlier occurrence of plant-water stress. All trends show a significant elevation gradient in either timing or magnitude.

To assess the sensitivity of the mountain snow cover to natural climate variability, and as forced by warming climate, snow cover development and melt during five snow seasons (1984, 1986, 1987, 2001, and 2006) were simulated under actual (base), warm (+2°C), and cold (-2°C) forcing climate scenarios, at the Reynolds Mountain East (RME) basin, a head water catchment of the RCEW. Selected seasons displayed tremendous variability in snow distribution, accumulation, and melt with snowcover during dry snow (1987, 2001) seasons substantially smaller, and peak snow accumulations and melts about a month earlier compared to wet snow seasons (1984, 1986, 2006). Results from altered climate scenario simulations show that colder conditions result in less rain and more snow, increase in SWE, later timing of peak SWE, and later snowmelt. The simulations with warm scenarios show more rain and less snow, decrease in SWE, earlier timing of peak SWE, and earlier timing of snowmelt. In general, seasonal snowcover shows greater sensitivity to warm scenarios than cold.

ACKNOWLEDGMENTS

With great pleasure and deep sense of gratitude, I take this opportunity to express my sense of indebtedness to my major professor, Dr. David G. Chandler, for providing me invaluable guidance, constant encouragement, and cooperation to achieve this dissertation a part of my PhD degree program. He has been always supportive and understanding, which helped me in taking off the excess stress during my research.

I also thank Dr. Danny Marks for the all-important technical inputs and guidance that he has been providing throughout my research work as well as for giving me the opportunity to use the research facilities available at the Northwest Watershed Research Center, Agricultural Research Service, United States Department of Agriculture (NWRC-ARS-USDA), Boise, Idaho.

I take this opportunity to extend my special thanks to my committee members, Dr. Gary Merkley, Dr. Christopher M. U. Neale, Dr. David G. Tarboton, and Dr. Larry E. Hippi, for their advice, assistance, and patience throughout my research.

I am grateful to Dr. Ronald C. Sims, head, Biological and Irrigation Engineering (BIE) Department, for helping me out during academic and financial difficulties. I am also grateful to the BIE faculty and staff. My personal thanks to Linda John and Anne Martin for making extra efforts several times whenever I needed, then Rebeca V. Olsen, and Jed Moss; and the Agricultural Science faculty and staff, including Keren Williams and Sally Maxwell, for maintaining my records and processing the required paperwork.

Sincere regards to Adam Winstral for giving his time and scientific inputs during this research. His support was very crucial for success completion of this research. I

deeply appreciate the help rendered by all the faculty and staff of NWRC-ARS-USDA, with special mention of Dr. Mark S. Seyfried and Michelle Reba.

Let me express my gratitude to Dr. Tim Link, assistant professor, Department of Forest Resources, University of Idaho, for helping me during financial need. I also would like to thank faculty and staff members at the Center for Ecohydraulics Research, University of Idaho, for providing me space and facilities to complete this research.

Life is incomplete without friends and fun so I would like to mention all of my friends who have been ever supportive. I would like to acknowledge my best friends, Deepak and Shantanu, for their unconditional support whenever I needed, then Ajay Prasad, Ashish Bhai, Anuj, Shashi, Ajay Kalra, Ritu, Sumit, Madhu, Tapan, Raghuveer, Sawan, Rahul, Nikhil, and Greg for being great friends. Thanks to Ajay Jain, Kaushal, and Sumit Paliwal who encouraged and supported me to seek higher education in the United States.

My parents are my biggest strength. Their constant support and faith in my abilities have always been a tremendous motivation. I would not forget my brothers, Amit and Rahul, and all of my relatives who have been praying and supporting me wholeheartedly.

Thanks to the Almighty Lord for the amazing grace and kindness that he has continuously bestowed on me.

Anurag Nayak

CONTENTS

	Page
ABSTRACT.....	iii
ACKNOWLEDGMENTS	v
LIST OF TABLES	x
LIST OF FIGURES	xiii
 CHAPTER	
1. INTRODUCTION	1
General.....	1
Objectives	6
References.....	7
2. OBJECTIVE SUB-DAILY DATA CORRECTION FOR WEIGHING BUCKET TYPE PRECIPITATION GAUGE MEASUREMENTS	11
Abstract.....	11
Introduction.....	12
Types of Mechanical Errors.....	15
Program Description.....	18
Out of Range Data Values	19
Scanning Cycle 1	20
Scanning Cycle 2.....	22
Test Data.....	24
Results and Discussion	26
Conclusion	31
Appendix.....	33
Acquiring the APCP Software	33
References.....	33

3. LONG-TERM SNOW, CLIMATE, AND STREAMFLOW TRENDS AT THE REYNOLDS CREEK EXPERIMENTAL WATHERSHED, OWYHEE MOUNTAINS, IDAHO, USA	38
Abstract	38
Introduction.....	39
The Reynolds Creek Experimental Watershed (RCEW).....	44
Meteorological Measurement Sites.....	45
Precipitation Measurement Sites.....	50
Snow Measurement Sites.....	51
Soil Temperature and Moisture Measurement Sites	52
Streamflow Measurement Sites	53
Data Presentation and Trend Analysis.....	53
The Statistical Significance Test.....	54
Air Temperature.....	55
Precipitation	58
Snowfall	60
Snow Measurements	63
Soil Freezing	68
Plant Water Stress	70
Streamflow.....	72
Discussion	77
Conclusions.....	86
References.....	88
4. SENSITIVITY OF SNOWCOVER TO CLIMATE WARMING IN A SEMI-ARID MOUNTAIN CATCHMENT	96
Abstract	96
Introduction.....	97
The Study Site.....	100
The Study Snow Seasons	102
The Modeling Approach.....	106

Experimental Design.....	110
Results and Discussion	111
Base-Condition Simulations	111
Base, -2°C, and +2°C Scenario Simulations: Basin Average Results.....	119
Base, -2°C, and +2°C Scenario Simulations: Spatial Distribution Results	129
Base, -2°C, and +2°C Scenario Simulations: Rain-on-Snow Sensitivity	135
1987 Mixed Rain-Snow, ROS event (3/5/1987- 3/13/1987).....	138
2006 Mixed Rain-Snow, ROS event (4/3/2006- 4/15/2006).....	140
Summary and Conclusions.....	142
References.....	145
5. SUMMARY	150
The Automated Precipitation Correction Program (APCP).....	150
Trend Analysis of Long-Term Hydro-Climatic Data	151
Sensitivity of Seasonal Snowcover to Warming Climate	153
References.....	157
APPENDICES	159
APPENDIX A. THE AUTOMATED PRECIPITATION CORRECTION PROGRAM (APCP).....	160
APPENDIX B. THE DUAL GAUGE WIND CORRECTION PROGRAM.....	178
APPENDIX C. PERMISSION LETTERS	189
CURRICULUM VITAE.....	194

LIST OF TABLES

Table	Page
2.1	Description of User defined parameters and variables used in APCP program.....19
2.2	Instantaneous precipitation occurrence frequency and cumulative annual depth for daily, hourly, and 15 min.....29
3.1	Long-term climate (T_a , RH), precipitation, snow, soil temperature and moisture measurement sites at the RCEW48
3.2	Long-term Streamflow Measurement Sites at the RCEW53
3.3	Trends (in °C per decade) in maximum and minimum temperature based on least square linear fitting and Mann-Kendall test. Bold numbers indicate significance level greater than 90%; Blue, bold-Italic numbers, significance level greater than 95%. Critical shifts caused by trends are highlighted in yellow57
3.4	Annual and seasonal precipitation for the period 1963-200659
3.5	Trends (in % per decade) in fraction (%) of precipitation falling as snow. Blue, bold-italic numbers: significance level greater than 95%. Critical shifts caused by trends are highlighted in yellow65
3.6	Trends (in mm per decade) in April 1 and May 1 SWE based on least square linear fitting and Mann-Kendall test for the water year period 1964-2006. Bold numbers indicate significance level greater than 90%; Blue, bold-italic numbers a significance level greater than 95%. The large, significant trend at <i>144_sc</i> caused by site modification (deforestation) is highlighted in yellow66
3.7	Trends in timing (days per decade) and depth (mm per decade) of peak SWE accumulation based on least square linear fitting and Mann-Kendall test for water year period 1964-2006. Bold numbers indicate a significance level greater than 90%; Blue, bold-italic numbers a significance level greater than 95%68
3.8	Trends (in number of days per decade) in soil <i>freeze days</i> at mid-elevation, low slope, and valley-bottom sites. Bold numbers indicate significance level greater than 90%; Blue, bold-italic numbers significance level greater than 95%69

Table	Page
3.9	Trends (in days per decade) in timing of plant water stress for high (<i>176_stm</i>), mid- (<i>127_stm</i>) and low slope (<i>098_stm</i>) soil measurement sites for 1976 – 2006 (31 water years) period of record. Plant water stress is defined as 45% of average peak <i>plant-available water</i> or “field capacity” in the top meter of soil at each site. Blue, bold-italic numbers indicate significance level greater than 95%72
3.10	a) Trends (in 10^6 m^3 per decade) in streamflow ($10^6 \text{ m}^3 \text{ WY}^{-1}$) based on least square linear fitting and Mann-Kendall test for the period record. B- e) Trends (in % per decade) in monthly distribution of streamflow as % of total water year streamflow over the Mar – Jun for the period of record. Bold numbers indicate significance level greater than 90%; Blue, bold-Italic numbers a significance level greater than 95%74
3.11	Annual Precipitation – Runoff relationship for RME (<i>166_sf</i>), Tollgate (<i>116_sf</i>) and the RCEW outlet (<i>036_sf</i>), for period prior to and after 1985. Slope, precipitation threshold (P_0), R^2 and standard error are presented.....77
4.1	Summary of conditions during selected <i>snow seasons</i>103
4.2	State variables predicted and forcing variables required by the <i>Isnobar</i> snow model107
4.3	Root mean square difference (RMSD), (2) mean bias difference (MBD) and (3) Nash-Sutcliffe model efficiency (ME) for daily simulated vs. measured SWE at the <i>grove site</i> from the start of snowcover to the end of the <i>snow season</i> , and cumulative simulated basin SWI vs. measured streamflow from peak SWE to the end of the <i>snow season</i> for each of the simulation years116
4.4	1984 <i>snow season</i> basin-average SWE for selected dates, date and depth of peak SWE, dates of 200 mm and 50% SWI, SWI occurring prior to peak SWE and precipitation and rain total. Percentages in parentheses (%) indicate the fraction of peak SWE, total SWI or the rain fraction of total precipitation. Positive or negative numbers in parentheses (+/-) indicate date advance or retreat from base conditions122

Table	Page
4.5	1986 <i>snow season</i> basin-average SWE for selected dates, date and depth of peak SWE, dates of 200 mm and 50% SWI, SWI occurring prior to peak SWE, and precipitation and rain totals. Percentages in parentheses (%) indicate the fraction of peak SWE, total SWI or the rain fraction of total precipitation. Positive or negative numbers in parentheses (+/-) indicate date advance or retreat from base conditions123
4.6	1987 <i>snow season</i> basin-average SWE for selected dates, date and depth of peak SWE, dates of 200 mm and 50% SWI, SWI occurring prior to peak SWE, and precipitation and rain totals. Percentages in parentheses (%) indicate the fraction of peak SWE, total SWI or the rain fraction of total precipitation. Positive or negative numbers in parentheses (+/-) indicate date advance or retreat from base conditions125
4.7	2001 <i>snow season</i> basin-average SWE for selected dates, date and depth of peak SWE, dates of 200 mm and 50% SWI, SWI occurring prior to peak SWE, and precipitation and rain totals. Percentages in parentheses (%) indicate the fraction of peak SWE, total SWI or the rain fraction of total precipitation. Positive or negative numbers in parentheses (+/-) indicate date advance or retreat from base conditions.126
4.8	2006 <i>snow season</i> basin-average SWE for selected dates, date and depth of peak SWE, dates of 200 mm and 50% SWI, SWI occurring prior to peak SWE, and precipitation and rain totals. Percentages in parentheses (%) indicate the fraction of peak SWE, total SWI or the rain fraction of total precipitation. Positive or negative numbers in parentheses (+/-) indicate date advance or retreat from base conditions127

LIST OF FIGURES

Figure	Page
2.1	Types of mechanical errors present in gauge measurements, pink hollow diamonds show unprocessed data and blue solid lines show data and blue solid lines show data processed using APCP. (a) Out of Range Data, (b) Bucket Decanting, (c) Bucket Recharge, (d) Intermittent Noise, (e) Periodic Noise, and (f) Episodic Noise.....17
2.2	Measured and corrected shielded gauge precipitation data using manual (only bucket decanting), RA and APCP techniques for site 176, water year 2004. Estimated catch is computed by adding bucket decanting depths to the recorded precipitation. Inserted figure shows differences in three correction approaches at sub-daily scale.....26
2.3	Errors with respect to estimated annual precipitation, solid diamonds show shielded and open boxes show unshielded gauges. (a) Rainfall Analyzer (RA). (b) Automated Precipitation Correction Program (APCP).....28
2.4	Frequency of instantaneous precipitation values following scan 1 and scan 2 of the Automated Precipitation Correction Program for daily, hourly, and 15-minute time steps.30
2.5	Noise removal from hourly TDR water content record with APCP Scan cycle 1 and (offset) comparative water content record from a calibrated Water Content Reflectometer.32
3.1	Topographic map of RCEW with long-term climate stations, precipitation gauges, snow courses, snow pillow, soil temperature and moisture measurement stations, and weirs.....46
3.2	Water year maximum and minimum temperatures for high (Site <i>176_met</i> , 2093 m), mid- (Site <i>127_met</i> , 1652 m), and low elevation (Site <i>076_met</i> , 1207 m) meteorological sites. Pink diamonds shows maximum and blue squares shows minimum temperature. Trend lines are indicated for each site, showing an increase in both minimum and maximum temperature at all sites.56
3.3	Seasonal precipitation as percentage of total water year (WY) precipitation at the high, mid- and low elevation measurement sites. Trend lines are indicated for each over the period of record.61

Figure	Page
3.4	Rain and snow fraction (percentage) of water year total precipitation at high (<i>176e_ppt</i>), mid- (<i>127_ppt</i>) and low (<i>076_ppt</i>) elevation measurement sites. Pink diamonds show snow, blue stars show rain. Trend lines indicated for each over the period of record showing a decrease in snow and an increase in rain at all elevations.64
3.5	May 1 st SWE (mm) for high elevation (<i>163c_sc</i> , 2125 m), mid-elevation (<i>176_sc</i> , 2056 m) and low elevation (<i>155_sc</i> , 1743 m) snow courses. Trend lines are indicated for period of record showing a consistent decrease at all elevations, with a strong decrease at the low elevation snow course (<i>155_sc</i>) in both months.67
3.6	Number of <i>soil freeze</i> days for mid-elevation (<i>127_stm</i> , 1652 m), low slope (<i>098_stm</i> , 1410 m) and valley-bottom (<i>076_stm</i> , 1207 m) sites. Vertical line shows the timing of temperature profile change. Note the discontinuity after the instrument change at the valley-bottom site (<i>076_stm</i>). Trend lines are indicated for each over the period of record showing a consistent decrease in the number of soil freeze days at all sites (though the trend at the valley-bottom site is clearly biased by the profile change discontinuity).70
3.7	Average monthly streamflow at the RME headwater catchment weir (<i>166_sf</i>), the Tollgate mid-elevation weir (<i>116_sf</i>) and the RCEW outlet weir (<i>036_sf</i>).73
3.8	Annual Precipitation – Runoff relationship for RME (<i>166_sf</i>), Tollgate (<i>116_sf</i>) and the RCEW outlet (<i>036_sf</i>), for period prior to and after 1985. Annual values, slope and +/- one standard error are plotted.76
4.1	The Reynolds Mountain East (RME) catchment, within the Reynolds Creek Experimental Watershed (RCEW). Locations of the outlet weir, ridge and grove measurement sites are indicated.101
4.2	Bi-weekly basin total precipitation (snow and rain) for the five selected <i>snow seasons</i>104
4.3	Base-condition simulation results for each of the selected <i>snow seasons</i> . A) <i>Grove site</i> snow pillow and snow course results are compared to SWE from the <i>grove site</i> simulation grid cell, and to simulated basin average SWE. B) daily total simulated surface water input (SWI) compared to measured streamflow.112

Figure	Page
4.4	Base-condition total <i>snow season</i> SWI and streamflow for each of the selected <i>snow seasons</i> . Note that in cold wet years streamflow is nearly equal to SWI, while in warm, wet years it is less, and in dry years it is substantially less.118
4.5	a) Daily basin-average SWE for the base, -2°C, and +2°C simulations for each of the selected <i>snow seasons</i> . B) Bi-weekly basin-total SWI hydrographs for the base, -2°C, and +2°C simulations for each of the selected <i>snow seasons</i>120
4.6	Bi-weekly basin area-normalized SCA (%), by SWE depth class for the base, -2°C, and +2°C simulations.130
4.7	Bi-weekly basin average depth-normalized SWE (mm), by SWE depth class for the base, -2°C, and +2°C simulations. Note that the y-axis is scaled 0–1000 mm SWE for 1984, 1986, & 2006, and 0–500 mm SWE for 1987 & 2001 <i>snow seasons</i>131
4.8	Spatial SWE images, 1987 snow season during snowcover development and ablation for base, -2°C, and +2°C simulations. Dec 5 through May 1 images presented. Average basin SWE and percent of peak SWE indicated for each image. Green colors indicate snow free areas.....133
4.9	Spatial SWE images, 2006 snow season during snowcover development and ablation for base, -2°C, and +2°C simulations. Dec 23 through May 24 images presented. Average basin SWE and percent of peak SWE indicated for each image. Green colors indicate snow free areas.136
4.10	Weather, precipitation and energy flux conditions during the March 5 – 13, 1987 mixed precipitation event for a) base, b) -2°C, and c) +2°C simulations.139
4.11	Weather, precipitation and energy flux conditions during the April 3 – 15, 2006 mixed precipitation event for a) base, b) -2°C, and c) +2°C simulations.141

CHAPTER 1

INTRODUCTION

1. General

Global surface temperature has risen by about 0.6-0.7 °C over the last 50 years (Trenberth et al. 2007). Further increase in global temperature by 1.1 to 6.4 °C is projected by the end of 21st century (Meehl et al. 2007). This increase in temperature is primarily attributed to anthropogenic increase in green-house gas concentrations in atmosphere. Substantial change in both at global and regional scales hydro-climate have been observed and predicted as a result of persistent warming (Leung and Ghan 1999; Manabe et al. 2004; Stewart et al. 2005; Leipprand and Gerten 2006; Trenberth et al. 2007; Randall et al. 2007).

Though increase in surface temperatures have been observed over the entire globe during past 50 years, the rate and nature of rise in temperature varies from one region to another. In western USA and Canada, regional surface temperature has increased by 1-3 °C since mid 20th century (Trenberth et al. 2007) with greater increase in winter temperatures. The trends of rising temperature are also diurnally asymmetric, with a larger increase in minimum temperature than maximum temperature and a decrease diurnal temperature range (Karl et al. 1984, 1993; Quintana-Gomez 1999; Brunetti et al. 2000; Trenberth et al. 2007).

Precipitation in much of the western USA and Canada is winter dominant, the majority of which falls as snow, especially at high elevations. Mountain snowpack plays an important role in regional hydrologic cycle by storing winter precipitation and

releasing melt water during late spring and summer, when ecological, agricultural and domestic water demand is at its peak. Warming climate conditions can substantially alter hydrologic cycle in these regions by altering snow deposition, accumulation and melt pattern.

Volume of water stored in mountain snowpack and timing of melt generated are very sensitive to climate conditions. A number of studies have reported impacts of warming climate on hydrologic cycle of these western mountains by means of decline in snow accumulation and spring snowpack (Mote 2003a, 2003b, 2006; Mote et al. 2005; Hamlet et al. 2005), decrease in fraction of precipitation that falls as snow (Aguado et al. 1992; Dettinger and Cayan 1995; Huntington et al. 2004; Regonda et al. 2005; Knowles et al. 2006), and a shift in the timing of snowmelt runoff toward earlier in the year (Aguado et al. 1992; Dettinger and Cayan 1995; Cayan et al. 2001; Stewart et al. 2004, 2005; Regonda et al. 2005).

In the western USA, hydrologic sensitivity of a basin to warming climate has shown to have strong correlation with elevation and low to mid elevation basins (with winter temperatures near freezing point) have displayed greater changes in streamflow timings and spring SWE than high elevation basins (with winter temperatures well below freezing point) (Stewart et al. 2004, 2005; Mote et al. 2005; Regonda et al. 2005; McCabe and Clark 2005). Similarly Knowles et al. (2006) reported that the greatest decline in fraction of precipitation as snow occurred in low to mid elevation basins where winter temperatures were warmer than -5°C . Though studies cited above clearly indicate a strong relationship between the basin elevation and Climate Change signal in the

western USA they were limited by the lack of coherent climate and snow data and by limited number of high elevation measurement sites.

It is clear that warming temperature has affected hydrologic cycle of the mountainous western USA. Most research, however focuses on the large scale changes in hydrologic regime and based on majority data collected at low to mid elevation sites near urban areas. This is primarily due to limited availability of quality data at remote mountainous locations (Hamlet et al. 2005).

Mountain basins of the western USA display tremendous spatial heterogeneity due to rapid change in elevation, slope, topography and vegetation. In these mountain basins precipitation typically increases with elevation (Hanson 1982, 2001; Cooley et al. 1988; Daly et al. 1994) and shows substantial differences between upwind and downwind slopes (Hanson 1982). These spatial heterogeneities and differences in precipitation lead to great disparities in snowpack development and melt within the basin. The large scale research studies cited earlier fail to clarify specific questions about differences in sensitivity of hydrologic cycle to the warming climate at range of elevations in these mountain basins.

Given the importance of mountain snowpack and snowmelt in regional hydrology, it is important to understand impacts of climate warming in these mountain basins. The Reynolds Creek Experimental Watershed (RCEW), a 238 km² semi-arid basin located in Owyhee Mountains, Idaho, is a densely instrumented watershed with sensors recording precipitation, climate data (temperature, wind speed and direction, solar radiation, evaporation, humidity etc.), snow, soil temperature and moisture, streamflow etc. at high temporal and spatial resolution. The available data make it an

ideal place to investigate impacts of warming climate on hydrologic cycle of mountain basins.

Climate data collected at RCEW (and other mountain locations) are subjected to noise and errors as instruments are affected by extreme weather conditions. Therefore careful quality checks and corrections in the climate data are necessary before their use in hydrologic studies and modeling. Precipitation measurements are most adversely affected by the systematic and mechanical errors in mountainous environments such as RCEW, where substantial amount of precipitation falls as snow. Techniques to correct precipitation data for systematic errors have already been developed (Hamon 1971, 1973; Goodison et al. 1998; Yang et al. 1998), but researchers have often relied on manual methods to remove mechanical errors. Manual removal of mechanical errors from the high frequency precipitation data is very tedious, requires operator expertise and may be affected by operator bias. Currently 26 dual gauge precipitation stations (two National Weather Service (NWS) weighing-recording gauges, one unshielded and the other shielded with Alter-type shield, located in close proximity) recording precipitation at 15 min or higher frequency, are in operation at RCEW. Manual removal of mechanical errors from high frequency precipitation data, in a heavily instrumented watershed like RCEW, is not practical and there is a need to develop automated techniques to remove mechanical noise signals from the precipitation data.

In mountain basins where topography, vegetation and climate conditions change rapidly with elevation, it is important to understand differences in impact of warming climate at range of elevations within the basin. Continuous records of hydro-climate and related data are available at a range of elevations of RCEW since early 1960's. Analyses

of these uniquely coherent long term hydro-climate data could be useful in understanding nature, extent and spatial differences in Climate Change signal in mountain basins.

There is a strong elevational gradient in precipitation at RECW, where the high elevation southern extent of the basin receives as much as 5-6 times more precipitation than the valley bottom (Hanson 2001). In RCEW, development of high elevation snow cover and subsequent release during late spring and summer is critical to sustaining the vegetation and ecosystems (Marks et al. 2001). Warming climate conditions could significantly alter snow cover development and melt pattern. Therefore it is important to understand the sensitivity of high elevation snowpack to the change in climate conditions.

The weather patterns at RCEW is related to oceanic circulations such as Pacific Decadal Oscillation (PDO) and El-Nino Southern Oscillation (ENSO) (Hurrell 1995; Hurrell and Van Loon, 1997; Dettinger et al. 1998) because of which the climate at RCEW shows great natural variability in precipitation (wet and dry cycles) and climate conditions (warm and cold phases). This natural variability in precipitation and climate conditions cause substantial year to year differences in snow accumulation and melt pattern at RCEW.

The studies cited above have reported that the warming climate has substantially altered the hydrologic regime of the mountainous western USA. These changes will continue at similar or accelerated rate if future climate predictions are true (Meehl et al. 2007). In order to prepare and adapt to the altered hydrologic regime due to climate warming, it is important to understand not only the long-term changes but also the variability associated with the hydrologic cycle.

2. Objectives

The overarching goal of this project is to clarify the processes by which warming climate conditions are affecting local scale hydrologic cycle in snowmelt dominated mountain catchments by altering precipitation (amount, distribution and phase), snow accumulation, and snowmelt timings. The main objectives of this research are:

1. Develop an automated technique to remove mechanical errors from the weighing-recording bucket precipitation gauges.
2. Investigate long-term (1960's to present) measurements of precipitation, temperature, humidity, snow, soil temperature and moisture and streamflow made at Reynolds Creek Experimental Watershed to quantify the extent of changes in temperature, precipitation (amount, distribution and phase), snow cover, and streamflow over a range of elevations.
3. Identify the impact of warming climate on snow accumulation, and melt of a mid-elevation mountain catchment during snow cover period in conjunction with natural climate variability.

These objectives were accomplished through a series of three papers presented as chapters in this dissertation. Each of these chapters contains necessary literature review and background information to make a case for the topic dealt in the chapter. Chapter 2 describes the development of an Automated Precipitation Correction Program (APCP) that can remove mechanical noise signals from the high frequency precipitation data collected using weighing-recording precipitation gauges. APCP was used to preprocess precipitation data collected at many stations in RCEW which was used in later part of the

research. Chapter 3 presents the trend analyses of carefully processed long term hydro-climate and related data collected at range of elevations of RCEW. In Chapter 4, sensitivity of seasonal snowcover to changing climate conditions, was tested for five snow seasons representing range of precipitation (from wet to dry) and climate (from warm to cold) conditions at Reynolds Mountain East, a high elevation headwater catchment of RCEW.

3. References

- Aguado, E., Cayan, D. R., Riddle, L., and Roos, M. (1992). "Climate fluctuations and the timing of west coast streamflow." *J. Clim.*, 5(12), 1468-1483.
- Brunetti, M., Burroni, L., Maugeri, M., and Nanni, T. (2000). "Trends of minimum and maximum daily temperatures in Italy from 1865 to 1996." *Theor. Appl. Climatol.*, 66, 49-60.
- Cayan, D. R., Kammerdiener, S. A., Dettinger, M. D., Caprio, J. M., and Peterson, D. H. (2001). "Changes in the onset of spring in the Western United States." *Bull. Am. Meteorol. Soc.*, 82(3), 399-415.
- Cooley, K. R., Hanson, C. L., and Johnson, C. W. (1988). "Precipitation erosivity index estimates in cold climates." *Trans. ASAE*, 31(5), 1445-1450.
- Daly, C., Neilson, R. P., and Phillips, D. L. (1994). "A statistical topographic model for mapping climatological precipitation over mountainous terrain." *J. Appl. Meteorol.*, 33, 140-158.
- Dettinger, M. D., and Cayan, D. R. (1995). "Large-scale atmospheric forcing of recent trends toward early snowmelt runoff in California." *J. Clim.*, 8, 606-623.
- Dettinger, M. D., Cayan, D. R., Diaz, H. F., and Meko, D. M. (1998). "North-south precipitation patterns in western north America on interannual-to-decadal timescales." *J. Clim.*, 11(12), 3095-3111.
- Goodison, B. E., Louie, P. Y. T., and Yang, D. (1998). "WMO solid precipitation measurement intercomparison, final report." *WMO/TD-No. 872*, World Meteorological Organization, Geneva.

- Hamlet, A. F., Mote, P. W., Clark, M. P., and Lettenmaier, D. P. (2005). "Effects of temperature and precipitation variability on snowpack trends in the Western United States." *J. Clim.*, 18, 4545-4561.
- Hamon, W. R. (1971). "Chapter 4 – Reynolds Creek, Idaho." *Agricultural Research Service Precipitation Facilities and Related Studies*. D. M. Hershfield ed., ARS-USDA, Washington, D.C.
- Hamon, W. R. (1973). "Computing actual precipitation: Distribution of precipitation in mountainous areas." *WMO Rep. No. 362*, World Meteorological Organization, Geneva, 1, 159-173.
- Hanson, C. L. (1982). "Distribution and stochastic generation of annual and monthly precipitation on a mountainous watershed in southwest Idaho." *Water Resour. Bull.*, 18(2), 875-883.
- Hanson, C. L. (2001). "Long-term precipitation database, Reynolds Creek Experimental Watershed, Idaho, United States." *Water Resour. Res.*, 37(11), 2831-2834.
- Huntington, T. G., Hodgkins, G. A., Keim, B. D. and Dudley R. W. (2004). "Changes in the proportion of precipitation occurring as snow in New England (1949-2000)." *J. Clim.*, 17(13), 2626-2636.
- Hurrell, J. W. (1995). "Decadal trends in the North Atlantic Oscillation: Regional temperatures and precipitation." *Science*, 269(5224), 676-679.
- Hurrell, J. W., and Van Loon, H. (1997). "Decadal variations in climate associated with the North Atlantic Oscillation." *Clim. Change*, 36(3-4), 301-326.
- Karl, T. R., Jones, P. D., Knight, R. W., Kukla, G., Plummer, N., Razuvayev, V., Gallo, K. P., Lindseay, J., Charlson, R., and Peterson, T. C. (1993). "A new prospective on recent global warming: Asymmetric trends of daily maximum and minimum temperature." *Bull. Am. Meteorol. Soc.*, 74(6), 1007-1023.
- Karl, T. R., Kukla, G., and Gavin, J. (1984). "Decreasing diurnal temperature range in the United States and Canada from 1941 through 1980." *J. Clim. Appl. Meteorol.*, 23(11), 1489-1504.
- Knowles, N., Dettinger, M. D., and Cayan, D. R. (2006). "Trends in snowfall versus rainfall in the Western United States." *J. Clim.*, 19(18), 4545-4559.
- Leipprand, A., and Gerten, D. (2006). "Global effects of doubled atmospheric CO₂ content on evapotranspiration, soil moisture and runoff under potential natural vegetation." *Hydrolog. Sciences*, 51(1), 171-185.

- Leung, L. R., and Ghan, S. J. (1999). "Pacific Northwest climate sensitivity simulated by a regional Climate Model driven by a GCM. Part II: 2xCO₂ Simulations." *J. Clim.*, 12, 2031-2053.
- Manabe, S., Milly, P. C. D., and Wetherald, R. (2004). "Simulated long-term changes in river discharge and soil moisture due to global warming." *Hydrolog. Sciences*, 49(4), 625-642.
- Marks, D., Cooley, K. R., Robertson, D. C., and Winstral, A. (2001). "Long-term snow database, Reynolds Creek Experimental Watershed, Idaho, United States." *Water Resour. Res.*, 37(11), 2835-2838.
- McCabe, G. J., and Clark, M. P. (2005). "Trends and variability in snowmelt runoff in the Western United States." *J. Hydrometeorol.*, 6, 476-482.
- Meehl, G. A., Stocker, T. F., Collins, W. D., Friedlingstein, P., Gaye, A. T., Gregory, J. M., Kitoh, A., Knutti, R., Murphy, J. M., Noda, A., Raper, S. C. B., Watterson, I. G., Weaver, A. J., and Zhao, Z. C. (2007). "Global climate projections." *Climate change 2007: The physical science basis*. Contributions of working group I to the fourth assessment report of the Intergovernmental Panel on Climate Change, S. Solomon, D. Qin, M. Manning, Z. Chen, M. Marquis, K. B. Averyt, M. Tignor, and H. L. Miller, eds., Cambridge University Press, Cambridge, UK and New York, 747-845.
- Mote, P. W. (2003a). "Trends in snow water equivalent in the Pacific Northwest and their climatic causes." *Geophys. Res. Lett.*, 30(12), 1601, doi:10.1029/2003GL017258, 2003.
- Mote, P. W. (2003b). "Twentieth-century fluctuations and trends in temperature, precipitation, and mountain snowpack in the Georgia Basin-Puget Sound region." *Can. Water Resour. J.*, 28(4), 567-585.
- Mote, P. W. (2006). "Climate-driven variability and trends in mountain snowpack in Western North America." *J. Clim.*, 19(23), 6209-6220.
- Mote, P. W., Hamlet, A. F., Clark, M. P., and Lettenmaier, D. P. (2005). "Declining mountain snowpack in Western North America." *Bull. Am. Meteorol. Soc.*, 86, 39-49.
- Quintana-Gomez, R. A. (1999). "Trends of maximum and minimum temperatures in Northern South America." *J. Clim.*, 12, 2104-2112.
- Randall, D. A., Wood, R. A., Bony, S., Colman, R., Fichet, T., Fyfe, J., Kattsov, V., Pitman, A., Shukla, J., Srinivasan, J., Stouffer, R. J., Sumi, A., and Taylor, K. E. (2007). "Climate models and their evaluation." *Climate change 2007: The*

physical science basis. Contributions of working group I to the fourth assessment report of the Intergovernmental Panel on Climate Change, S. Solomon, D. Quin, M. Manning, Z. Chen, M. Marquis, K. B. Averyt, M. Tignor, and H. L. Miller, eds., Cambridge University Press, Cambridge, UK and New York, 589-662.

Regonda, S. K., Rajgopalan, B., Clark, M., and Pitlick, J. (2005). "Seasonal cycle shifts in hydroclimatology over the Western United States." *J. Clim.*, 18, 372-384.

Stewart, I. T., Cayan, D. R., and Dettinger, M. D. (2004). "Changes in snowmelt runoff timing in Western North America under a 'Business As Usual' Climate Change scenario." *Clim. Change*, 62, 217-232.

Stewart, I. T., Cayan, D. R., and Dettinger, M. D. (2005). "Changes towards earlier streamflow timing across Western North America." *J. Clim.*, 18, 1136-1155.

Trenberth, K. E., Jones, P. D., Ambenje, P., Bojariu, R., Easterling, D., Tank, A. K., Parker, D., Rahimzadeh, F., Renwick, J. A., Rusticucci, M., Soden, B., and Zhai, P. (2007). "Observations: Surface and atmospheric climate change." *Climate change 2007: The physical science basis*. Contributions of working group I to the fourth assessment report of the Intergovernmental Panel on Climate Change, S. Solomon, D. Quin, M. Manning, Z. Chen, M. Marquis, K. B. Averyt, M. Tignor, and H. L. Miller, eds., Cambridge University Press, Cambridge, UK and New York, 235-336.

Yang, D., Goodison, B. E., Metcalfe, J. R., Golubev, V. S., Bates, R., Pangburn, T., and Hanson, C. L. (1998). "Accuracy of NWS 8" standard nonrecording precipitation gauge: results and application of WMO Intercomparison." *J. Atmos. Oceanic Technol.*, 15(1), 54-68.

CHAPTER 2

OBJECTIVE SUB-DAILY DATA CORRECTION FOR WEIGHING BUCKET TYPE PRECIPITATION GAUGE MEASUREMENTS¹

Abstract

Electronic sensors generate valuable streams of forcing and validation data for hydrologic models, but are often subject to noise which must be removed as part of model input and testing database development. We developed Automated Precipitation Correction Program (APCP) for weighing bucket precipitation gauge records, which are subject to several types of mechanical and electronic noise and discontinuities including gauge maintenance, missing data, wind vibration and sensor drift. Corrected cumulative water year precipitation from APCP did not exhibit an error bias and matched measured water year total precipitation within 2.1 % for 58 station-years tested. Removal of low amplitude periodic noise was especially important for developing accurate instantaneous precipitation records at sub-daily time steps. Model flexibility for use with other data types is demonstrated through application to time domain reflectometry soil moisture content data, which is also frequently subject to substantial noise.

¹ Coauthored by A. Nayak, D.G. Chandler, D. Marks, J. P. McNamara, and M. Seyfried. Submitted for publication to the *Water Resources Research*, American Geophysical Union.

1. Introduction

Precipitation and soil moisture are two of the most commonly measured components in catchment water balance studies. Continuous and accurate data for these and other variables are critical for driving and validating hydrological models. Many hydrological processes occur at sub-daily time steps and modeling these processes requires either accurate forcing data at the time step of the model (Haddeland et al. 2006) or a scaling approach (Waichler and Wigmosta 2003; Kandel et al. 2005) to use daily data.

Building accurate sub-daily time step hydrometeorological data sets is also an important step in reconstructing land surface atmosphere interactions through hydrological modeling (Ngo-Duc et al. 2005), especially for mountain environments and snowmelt conditions where distributed data sets are limited (Arnold et al. 1998; Schnorbus and Alia 2004; Lehning et al. 2006). Generally these data are difficult to acquire and limit the temporal extent of the simulation (Link and Marks 1999a&b; Winstral and Marks 2002). If high quality data are available, snow cover simulation for entire snow season is possible (Marks et al. 1999; Susong et al. 1999; Garen and Marks 2005).

Precipitation gauge measurements are subject to a wide range of errors that may affect the precipitation record and require assessment and correction. These may be broadly divided into two groups: mechanical errors and systematic errors. The magnitude of these errors and the techniques required to correct them depend on the meteorological conditions and type of gauge. The most prevalent recording gauge types are tipping bucket and weighing bucket.

The influence of mechanical errors on precipitation records has been well investigated for tipping bucket type gauges (La Barbera et al. 2002; Molini et al. 2005a). Sources of mechanical error in tipping bucket gauge data include incomplete dumping (Vasvari 2005) and can be associated with high rainfall intensity (Molini et al. 2005a) or data processing strategy (Ciach 2003). Several sensor calibration approaches have been developed (Calder and Kidd 1978; Marsalek 1981; Molini et al. 2005b).

The weighing bucket precipitation gauge is most common in environments receiving precipitation both as rain and snow, where tipping bucket gauge records are unreliable (Kuligowski 1997). Systematic errors in weighing bucket type gauges have been well investigated and are known to occur due to wind field deformation above the gauge-rim, evaporation (Yang et al. 1999; Hanson 2001), splashing of raindrops and blowing of snow (Sevruk 1982). Evaporative losses from weighing bucket gauges in colder climates range from 0.1-0.2 mm/day (Goodison et al. 1998) and can be minimized by adding mineral oil into the precipitation bucket (Kuligowski 1997). Under catch due to wind may reach 10-20% for liquid precipitation and 75-80% for snow and can be corrected through the use of paired shielded and unshielded gauges (Hamon 1971, 1973) or empirical equations (Goodison et al. 1998; Yang et al. 1998, 1999, 2000). Appropriate use of systematic error correction algorithms requires prior removal of mechanical errors from the data record. However, mechanical errors associated with weighing bucket gauges have received only passing attention as part of comparative studies (Nystuen 1999; Duchon and Essenberg 2001). In this paper we will focus primarily on automated correction of mechanical errors typical of electronically recorded weighing bucket type gauges.

Weighing bucket precipitation gauge data are intrinsically cumulative. While this type of data is convenient when long term (such as daily, monthly or annual) total precipitation volume is of interest, for many hydrologic applications, discrete values in a time series with a fixed interval of minutes to hours are required. To process time-series precipitation values from cumulative data, it is necessary to derive unbiased instantaneous differences from the cumulative record. Even small errors in instantaneous time-series precipitation values become additive in the cumulative annual record and can result in relatively large differences between physically measured volume and calculated cumulative precipitation.

Manual removal of mechanical errors and electronic noise from data is tedious and can be time consuming. Discontinuities and errors in weighing type precipitation gauge data due to maintenance activities such as bucket recharge, addition of mineral oil and antifreeze and malfunctioning of the gauge-data logger assembly are easily identified as distinct discontinuities in measured precipitation volume and can be simply removed in a spreadsheet. However, small oscillations induced by wind vibration, or thermal expansion and contraction of weighing equipment are more difficult to separate from precipitation input in the data record. Fluctuations caused by wind vibration can have an affect on gauge measurements for periods from a few hours to a few days depending on conditions while fluctuations due to temperature are cyclic in nature. Here we present an automated precipitation correction program (APCP) to remove mechanical errors from continuous time series data obtained from weighing bucket precipitation gauges.

Although the ACPC program was written specifically to address weighing bucket precipitation data, and some of the features are unique to that kind of data, the data

smoothing and filling algorithms are basically generic and can be applied, with minimal modification, to other types of data. We demonstrate this more general applicability of the program by applying it to soil moisture data collected with automated time domain reflectometry (TDR) to demonstrate other uses of the algorithm. TDR pulse generator/analyzers can contain sufficient instrument errors to render the data impractical to use. Such errors are commonly caused by misinterpretation of waveform reflection points and result in values outside of the expected range for soil moisture and instrument error values (e.g. -6999, -9999). In addition to out of range values, many values, though clearly incorrect in the context of the environment, are not out of range of the likely values.

2. Types of Mechanical Errors

We classify the various types of mechanical errors present in weighing bucket gauges as a) out of range data values, b) bucket decanting, c) bucket recharge, d) intermittent noise, e) periodic noise, and f) episodic noise (**Figure 2.1**). Based on the noise signal amplitude, errors due to out of range data values, bucket decanting, bucket recharge and intermittent noise can be classified as high amplitude noise signals, while small vibrations in the data record due to wind (episodic noise) and temperature fluctuations (periodic noise) can be classified as low amplitude noise.

Periods of instrument or data logger failure are recorded by Campbell Scientific data loggers as extreme negative values (e.g. -6999, -9999) that cause discontinuities in the precipitation records during these periods of out of range data (**Figure 2.1a**). During instrument servicing the gauge bucket is removed from the load cell-weighing

mechanism, decanted and then recharged with mineral oil (to prevent evaporation) and anti-freeze (to melt snow, only during snow season) before returning the bucket to the gauge. This activity introduces large instantaneous changes in the load cell records. Such discontinuities in the record are generally negative (bucket decanting; **Figure 2.1b**), but can be positive depending on the mass of mineral oil and/or anti-freeze added to the measurement buckets (bucket recharge; **Figure 2.1c**). Occasionally, the gauge record is subject to large instantaneous changes or fluctuations from intermittent electronic noise (**Figure 2.1d**).

Low amplitude noise signals may be introduced by load cell sensitivity to temperature fluctuations, diurnal changes in the data-logger power supply, wind or barometric pressure changes. These effects can be broken into periodic noise, which follows the diurnal cycle (**Figure 2.1e**) and episodic noise which is characterized by irregular, low amplitude, high frequency fluctuations near to the mean of the values (**Figure 2.1f**). Some of the gauge systems located at RCEW show a diurnal variation up to 0.4 mm (Hanson et al., 2001). This diurnal variation can be attributed to solar heating and cooling of load cell-gauge system and is more pronounced in summer (Hanson et al., 2001). Shielded gauges at windy sites can be subject to frequent episodic noise due to wind induced vibrations if the shield is mounted to the same post as the gauge (Hanson et al., 1979). Although such low amplitude noise does not affect long-term aggregate precipitation measurements, it is difficult to manually separate from sub-daily (15 min, hourly, etc.) precipitation data and can obscure the beginning and end of precipitation events.

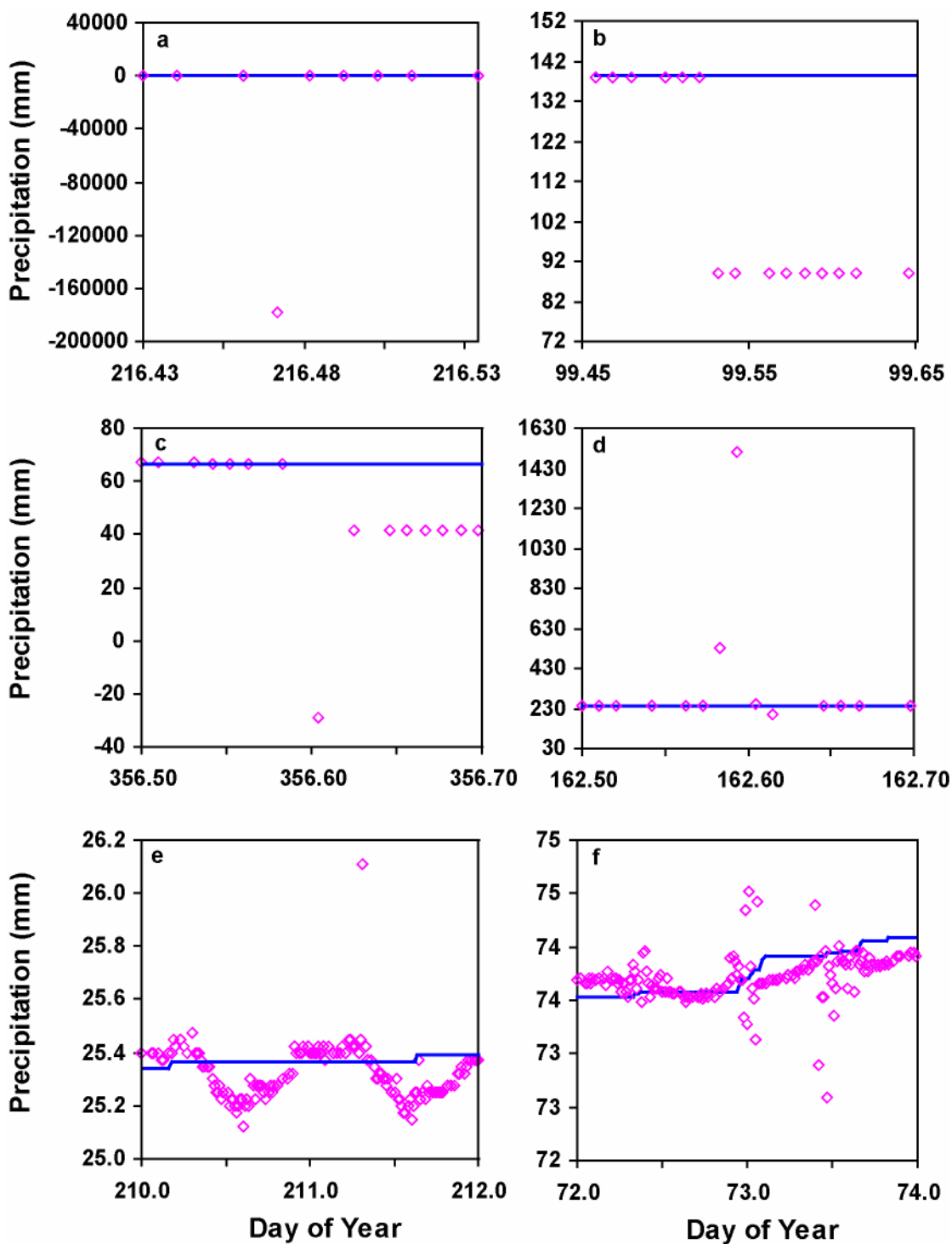


Figure 2.1: Types of mechanical errors present in gauge measurements, pink hollow diamonds show unprocessed data and blue solid lines show data processed using APCP. (a) Out of Range Data, (b) Bucket Decanting, (c) Bucket Recharge, (d) Intermittent Noise, (e) Periodic Noise, and (f) Episodic Noise

3. Program Description

The APCP utility was developed in 'Visual Basic 6.0' to process high frequency cumulative precipitation records, fill data gaps, remove discontinuous data and filter mechanical and electronic noise from the file. APCP is designed to process data one year at a time, and will accept any regular or irregular input time interval. User-defined parameters include: out of range data value indicator, *NoData*; bucket decanting limit, *BucketDecanting*; bucket recharge limit, *BucketRecharge*; and noise limit, *Noise*. By default APCP generates a processed output data file following the time steps of input data file but it can also generate output data file at any user specified time interval (such as 15 min, 1 hour or 3 hours, etc.). The value of the parameter *NoData* should be selected based on data-logger settings (e.g. -6999, -9999). Prior to running the program input data files should be inspected carefully, to verify that the initial values are accurate, to identify extended periods of missing data, and to ensure reasonable selection of values for other user defined parameters. Both *BucketDecanting* and *BucketRecharge* limits should be set smaller than the minimum absolute change in data records due to bucket decanting and bucket recharge respectively, but greater than the *Noise* limit. The *Noise* limit, which separates high and low amplitude noise signals, should smaller than the minimum change due to high amplitude noise but greater than the maximum change due to low amplitude fluctuations in input data file.

APCP scans the data and compares the difference in consecutive records to the user-defined limits in two separate cycles. In the first scanning cycle, APCP removes high amplitude noise and discontinuities including missing records, bucket decanting, bucket recharge and intermittent noise. In the second scanning cycle APCP removes low

amplitude noise and fluctuations due to diurnal temperature variations and vibrations from wind. A list of user defined parameters and program variables used by APCP is given in **Table 2.1**. Symbols used to describe programming logic are described in the Appendix (Section 7 of this chapter).

Table 2.1: Description of User defined parameters and variables used in APCP program

User Defined Parameters	
<i>BucketDecanting</i>	Bucket decanting limit
<i>BucketRecharge</i>	Bucket recharge limit
<i>Noise</i>	Threshold of high magnitude noise
<i>NoData</i>	Out of range data value.
Program Variables	
Records	Number of data points in the input file
i	Counter used to limit the scanning cycles
j	Counter from beginning to end of noise
p	Value of 'i' at start of noise
n	Value of 'i' at end of noise
CumPPT	Cumulative precipitation
PPT, PPTB, PPTE	Incremental precipitation

3.1. Out of Range Data Values

Out of range data values are first replaced to make the data record continuous.

Most data of this type are of short duration and are automatically filled by APCP by uniformly distributing the difference between previous and next available valid data over the period of out of range data points. The value of the cumulative precipitation record (CumPPT) at each time step (i) is first compared to *NoData*, to identify out of range data. APCP sets a marker (p) at the end of noise-free values to identify beginning of the period of the out of range data values.

$$Re\ cords_{i=2} \left| CumPPT(i) = NoData \ ? \ p = i - 1 \right.$$

Since an out of range data value is assumed to be an extreme negative value, APCP sets a second marker (n) at the point where data resume.

$$\left. \begin{array}{l} \text{Records} \\ j=p+1 \end{array} \right| \text{CumPPT}(j) \geq 0 \ \& \ \text{CumPPT}(j) \neq \text{NoData?} \ n = j$$

In some cases out of range data values are generated during gauge maintenance. If the collection bucket was decanted or recharged during the period of out of range data, no precipitation is assumed. Otherwise, the difference in cumulative precipitation is distributed evenly throughout the period.

$$\text{CumPPT}(p) - \text{CumPPT}(n) > \text{BucketDecanting} \ \parallel \ -(\text{CumPPT}(p) - \text{CumPPT}(n)) > \text{BucketRecharge?}$$

$$\left. \begin{array}{l} n-1 \\ j=p+1 \end{array} \right| \text{CumPPT}(j) = \text{CumPPT}(p) : \left. \begin{array}{l} n-1 \\ j=p+1 \end{array} \right| \text{CumPPT}(j) = \text{CumPPT}(p) + (j-p) \times \frac{\text{CumPPT}(n) - \text{CumPPT}(p)}{n-p}$$

3.2. Scanning Cycle 1

After removal of out of range values from the data record, high amplitude noise signals are identified and removed using the user specified limit, *Noise* in the first scanning cycle. If the absolute difference of two successive data values is greater than the *Noise* limit, the second value is identified as affected by noise and a marker 'p' is set before the beginning of noise signal.

$$\left. \begin{array}{l} \text{Records} \\ i=2 \end{array} \right| \left| (\text{CumPPT}(i) - \text{CumPPT}(i-1)) \right| > \text{Noise?} \ p = i - 1$$

The end of a noise period in the data is identified by at least five successive data values for which the absolute values of the successive differences are all less than the *Noise* limit and a marker 'n' is set at next good value after the end of the noise signal.

$$\begin{array}{l}
\text{Records-3} \\
\left. \begin{array}{l}
\left| \text{CumPPT}(j+4) - \text{CumPPT}(j+3) \right| > \text{Noise} \ \& \\
\left| \text{CumPPT}(j+3) - \text{CumPPT}(j+2) \right| > \text{Noise} \ \& \\
\left| \text{CumPPT}(j+2) - \text{CumPPT}(j+1) \right| > \text{Noise} \ \& \\
\left| \text{CumPPT}(j+1) - \text{CumPPT}(j) \right| > \text{Noise} \ ? \ n = j
\end{array} \right\} \\
j=p+1
\end{array}$$

APCP then identifies instances of bucket decanting (and recharge) within the period of noise. If the positive (or negative) difference in recorded cumulative precipitation before and after the noise signal is greater than the *BucketDecanting* (or *BucketRecharge*) limit then all instantaneous precipitation values during the period are set equal to zero.

$$\begin{array}{l}
\text{CumPPT}(p) - \text{CumPPT}(n) > \text{BucketDecanting} \ \parallel \\
-(\text{CumPPT}(p) - \text{CumPPT}(n)) > \text{BucketRecharge} \ ? \ \left. \begin{array}{l} n-1 \\ j=p+1 \end{array} \right| \text{PPT}(j) = 0
\end{array}$$

If the absolute difference in cumulative precipitation over the period of noise is less than the *Noise* limit, any difference in cumulative precipitation over the period is distributed uniformly over the records within that period.

$$\left| \text{CumPPT}(n) - \text{CumPPT}(p) \right| \leq \text{Noise} \ ? \ \left. \begin{array}{l} n-1 \\ j=p+1 \end{array} \right| \text{PPT}(j) = \frac{\text{CumPPT}(n) - \text{CumPPT}(p)}{n - p}$$

High variation in successive values may also occur due to precipitation intensity greater than the specified *Noise* limit. An increase in the cumulative precipitation over the period of noise that exceeds *Noise* but not *BucketRecharge* it is attributed to high intensity precipitation. Instantaneous precipitation during high intensity precipitation events is calculated by subtracting previous cumulative precipitation value from the current cumulative precipitation value.

$$CumPPT(n) - CumPPT(p) \leq BucketRecharge \ \& \ CumPPT(n) - CumPPT(p) > Noise ?$$

$${}_{j=p+1}^{n-1} PPT(j) = CumPPT(j) - CumPPT(j-1)$$

Similarly if the absolute difference between two successive data values is less than the *Noise* limit, instantaneous precipitation is calculated by subtracting previous cumulative precipitation value from the current cumulative precipitation value.

$${}_{i=2}^{Records} \left| (CumPPT(i) - CumPPT(i-1)) \right| \leq Noise ? \ PPT(i) = CumPPT(i) - CumPPT(i-1)$$

3.3. Scanning Cycle 2

After all high amplitude noise signals have been removed from the record in scanning cycle 1, low amplitude episodic and periodic noise are removed in the second scanning cycle. Low amplitude noise does not affect the long term total catch volume, but introduces negative values when instantaneous precipitation (PPT) is calculated from the cumulative record, as at the end of scanning cycle 1. APCP identifies episodic or periodic noise as negative instantaneous precipitation values and uses an averaging approach to distribute them over the two previous and two successive precipitation values, thereby smoothing the data without changing the total cumulative record value. The approach assumes that actual precipitation during periods of episodic or periodic noise is reasonably approximated by the generated mean values.

In scanning cycle 2, the array containing instantaneous precipitation after scanning cycle 1 (PPT) is first copied in two separate arrays: one is smoothed from the beginning of file to the end (PPTB) and the other is smoothed from the end of file to the beginning (PPTE). It is important to note that scanning cycle 1 assigns values in array PPT from cells 2 to *Records* while value in first cell is by default assigned as zero.

$$\text{Records}_{i=1} | PPTB(i) = PPTE(i) = PPT(i)$$

In order to implement the program, noise free conditions are required for the second and third values of PPT. This is achieved by moving any errors to successive values of PPT:

$$PPTB(2) < 0 ? PPT(3) = PPTB(2) + PPTB(3) \ \& \ PPTB(2) = 0$$

and

$$PPTB(3) < 0 ?$$

$$\sum_{i=2}^4 PPTB(i) \geq 0 ? \ \text{Records}_{i=2}^4 | PPTB(i) = \frac{\sum_{i=2}^4 PPTB(i)}{3} : PPTB(4) = \sum_{i=2}^4 PPTB(i) \ \& \ PPTB(2) = PPTB(3) = 0$$

For the remainder of the array, periods of five values with a central instantaneous negative value are assigned the average of these five values or the net negative value is assigned to the $i+2^{th}$ value:

$$\text{Records}_{i=4}^{-2} | PPTB(i) < 0 ?$$

$$\sum_{j=i-2}^{i+2} PPTB(j) \geq 0 ? \ \text{Records}_{j=i-2}^{i+2} | PPTB(j) = \frac{\sum_{j=i-2}^{i+2} PPTB(j)}{5} : PPTB(i+2) = \sum_{j=i-2}^{i+2} PPTB(j) \ \& \ \text{Records}_{j=i-2}^{i+1} | PPTB(j) = 0$$

The second array is scanned in the same manner, but in reverse order, i.e. from *Records-2* to 4. Finally, the instantaneous values for each time step of the two arrays are averaged to return the corrected instantaneous precipitation.

$$\text{Records}_{i=1} | PPT(i) = (PPTB(i) + PPTE(i))/2$$

4. Test Data

The U.S. Department of Agriculture Agricultural Research Service-Northwest Watershed Research Center (ARS-NWRC) is operating a dense network of precipitation gauges in Reynolds Creek Experimental Watershed (RCEW) since 1962. The watershed is located in the Owyhee Mountains of southwestern Idaho, approximately 80 km southwest of Boise and experiences a wide range of meteorological conditions (Slaughter et al. 2001). The current network is a dual-gauge system consisting of one unshielded and one shielded Belford universal recording gauge with orifice diameter of 203 mm, capacity 305 mm (Hamon 1971, 1973; Hanson et al. 1999, 2001; Hanson 2001) and an absolute sensitivity of +/-0.25 mm (Kuligowski 1997). Through time, the weighing mechanisms have also been updated to improve measurement accuracy and sensitivity. In their current configuration, a data logger records the load cell output of precipitation depth in the gauge collection bucket at 15 minute intervals (Hanson et al. 2001).

Experience with weighing bucket gauge data has led NWRC to develop extensive quality control protocols and quality analysis techniques. Through 2004, NWRC used the graphical tool 'Rainfall Analyzer' (RA) to manually filter, correct and process raw precipitation data. This method requires 1-3 days per station-year depending on operator training, skill, judgment, and patience. Internal comparisons have shown that RA results are somewhat subject to operator bias and are not exactly reproducible even when repeated by the same operator. Nevertheless, to our knowledge RA is the most sophisticated data filter available for weighing type bucket gauges. *Estimated total annual gauge catch* was added as a supplemental measure of quality analysis. This value is the sum of total collected gauge bucket volume changes, recorded from field records of

gauge maintenance. It is the most objective measure available of actual cumulative precipitation at RCEW.

The APCP correction technique was applied to 22 dual gauge stations in RCEW for water years 1997-2005 (October through September). The gauge sites span an elevation range from 1177 to 2169 m and mean annual precipitation from 236 to 1123 mm (Hanson 2001). Corrected data from APCP and RA are compared to *estimated total annual gauge catch* for eleven dual gauge stations for water years 2002-2004 for a total of 58 station-years. These sites and station years were selected for availability of both RA corrected precipitation records and field maintenance records to estimate total annual gauge catch. To assess the effect of the APCP on sub-daily precipitation data, we compare precipitation records following scanning cycle 1, which is similar to records following manual correction of out of range data and gauge servicing, to information following scanning cycle 2, which removes low amplitude noise for daily, hourly and 15 minute time steps (**Figure 2.2**).

As a demonstration of the capability of APCP to remove random noise from other data, we applied the program to TDR data. The data were collected in the Dry Creek Experimental Watershed near Boise, Idaho, in coarse-loamy, mixed mesic Ultic Haploxerolls (Harkness 1997; McNamara et al. 2005). The TDR waveguides were 30 cm in length and logged hourly using TDR100, coaxial multiplexers and CR10X data loggers (Campbell Scientific, Logan, UT). Data filtering was performed with the first scanning cycle of APCP only, since these data are not cumulative. In this case Noise limit is set to 0.025. Bucket decanting and recharge limits are set to very high values (50) to only

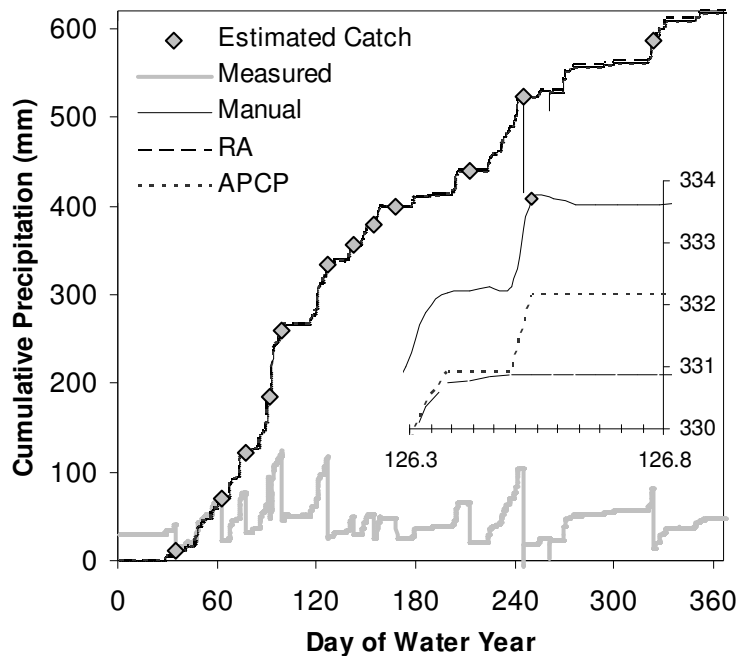


Figure 2.2: Measured and corrected shielded gauge precipitation data using manual (only bucket decanting), RA and APCP techniques for site 176, water year 2004. Estimated catch is computed by adding bucket decanting depths to the recorded precipitation. Inserted figure shows differences in three correction approaches at sub-daily scale.

Remove extreme data spikes and out of range data value was set to -6999.

Contemporaneous data from a proximal Water Content Reflectometer (WCR) which was previously calibrated with TDR (Chandler et al. 2004) is provided for comparison.

5. Results and Discussion

The goal of data processing is noise and error removal without introducing bias. To demonstrate the function of APCP for each defined category of mechanical error, we present example comparisons of raw and APCP processed data at the scale of each error (**Figure 2.1**). The error categories “Out of Range Data,” “Bucket Decanting,” “Bucket Recharge,” and “Intermittent Noise” occur as instances or constant value shifts from a

baseline and are simply corrected relative to local baseline cumulative precipitation by scanning cycle 1. Establishing a local baseline is more complicated over the temporal scale of “Periodic Noise,” which is by definition a quasi-regular waveform around the expected value and for “Episodic Noise,” which superimposes random noise onto the diurnal signal of “Periodic Noise” (Figure 2.1e, f). The uncertainty in baseline cumulative precipitation during Periodic and Episodic Noise, as complicated by contemporaneous noise and precipitation, is the greatest potential source of error and bias in data correction for cumulative gauge records.

In the case of cumulative precipitation, the match between processed and raw cumulative gauge-catch data is a qualitative measure of the efficacy of data processing techniques. Such a comparison requires developing a cumulative record from raw data by correction of negative steps in the measured record from bucket decanting, for instance by APCP scanning cycle 1. Comparison of the raw 15 minute interval data from the shielded gauge at site 176, to the cumulative series following manual adjustment for bucket decanting, output from APCP and RA is presented in **Figure 2.2**. All three correction approaches maintain the basic structure of the time series data and match the incremental estimated catch at the annual time scale. However, at sub-daily time scale, the cumulative records for manual correction, RA and APCP often diverge at the mm scale (**Figure 2.2**, inset) due to differences in the approach to processing Periodic and Episodic Noise. Bias is therefore inherent in both methods of processing precipitation data.

For 58 station-years tested, the bias between processed cumulative gauge precipitation and estimated actual gage catch is lower for APCP than RA (**Figure 2.3**).

APCP annual total is consistently close to the estimated total annual precipitation, with a mean difference and standard deviation (SD) of about -0.6 mm (-0.1%) and 3.4 mm (0.6%) respectively for shielded gauge and -0.2 mm (-0.02%) and 2.1 mm (0.5%) respectively for unshielded gauges. In contrast, RA results show a mean difference and standard deviation of -2.7 mm (-0.5%) and 11.3 mm (2.1%), respectively, for shielded gauge and -1.0 mm (0.4%) and 12.9 mm (3.4%) for unshielded gauge. Because APCP is not affected by operator bias, total water year precipitation for data processed by APCP can be exactly repeated and processing and depending on the operator, APCP can process one station year in a few minutes. Depending on the extent of noise, spreadsheet and RA processing may take 1-3 days per station year.

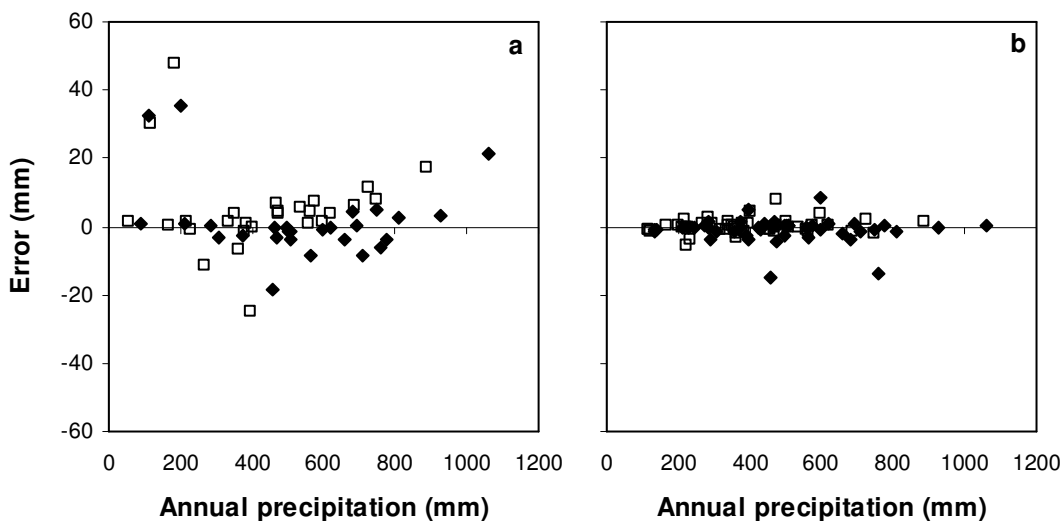


Figure 2.3: Errors with respect to *estimated total annual precipitation*, solid diamonds show shielded and open boxes show unshielded gauges. (a) Rainfall Analyzer (RA). (b) Automated Precipitation Correction Program (APCP).

Ultimately, the goal of removing low amplitude noise from the record is to generate a reliable instantaneous precipitation record at sub daily time steps. As an example of the temporal scale dependence of the influence of low amplitude noise on the instantaneous precipitation record, we compare distributions for daily hourly and 15 minute time steps for a single station year (**Figure 2.4**). Once again, APCP scan 1 is used to remove all major noise and scan 2 is then used to filter the low amplitude noise. Excluding the nil instantaneous precipitation data, which were most frequent for all time steps, two clear trends emerge: First, the instances of precipitation represented by scan 1 exceed those by scan 2 at all time steps. Second, the number of representations of negative precipitation increases with decreasing time step (**Figure 2.4**). Whereas the positive and negative instantaneous precipitation values balance in the annual record at all time steps, manual correction of erroneous instantaneous precipitation values is clearly impractical for hourly and 15 minute records due to the exponential increase in number of errors at shorter time steps (**Table 2.2**).

Table 2.2: Instantaneous precipitation occurrence frequency and cumulative annual depth for daily, hourly, and 15 min

	scan 1				scan 2	
	<u>positive event</u> number	sum (mm)	<u>negative event</u> number	sum (mm)	<u>positive event</u> number	sum (mm)
daily	188	491	130	-28	95	463
hourly	3895	721	3098	-246	885	475
15 min	13912	1328	12030	-853	2081	475

APCP does not eliminate the requirement for careful observation of raw data and field notes. APCP may not remove all noise satisfactorily when the amplitude of noise

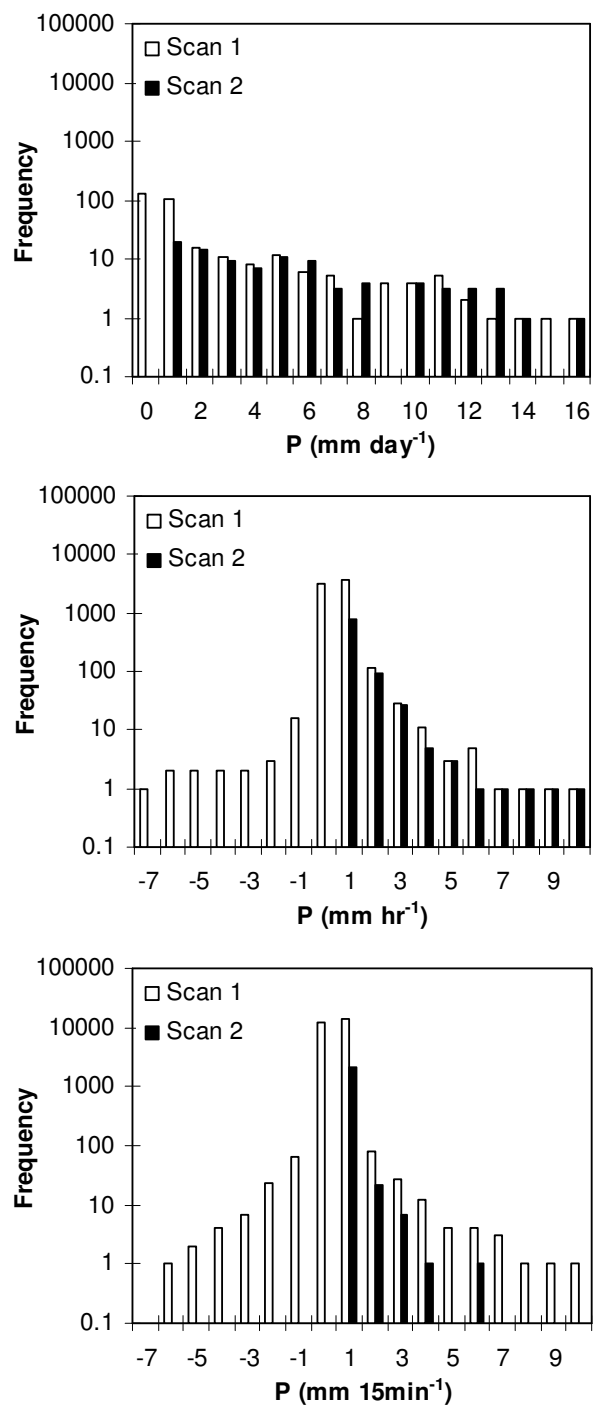


Figure 2.4: Frequency of instantaneous precipitation values following scan 1 and scan 2 of the Automated Precipitation Correction Program for daily, hourly, and 15-minute time steps.

Caused by site maintenance is very small. In this case it is necessary to remove these errors from the raw precipitation record before using APCP. It is also recommended that the processed data generated by APCP be checked by comparison with estimated total annual gauge catch and visual inspection of raw data to verify that all noise and discontinuities have been removed satisfactorily.

The result of application of APCP to hourly TDR data is shown in **Figure 2.5**. In this case, the assumption that instantaneous change in the hourly water content record greater than $0.025 \text{ m}^3 \text{ m}^{-3}$ were noise. This approach identified 459 data records as noise and adjusted them to the local average. Of the records identified as noise, 70 were greater than $0.4 \text{ m}^3 \text{ m}^{-3}$, 83 were less than the apparent residual moisture content of $0.045 \text{ m}^3 \text{ m}^{-3}$ (29 were negative). Of the 306 adjusted data values within the possible range of soil moisture ($0.045\text{-}0.40 \text{ m}^3 \text{ m}^{-3}$), 128 were greater than the apparent field capacity ($0.24\text{-}0.40 \text{ m}^3 \text{ m}^{-3}$). The remaining 178 identified errors were random changes greater than the assumed noise limit within the expected range of soil moisture, for example the spikes near Julian day 160 (**Figure 2.5**). The corrected TDR record is comparable to the calibrated WCR record, which tend not to be subject to similar noise problems.

6. Conclusion

The APCP precipitation correction utility, developed to filter mechanical errors from raw precipitation data, was applied successfully to process data collected at 22 dual gauge stations for water years 1997-2005 and tested against the data processed using RA and estimated total annual gauge catch at 11 dual gauge sites for water years 2002-2004. APCP was capable of rapidly and accurately filtering noise and discontinuities from the

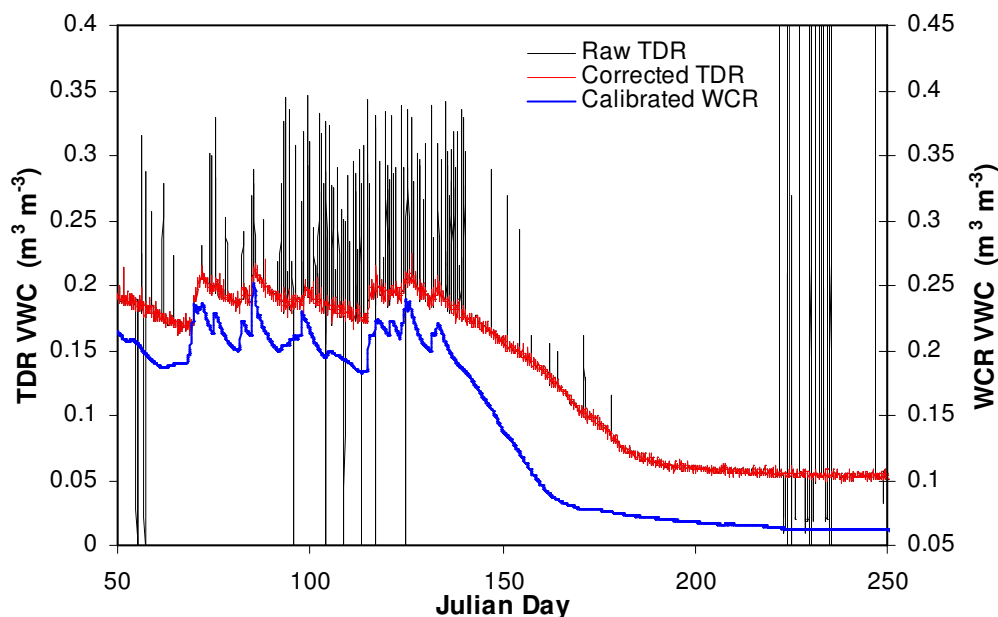


Figure 2.5: Noise removal from hourly TDR water content record with APCP Scan cycle 1 and (offset) comparative water content record from a calibrated Water Content Reflectometer.

Raw precipitation data. The data processed by APCP has smaller mean and standard deviation of error than the graphical RA correction. This can be attributed to the fact that APCP is automated, repeatable and eliminates the effect of operator bias. The time required to process the raw high frequency precipitation data using APCP is significantly less than the graphical RA approach, which is important in extensively instrumented watersheds like RCEW. The success of the APCP correction of TDR data indicates further that the model uses a robust approach to filtering and filling data that can be applied to different sources of continuous data.

7. Appendix

The following notation has been used in this paper

$\prod_{i=1}^n$	=	for i = 1 to n
A ? B	=	If 'A' is true then 'B'.
A ? B : C	=	If 'A' is true then 'B' otherwise 'C'.
A B	=	'A' or 'B'
A & B	=	'A' and 'B'
A	=	Absolute of 'A'
$\sum_{i=1}^n A(i)$	=	Sum of A(i) from i=1 to n

8. Acquiring the APCP Software

Detail description of the APCP software and programming code is presented in Appendix A. The APCP software is available for download in the 'apcp' directory at the anonymous ftp site <ftp://cirque.nwrc.ars.usda.gov/pub/> maintained by the U.S.

Department of Agriculture Agricultural Research Service, Northwest Watershed Research Center in Boise Idaho, United States. Questions may be addressed to Anurag Nayak (anurag.nayak@aggiemail.usu.edu) or Dr. Danny Marks (danny@nwrc.ars.usda.gov). Note that any reference to specific equipment types or manufacturers is for information purposes, and does not represent a product endorsement.

9. References

Arnold, N., Richards, K., Willis, I., and Sharp, M. (1998). "Initial results from a distributed, physically based model of glacier hydrology." *Hydrolog. Process.*, 12(2), 191-219.

- Calder, I. R., and Kidd, C. H. R. (1978). "Note on the dynamic calibration of tipping-bucket gauges." *J. Hydrol.*, 39(3-4), 383-386.
- Chandler, D.G., Seyfried, M., Murdock, M., and McNamara, J. (2004). "Field calibration of water content reflectometers." *Soil Sci. Soc. Am. J.*, 68,1501-1507.
- Ciach, G. J. (2003). "Local random errors in tipping-bucket rain gauge measurements." *J. Atmos. Oceanic Technol.*, 20(5), 752-759.
- Duchon, C. E., and Essenberg, G. R. (2001). "Comparative rainfall observations from pit and above ground rain gauges with and without wind shields." *Water Resour. Res.*, 37(12), 3253-3263.
- Garen, D. C., and Marks, D. (2005). "Spatially distributed energy balance snowmelt modeling in a mountainous river basin: estimation of meteorological inputs and verification of model results." *J. Hydrol.*, 315(1-4), 126-153.
- Goodison, B. E., Louie, P. Y. T., and Yang, D. (1998). "WMO solid precipitation measurement intercomparison, final report." *WMO/TD-No. 872*, World Meteorological Organization, Geneva.
- Haddeland, I., Lettenmaier, D. P., and Skaugen, T. (2006). "Reconciling simulated moisture fluxes resulting from alternate hydrologic model time steps and energy budget closure assumptions." *J. Hydrometeorol.*, 7(3), 355-370.
- Hamon, W. R. (1971). "Chapter 4 – Reynolds Creek, Idaho." *Agricultural Research Service Precipitation Facilities and Related Studies*. D. M. Hershfield ed., ARS-USDA, Washington, D.C.
- Hamon, W. R. (1973). "Computing actual precipitation: Distribution of precipitation in mountainous areas." *WMO Rep. No. 362*, World Meteorological Organization, Geneva, 1, 159-173.
- Hanson, C. L. (2001). "Long-term precipitation database, Reynolds Creek Experimental Watershed, Idaho, United States." *Water Resour. Res.*, 37(11), 2831-2834.
- Hanson, C. L., Burgess, M. D., Windom, J. D., and Hartzmann, R. J. (2001). "New weighing mechanism for precipitation gauges." *J. Hydrol. Eng.*, 6(1), 75-77.
- Hanson, C. L., Morris, R. P., and Coon, D. L. (1979). "A note on the Dual-gage and Wyoming shield precipitation measurement systems." *Water Resour. Res.*, 15(4), 956-960.

- Harkness, A. (1997). "Soil survey of Boise front project, Idaho: Interim and supplemental Report.", US Department of Agriculture in cooperation with Boise City and Ada County, Boise, ID.
- Kandel, D. D., Westernand, A. W., and Grayson, R. B. (2005). "Scaling from process timescales to daily time steps: A distribution function approach." *Water Resour. Res.*, 41(2), Art. No. W02003.
- Kuligowski, R. J. (1997). "An overview of national weather service quantitative precipitation estimates." U. S. Department of Commerce, National oceanic and atmospheric administration, N. W. S.
- La Barbera, P., Lanza, L. G., and Stagi, L. (2002). "Tipping bucket mechanical errors and their influence on rainfall statistics and extremes." *Water Sci. Technol.*, 45(2), 1-10.
- Lehning, M., Volksch, I., Gustafsson, D., Nguyen, T. A., Stahli, M., and Zappa, M. (2006). "ALPINE3D: A detailed model of mountain surface processes and its application to snow hydrology." *Hydrolog. Process.*, 20(10), 2111-2128.
- Link, T., and Marks, D. (1999a). "Distributed simulation of snowcover mass and energy balance in a boreal forest." *Hydrolog. Process.*, 13(13-14), 2439-2452.
- Link, T., and Marks, D. (1999b). "Point simulation of seasonal snowcover dynamics beneath a boreal forest canopies." *J. Geophys. Res.*, 104(D22), 27841-27858.
- Marks, D., Domingo, J., Susong, D., Link, T., and Garen, D. (1999). "A spatially distributed energy balance snowmelt model for application in mountain basins." *Hydrolog. Process.*, 13(12-13), 1935-1959.
- Marsalek, J. (1981). "Calibration of the tipping bucket rain gauge." *J. Hydrol.*, 53(3-4), 343-354.
- McNamara, J. P., Chandler, D. G., Seyfried, M., and Achet, S. (2005). "Soil moisture states, lateral flow, and streamflow generation in a semi-arid, snowmelt-driven catchment." *Hydrolog. Process.*, 19, 4023-4038.
- Molini, A., Lanza, L. G., and La Barbera, P. (2005a). "The impact of tipping-bucket rain gauge measurement errors on design rainfall for urban-scale applications." *Hydrolog. Process.*, 19(5), 1073-1088.
- Molini, A., Lanza, L. G., and La Barbera, P. (2005b). "Improving the accuracy of tipping-bucket rain records using disaggregation techniques." *Atmos. Res.*, 77(1-4), 203-217.

- Ngo-Duc, T., Polcher, J., and Ianval, K. (2005). "A 53-year forcing data set for land surface models." *J. Geophys. Res.*, 110(D6), Art. No. D06116.
- Nystuen, J. A. (1999). "Relative performance of automatic rain gauges under different rainfall conditions." *J. Atmos. Oceanic Technol.*, 16(8), 1025-1044.
- Schnorbus, M., and Alia, Y. (2004). "Generation of an hourly meteorological time series for an alpine basin in British Columbia for use in numerical hydrological modeling." *J. Hydrometeorol.*, 5(5), 862-882.
- Sevruk, B. (1982). "Methods of correction for systematic error in point precipitation measurement for operational use." *Operational Hydrology Report No. 21*, World Meteorological Organization, Geneva, Switzerland.
- Slaughter, C. W., Marks, D., Flerchinger, G. N., Van Vactor, S. S., and Burgess, M. D. (2001). "Thirty-five years of research data collection at Reynolds Creek Experimental Watershed, Idaho, United States." *Water Resour. Res.*, 37(11), 2819-2823.
- Susong, D., Marks, D., and Garen, D. (1999). "Methods for developing time-series climate surfaces to drive topographically distributed energy- and water-balance models." *Hydrolog. Process.*, 13(12-13), 2003-2021.
- Vasvari, V. (2005). "Calibration of tipping bucket rain gauges in Graz urban research area." *Atmos. Res.*, 77(1-4), 18-128.
- Waichler, S. R., and Wigmosta, M. S. (2003). "Development of hourly meteorological values from daily data and significance to hydrological modeling at H. J. Andrews experimental forest." *J. Hydrometeorol.*, 4(2), 251-263.
- Winstral, A., and Marks, D. (2002). "Simulating wind fields and snow redistribution using terrain-based parameters to model snow accumulation and melt over a semi-arid mountain catchment." *Hydrolog. Process.*, 16(18), 3585-3603.
- Yang, D., Goodison, B. E., Metcalfe, J. R., Golubev, V. S., Bates, R., Pangburn, T., and Hanson, C. L. (1998). "Accuracy of NWS 8" standard nonrecording precipitation gauge: results and application of WMO Intercomparison." *J. Atmos. Oceanic Technol.*, 15(1), 54-68.
- Yang, D., Goodison, B. E., Metcalfe, J. R., Louie, P., Leavesley, G., Emerson, D., Hanson, C. L., Golubev, V. S., Elomaa, E., Gunther, T., Pangburn, T., Kang, E., and Milkovic, J. (1999). "Quantification of precipitation measurement discontinuity induced by wind shields on national gauges." *Water Resour. Res.*, 35(2), 491-508.

Yang, D., Kane, D. L., D., H. L., Goodison, B. E., Metcalfe, J. R., Louie, P. Y. T., Leavesley, G. H., Emerson, D. G., and Hanson, C. L. (2000). "An evaluation of the Wyoming gauge system for snowfall measurement." *Water Resour. Res.*, 36(9), 2665-2677.

CHAPTER 3

LONG-TERM SNOW, CLIMATE, AND STREAMFLOW TRENDS AT THE REYNOLDS CREEK EXPERIMENTAL WATERSHED, OWYHEE MOUNTAINS, IDAHO, USA²

Abstract

Forty-five water years (1962 – 2006) of carefully measured data on temperature, precipitation, streamflow, snow, soil temperature, and moisture for valley bottom, mid-elevation, and high elevation sites within the Reynolds Creek Experimental Watershed (RCEW) were analyzed to evaluate the extent and magnitude of the impact of climate warming on the hydrology and related resources in the interior northwestern U.S. This analysis shows significant trends of increasing temperature at all elevations, with larger increases in daily minimum than daily maximum. The proportion of snow to rain has decreased at all elevations, with the largest and most significant decreases at mid- and low elevations. Maximum snow water equivalent (SWE) has decreased at all elevations, again with the most significant decreases at lower elevations and the length of the snow season has decreased by nearly a month. Changes in air temperature and snow cover affect the duration of soil freezing (a reduction by about half the number of freezing days) at low and mid-elevations, and the onset of plant-water stress, which occurs about 3 weeks earlier at high elevations. All trends show a significant elevation gradient in either timing or magnitude. Though inter-annual variability is large, there has been no change in water year total precipitation or streamflow. Streamflow shows a seasonal shift,

² Coauthored by A. Nayak, D. Marks, D.G. Chandler, and M. Seyfried. To be submitted for publication in *The Cryosphere*, European Geosciences Union.

stronger at high elevation and delayed at lower elevations, to larger winter and early spring flows, and reduced late-spring and summer flows.

1. Introduction

In the mountainous western U.S. and Canada the seasonal snowcover is a critical component of the hydrologic cycle. Most precipitation falls during winter, with significant snowfall in the mountains. Mountain snowcovers provide both the primary supply and storage reservoir for water in the region. In the western U.S., water management is largely based on the belief that, in these mountain basins, there is a stable and robust relationship between snow deposition and the timing and magnitude of melt from the snowcover. From this it follows that if climate warming alters patterns of snow deposition, the timing of melt, and the delivery of melt-water to soil, streams and rivers, water supplies and water resource management in the region will be substantially affected.

Since the beginning of the 20th century, Earth's mean surface temperature has increased by about 1°C (IPCC 2007; Trenberth et al. 2007), with greater temperature increases in mountainous regions and strong effects on the seasonal snow cover (Lemke et al. 2007; Randall et al. 2007). Observations and model predictions indicate that persistent warming will substantially alter hydro-climate, both at global and regional scales (Leung and Ghan 1999; Manabe et al. 2004; Stewart et al. 2005; Leipprand and Gerten 2006; Trenberth et al. 2007; Randall et al. 2007). In the western U.S. and Canada mean surface temperature has increased by 1 – 3°C over the last 50 years (0.2 – 0.5°C per decade), with larger increases during winter (Dec, Jan, Feb) (0.7 – 0.9°C per decade;

Trenberth et al. 2007). The trend in warming is diurnally asymmetric, with a larger increase in minimum temperature and a decreased diurnal temperature range (Karl et al. 1984, 1993; Quintana-Gomez 1999; Brunetti et al. 2000; Trenberth et al. 2007).

The effect of climate warming on precipitation is not definitive, particularly in mountainous regions of the western United States where the density of representative measurement stations is limited, and the change in phase from rain to snow as storms progress from valley bottoms to higher elevations is difficult to assess. In the United States and Canada it is reported that total annual precipitation has increased slightly (Groisman and Easterling 1994; Karl and Knight 1998; Hu et al. 1998; Akinremi et al. 1999; Easterling et al. 2000; Garbrecht et al. 2004; Hamlet et al. 2005; Trenberth et al. 2007), though some regions have reported persistent drought. The studies cited above are generalizations, extending over hemispheric or continental regions, or are limited to plains and prairie, due to the difficulty of modeling snow deposition and melt across mountainous areas of the western U.S. and Canada.

In mountainous western U.S. and Canada, much of the precipitation falls during winter as snow, to be released as melt water during spring and early summer. Topographic and vegetation canopy controls on wind fields, spatial and temporal patterns of precipitation, snow deposition, snowcover energy balance and drainage from snowmelt in mountains results in highly complex spatial and temporal patterns of runoff generation. Precipitation intensity and volume over the western mountains are strongly influenced by storm track and air mass characteristics associated with ocean circulation features such as the El Nino-Southern Oscillation (ENSO) and the Pacific Decadal Oscillation (PDO) (Hurrell 1995; Hurrell and Van Loon 1997; Dettinger et al. 1998), but the dynamics of

ocean circulation and temperature are poorly monitored (Bindoff et al. 2007) and subsequent linkages between atmosphere – ocean interactions and precipitation in mountainous regions of the Western U.S. and Canada are not well understood (Trenberth et al. 2007).

The timing and magnitude of snowmelt in the mountains of the western U.S. is very sensitive to climate conditions. Along with warmer temperatures a number of studies have shown substantial changes in snow deposition and melt patterns, reduced fraction of precipitation that falls as snow over western U.S. and Canada (Aguado et al. 1992; Dettinger and Cayan 1995; Huntington et al. 2004; Regonda et al. 2005; Knowles et al. 2006), and a shift in the timing of snowmelt runoff toward earlier in the year (Aguado et al. 1992; Dettinger and Cayan 1995; Cayan et al. 2001; Stewart et al. 2004, 2005). Indications of this shift have been earlier timing of the initial pulse of snowmelt runoff (Cayan et al. 2001; Stewart et al. 2004, 2005), declines in snowcover and spring snow water equivalent (Mote 2003a&b, 2006; Mote et al. 2005), earlier timing of the peak runoff, and a redistribution of the average monthly or seasonal fractional flow (Aguado et al. 1992; Cayan et al. 2001; McCabe and Clark 2005; Regonda et al. 2005).

While the studies cited above show the general sensitivity of the seasonal snowcover to climate warming, they give us little insight into how that sensitivity will vary with elevation, site or climate conditions other than temperature. We expect that snow in low to mid-elevations (the so-called “rain – snow transition zone”) within a mountain basin will be more affected by climate warming than snow at higher elevations, but few data are available to test this hypothesis, and most of the conclusions reached are circumstantial or anecdotal. McCabe and Clark (2005) evaluated streamflow timing for

84 rivers in the western U.S. showing a systematic shift toward earlier flows in all regions, with the strongest trend in the Pacific Northwest. This work shows increased trend significance for lower elevation rivers, but the comparison is limited by the data used for the analysis. Many of the high significance trends are for low elevation sites located in the Cascade Mountains of the Pacific Northwest, with weaker trends for higher elevation sites in the Upper Colorado, Great Basin and California, which include the Rocky Mountains, Wasatch and Sierra Nevada. While their analysis does indicate that the Pacific Northwest may be more sensitive to warming than other regions of the west, because the low elevation rivers are geographically removed from the high elevation rivers, the effect of elevation on the trend is not direct.

Hamlet et al. (2005) and Mote et al. (2005) used a modeling approach to evaluate the sensitivity of trends in snow water equivalent (SWE) across the western U.S. to changes in temperature and precipitation. Both compared simulated SWE across the western U.S. to measured values, and both attempted to separate the effects of changes in temperature from changes in precipitation. These studies show that SWE is decreasing, that peak SWE is occurring earlier, and that these trends – across the west – are not the result of changes in precipitation but are strongly correlated to increases in temperature. The decrease in SWE was again greatest in the Pacific Northwest. However, both studies were limited by the lack of climate and snow data, and by a limited range of elevations where data were collected within the same geographic area. Though the western U.S. has probably the most extensive mountain snow measurement program in the world, the NRCS SNOTEL system (Serreze et al. 1999), the sites are generally located in protected, mid-elevation locations. Few sites are located in higher elevations, and while a few

SNOTEL sites include meteorological instrumentation, most do not. The analysis presented by Hamlet et al. (2005) and Mote et al. (2005), though carefully done and clearly presented, was based on extrapolated data across a range of elevations that extended far beyond that of the measurement sites. Temperature measurement sites were typically in valley bottoms, and may have been a km or more below the snow and precipitation sites, and precipitation at higher elevations was based on estimated lapse rates that could not be validated.

It is clear that temperatures across the west have increased, and that the seasonal snowcover has been affected. Most research, however, has focused on large-scale analysis, leaving many questions about specific impacts of climate warming, particularly how the mountain snowcover across a range of elevations within a mountain basin may be differently affected. Few locations exist where climate, precipitation and snow measurement sites are co-located, and fewer still where these are located along a range of elevations from the valley bottom to headwaters in a mountain basin. In mountain basins the distribution of the snowcover, snowmelt and the generation of runoff are heterogeneously distributed across the landscape as a function of terrain structure (elevation, slope and aspect), wind exposure and land cover (Marks and Dozier 1992; Marks and Winstral 2001; Winstral and Marks 2002; Marks et al. 1999, 2002; Garen and Marks 2005). To better understand how climate warming has affected, and in the future, may further affect the mountain snowcover, snowmelt, streamflow and catchment hydrology in the western U.S., coherent, long-term data from a range of elevations within a mountain basin on snow, precipitation, temperature, humidity, streamflow, and related parameters are required.

Detailed and carefully collected data from 45 years of monitoring (1962-2006 water years³) within the Reynolds Creek Experimental Watershed (RCEW), a USDA Agricultural Research Service watershed in the Owyhee Mountains of Idaho (Robins et al. 1965; Marks 2001; Flerchinger et al. 2007; Marks et al. 2008), are analyzed in this paper. Temporal trends in temperature and precipitation are analyzed by year and season, followed by seasonal analysis of precipitation phase (snow or rain), peak, April 1 and May 1 SWE, snowcover initiation and meltout dates, soil freezing days, the date of plant-water stress onset and streamflow for sites across the full range of elevations and site conditions found within the RCEW. This analysis shows similar hydro-climate trends to those reported in the literature. Further, the more complete meteorological record and data from a range of elevations and site conditions within the RCEW, indicates that there are elevational gradients and seasonal differences to climate warming and its effects that may have significant hydrologic impacts in the region. We highlight the implications of global warming for water management by comparing temporal trends in hydrometeorological forcing variables to changes in precipitation runoff-relationships for nested watersheds at RCEW for twenty year periods before and after the year 1985.

2. The Reynolds Creek Experimental Watershed (RCEW)

The Reynolds Creek Experimental Watershed (RCEW), a 238 km² drainage with an elevation range of 1145 m (1099–2244 m AMSL) is located in the Owyhee Mountains near Boise, Idaho, and has been continuously monitored since the early 1960's. The

³ A water year (WY) runs from October through September, so the 1962 WY extends from Oct 1961 thru Sept 1962. The WY is used in the western US because most precipitation falls during fall – spring months of Nov – April. The WY includes an entire precipitation cycle, whereas a calendar year would include the last part of one annual precipitation cycle, and the first part of the next.

vision for RCEW as an outdoor hydrologic laboratory in which watershed research would be supported by sustained, long-term monitoring of basic hydro-climatic parameters was first described in 1965 in the first volume of *Water Resour. Res.* (Robins et al. 1965), the first 35 years of data presented in a series of papers in 2001 (Marks 2001) and updated descriptions presented by Flerchinger et al. (2007) and Marks et al. (2008).

Research at the RCEW is supported by monitoring at 9 weirs, 32 primary and 5 secondary meteorological measurement stations, 5 tower profile sites, 26 precipitation stations, 8 snow course and 5 snow study sites, 27 soil temperature and moisture measurement sites with 5 sub-surface hill-slope hydrology sites and 5 Eddy Covariance (EC) systems, including measurements over low sage, big mountain sage, and above and below aspen. All data are ingested into a computer database, and available to the public via both web-based and on-line ftp access (Slaughter et al. 2001; <ftp://ftp.ars.usda.gov/>). In this study, data collected at 3 meteorological stations, 12 precipitation stations, 3 weirs, 8 snow courses, 1 snow pillow and 4 soil temperature and moisture measurement stations were selected based on length and continuity of data records, to investigate the impact of climate warming on hydrology and related resources at the RCEW (**Figure 3.1**). Detailed descriptions of selected stations are presented in sections below.

2.1. Meteorological Measurement Sites

Of the 37 meteorological measurement sites currently within the RCEW, data from three, which have been operated continuously since the 1960's, are used for this study. As reported by Hanson et al. (2001) these were the primary meteorological monitoring sites within RCEW for the first 35 years that the watershed was operated.

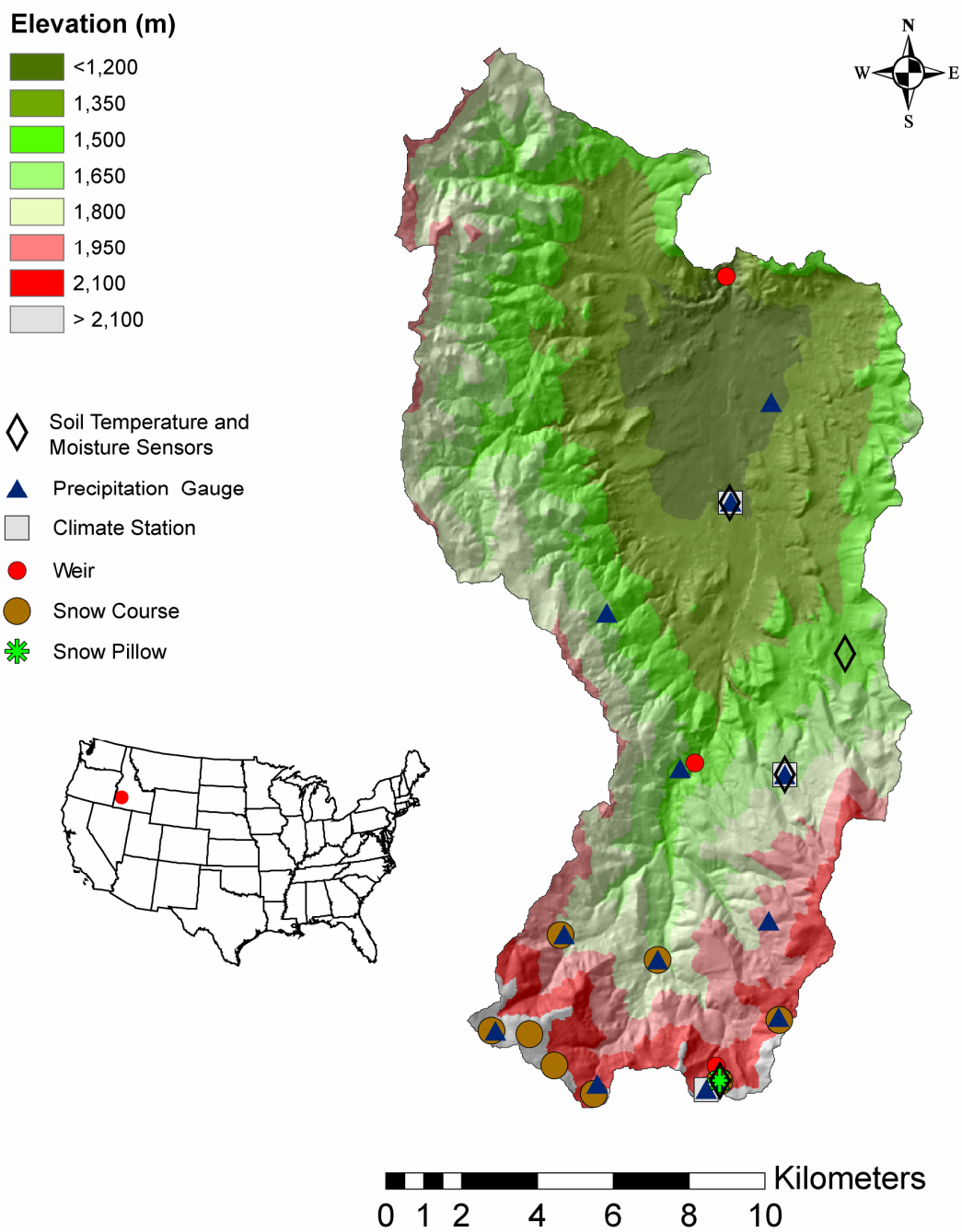


Figure 3.1: Topographic map of RCEW with long-term climate stations, precipitation gauges, snow courses, snow pillow, soil temperature and moisture measurement stations, and weirs.

They represent nearly the full range of elevations within RCEW, and are co-located with precipitation and soil moisture and temperature measurement sites (**Table 3.1**). These sites were initially established to monitor daily climate conditions (max/min temperature & RH, and pan evaporation during summer) at a range of elevations within the RCEW. As digital data loggers became available in the 1970's and early 1980's, they were converted to full micro-meteorological stations, providing hourly records of temperature, humidity, wind, and radiation.

The low elevation meteorological site (site *076_met*, also referred to as the “Quonset”) is located at the operational headquarters for the RCEW. Precipitation (*076_ppt*) and soil temperature and moisture (*076_stm*) measurements are co-located at this site. This site is in a relatively broad, flat valley bottom approximately centered within the RCEW (see **Figure 3.1**). At an elevation of 1207 m, it is only 108 m above the RCEW Outlet weir, but it is nearly 10 km distant. Site *076_met* vegetation is Wyoming Big Mountain sagebrush with some low sage, which is representative of valley bottom vegetation in the RCEW. Annual average wind-corrected precipitation is less than 280 mm, mean annual temperature is 9.8°C, with an average daily max of 15.7°C and a min of 2.4°C, annual average wind speed is 2.3 ms⁻¹ (1981-2006), growing season pan evaporation is 1250 mm (1964-2001), and dew point temperature is -0.8°C (1981-2006).

The mid-elevation meteorological site (site *127_met*, also referred to as “Lower Sheep Creek” or *LSC*) is located on the eastern side and about half way between *076_met* and the southern – and highest elevation – boundary of the RCEW (see **Figure 3.1**). Precipitation (*127_ppt*) and soil temperature and moisture (*127_stm*) measurements are co-located at this site. At an elevation of 1652 m, it is 66 m below the mid-point

Table 3.1: Long-term climate (T_a , RH), precipitation, snow, soil temperature and moisture measurement sites at the RCEW.

Site ID	Location ⁴		Elevation (m)	Data Records	
	Easting (m)	Northing (m)		Type	Records Begin
<i>163_ppt</i>	514,134	4,764,430	2170	Precip.	1962
<i>163_sc</i>	514,042	4,769,428	2162	Snow Course	1961
<i>163b_sc</i>	515,042	4,769,342	2147	Snow Course	1961
<i>163c_sc</i>	515,689	4,768,520	2125	Snow Course	1961
<i>176_ppt</i>	519,693	4,767,923	2097	Precip.	1968
<i>176_stm</i>	519,693	4,767,923	2097	Soil T	1981
				Soil Moisture	1973
<i>176_met</i>	519,686	4,767,924	2093	Daily T, RH	1967
				Hourly Micromet	1983
<i>174_ppt</i>	516,815	4,768,026	2074	Precip.	1962
<i>174_sc</i>	516,731	4,767,765	2073	Snow Course	1961
<i>176e_ppt</i>	520,055	4,768,117	2056	Precip.	1962
<i>176e_sc</i>	520,040	4,768,108	2056	Snow Course	1961
<i>176e_sp</i>	520,047	4,768,115	2056	Snow Pillow	1982
<i>167_ppt</i>	521,596	4,769,779	2003	Precip.	1962
<i>147_ppt</i>	521,336	4,772,334	1872	Precip.	1962
<i>144_ppt</i>	515,945	4,771,988	1815	Precip.	1962
<i>144_sc</i>	515,862	4,771,963	1815	Snow Course	1961
<i>155_ppt</i>	518,424	4,771,320	1654	Precip.	1962
<i>155_sc</i>	517,893	4,770,341	1743	Snow Course	1961
<i>127_ppt</i>	521,742	4,776,189	1652	Precip.	1962
<i>127_met</i>	521,742	4,776,195	1652	Daily T, RH	1967
				Hourly Met	1984
<i>127_stm</i>	521,742	4,776,195	1652	Soil T	1982
				Soil Moisture	1970
<i>116_ppt</i>	519,008	4,776,343	1459	Precip.	1962
<i>098_stm</i>	523,353	4,779,404	1259	Soil T	1981
				Soil Moisture	1971
<i>076_ppt</i>	520,367	4,783,418	1207	Precip.	1962
<i>076_met</i>	520,365	4,783,423	1207	Daily T, RH	1964
				Hourly Met	1981
<i>076_stm</i>	520,367	4,783,418	1207	Soil T	1981
				Soil Moisture	1981
<i>057_ppt</i>	521,390	4,786,033	1188	Precip.	1962

⁴ UTM zone 11, North American Datum 1927.

elevation (1718 m) of the watershed, but half way between the low (*076_met*) and high elevation (*176_met*) sites. Site *127_met* vegetation is low sagebrush, with some bare ground, which is representative of mid-elevation vegetation on the eastern side of the RCEW. On the western side there is less bare ground, more of a mix of Wyoming Big Mountain and low sagebrush with some Juniper encroachment. Annual average wind-corrected precipitation is 350 mm, temperature is 8.8°C, with an average daily max of 12.2°C and a min of 3.9°C, wind speed is 3.4 m s⁻¹ (1984-2006), growing season pan evaporation was 1082 mm (1964-2001), and dew point temperature is -2.5°C (1984-2006).

The high elevation meteorological site (*176_met*, also referred to as “Reynolds Mountain East” or *RME*) is located in a headwater catchment on the southern rim of the RCEW (see **Figure 3.1**). This is an exposed area where the few trees and larger shrubs in and around the site offer only limited protection from the wind. Precipitation (*176_ppt*) measurement is co-located at this site, but is also measured in a wind-sheltered clearing in an Aspen grove 300 m to the northeast and 36 m below (site *176e_ppt*, 2061 m). Soil temperature and moisture (*176_stm*) measurements are co-located at this site. At an elevation of 2093 m, it is located 150 m below the peak elevation (2242 m) of the watershed on the southern rim of the RCEW. Site *176_met* vegetation is not as uniform as *076_met* and *127_met*, but is a mix of Wyoming Big Mountain and low sagebrush, with a few shrub stands of Bitter Brush and Mountain Mahogany. Adjacent to the site are Douglas fir and a few Aspen trees. This heterogeneous mix of vegetation is characteristic of higher elevations within southeastern regions of the RCEW. Further to the west along the high rim are more extensive stands of fir and aspen. Annual average

wind-corrected precipitation is 795 mm at the wind-exposed site *176_ppt*, and 996 mm at the sheltered site *176e_ppt*. Annual average temperature is 5.1°C, with an average daily max of 8.9°C and a min of 0.9°C, wind speed is 4.2 m s⁻¹ (1983-2006), growing season pan evaporation was 795 mm (1964-2001), and dew point temperature is -3.6°C (1983-2006).

2.2. Precipitation Measurement Sites

Of the 26 active precipitation measurement sites in the RCEW, data from 11 of the 12 long term sites listed in **Table 3.1** were selected for this study. These sites were selected because they had a long period of record (45+ water years) and represented a range of elevations, site and wind exposure conditions. Data from site *176_ppt* was omitted from this part of the analysis because it had a shorter record (1968-2006, 38 water years) and because of its close proximity to site *176e_ppt*. Because much of the precipitation across the RCEW falls as snow, a significant wind-induced under-catch occurs. Wind correction of the recorded gauge catch is critical. Each precipitation measurement site consists of a pair of 30.48 cm (12 inch) orifice (orifice height is 3 m), weighing-recording gauges, one unshielded, and the other with an Alter-type wind shield, baffles individually constrained at 30° from vertical. This system supports the dual-gauge wind correction technique developed by Hamon (1973) (see also Hanson et al. 1999). The dual gauge method uses the ratio of shielded to unshielded catch as an indication of wind-induced under-catch. The method was evaluated as part of the WMO solid precipitation measurement experiment (Yang et al. 1999, 2001; Hanson et al. 1999, 2004), and was found to be comparable to the standard WMO wind correction, and to

reliably reproduce reference values based on the Wyoming shield over a wide range of wind, temperature and precipitation intensity conditions.

Though wind is currently measured at all precipitation measurement sites in the RCEW, this was not the case until recently. Because the dual-gauge method is based on the ratio of shielded to unshielded gauge catch, it allows wind correction of recorded gauge catch without wind data. Therefore because wind data are not available at the precipitation measurement sites for most of the period of record, application of the dual-gauge wind correction method is critical to the analysis presented here. Shielded and unshielded data from the period of record for all 12 sites were processed, integrated to an hourly time-step, and noise and discontinuities removed using a utility presented in Chapter 2 and then dual gauge wind corrections were performed using the Dual Gauge Wind Correction Program as described in Appendix B. Only wind-corrected values were used in the analysis presented in this paper.

2.3. Snow Measurement Sites

Seven bi-weekly snow courses have been operated at the RCEW since the early 1960's, with one additional added in 1970. These represent the upper 25% of the RCEW with a range of elevations from 1743 – 2162 m (**Table 3.1**). Only during cold, wet years does a continuous seasonal snowcover develop in the upper 50% of the RCEW (elevations above 1500 m) and hardly ever below that level. All sites are classical snow courses, with a fixed number of samples along a pre-determined track. Samples of depth and mass are taken with a Rosen Sampler, which tends to show improved sampling when compared to the Standard Federal Sampler (see Marks et al. 2001a). Twelve depth and

mass samples are taken at each snow course. Prior to 1970, samples were sporadic and did not always occur at two-week intervals, but after that care was taken to insure that the bi-weekly interval was maintained between December 1 and May 15. Depending on snow conditions, samples may be taken prior to December 1 and/or after May 15. If the ground is bare during a sample visit, zero values are recorded. All sites have been carefully maintained over the period of record to avoid the effects of site disturbance, vegetation removal or overgrowth.

A snow pillow has been maintained at a site just adjacent to the snow course *176e_sc*, and next to the precipitation measurement site *176e_ppt* since 1982. This site is a wind-protected clearing in an Aspen grove, similar to NRCS Snotel sites across the western U.S. (Serreze et al. 1999). The snow pillow is a 3 m diameter butyl-rubber device filled with a mix of anti-freeze, alcohol and water for measuring snowcover mass with a pair of pressure transducers. Hourly data on depth of SWE are recorded.

2.4. Soil Temperature and Moisture Measurement Sites

Data from four soil temperature and moisture measurement sites over range in elevation from 1207 – 2098 m were selected for analysis (**Table 3.1**). Data from these sites begin in the early 1980's, include sub-daily or hourly soil temperature from multiple depths, and bi-weekly neutron probe data from a tube located just adjacent to the temperature measurement site. Soil temperature was measured with thermistors and logged hourly at each site at multiple depths (Seyfried et al. 2001a). We analyzed data collected at a depth of 10cm to reflect soil-freezing conditions. Soil water content measurements were made every two weeks for most of the time period using the neutron

moderation method as described by Seyfried et al. (2001b). Individual depth increment measurements were combined to produce root zone water content estimates (Seyfried et al. 2001c).

2.5. Streamflow Measurement Sites

Of the 9 active weirs within the RCEW, data from three were selected for location and the availability of hourly streamflow records that begin in the early to mid-1960's (Pierson et al. 2001). These weirs include the *Reynolds Mtn. East* weir (*166_sf*), which drains the 0.38 km² headwater catchment, the *Tollgate* weir (*116_sf*) which drains the 55 km² *Tollgate* sub-basin, and the *Outlet* weir (*036_sf*), which drains the 238 km² RCEW basin (**Table 3.2**).

Table 3.2: Long-term Streamflow Measurement Sites at the RCEW

Site ID	Location		Elevation (m)	Records Begin	Area (km ²)	Elevation Range, m	Mean WY Streamflow
	Easting (m)	Northing (m)					
<i>166_sf</i>	519,952	4,768,494	2024	1963	0.38	2024-2139	6.7 ls ⁻¹
<i>116_sf</i>	519,392	4,776,492	1404	1966	54.7	1398-2244	0.424 m ³ s ⁻¹
<i>036_sf</i>	520,109	4,789,673	1099	1963	238.2	1099-2244	0.560 m ³ s ⁻¹

3. Data Presentation and Trend Analysis

In this section data from the Reynolds Creek Experimental Watershed are presented and analyzed for trends over the period of record. First temperature data from the three meteorological measurement sites are presented, followed by precipitation. These are followed by presentation of analyses of trends in precipitation phase, snow, soil moisture and temperature, and finally streamflow. To capture the annual hydrologic cycle, which begins in fall and ends in summer, annual trend analysis was conducted over

water year (WY) intervals (October – September). For seasonal analysis, the water year is divided into four seasons, fall (Oct – Dec), winter (Jan – Mar), spring (Apr – Jun), and summer (Jul – Sep).

3.1. The Statistical Significance Test

The significance of temporal trends present in the hydro-climatic observations is evaluated using the Mann-Kendall statistic (Hirsh and Slack 1984; Lettenmaier et al. 1994; Yue et al. 2002). The null hypothesis, H_0 , is that the variables are independent and randomly distributed. The test statistic is:

$$S = \sum_{i=1}^{n-1} \sum_{j=i+1}^n \text{sgn}(X_j - X_i)$$

where $\text{sgn}(X)$ can be +1, 0 or -1 depending on whether X is greater than, equal to or less than zero, respectively. In the absence of ties, the variance of S is calculated as:

$$\text{Var}[S] = \frac{n(n-1)(2n+5)}{18}$$

and the test statistic computed as:

$$Z = \frac{S - \text{sgn}(S)}{\sqrt{\text{Var}[S]}}$$

It is assumed that statistically significant trends are present if $|Z| > Z_{1-\alpha}$, at a selected significance level, α . In this study, trends were tested for significance at $\alpha = 0.10$

and 0.05 (90 & 95% confidence levels). The value of statistic $Z_{1-\alpha}$ can be found in standard normal distribution statistical tables.

We test the temporal stationarity of runoff by comparing three aspects of precipitation – runoff relationships at nested watersheds; threshold to runoff, runoff response rate and prediction interval of the relationship. The linear regression constants and statistics are calculated matrix linear regression using SimaStat (Systat Software, Point Richmond, CA).

3.2. Air Temperature

A systematic increase in temperature over the period 1965 – 2006 is indicated at all three elevations for annual average daily minimum and maximum temperatures, though the extent of change depends on elevation (**Figure 3.2**). Water year minimum daily temperatures increase about 30% more than maximum daily temperatures, and temperature trends at low elevations (*076_met*) are 50 – 60% that at mid- and high elevations (*127_met*, *176_met*). The greatest increase in annual average daily minimum temperature ($0.55 \pm 0.69^{\circ}\text{C}$ per decade) is found at the mid elevation site (**Table 3.3**).

As with water year trends, all seasons show warming, and minimum temperatures increase the most (**Tables 3.3b –e**). At low elevation (*076_met*), winter and spring increases in minimum daily temperature show strong trends that are significant at the 95% level, and both summer minimum and maximum daily temperature increases show strong trends that are significant at the 95% level. However, fall minimum and maximum daily temperature and winter and spring maximum daily temperature increases show weak trends that are not significant at the 90% level.

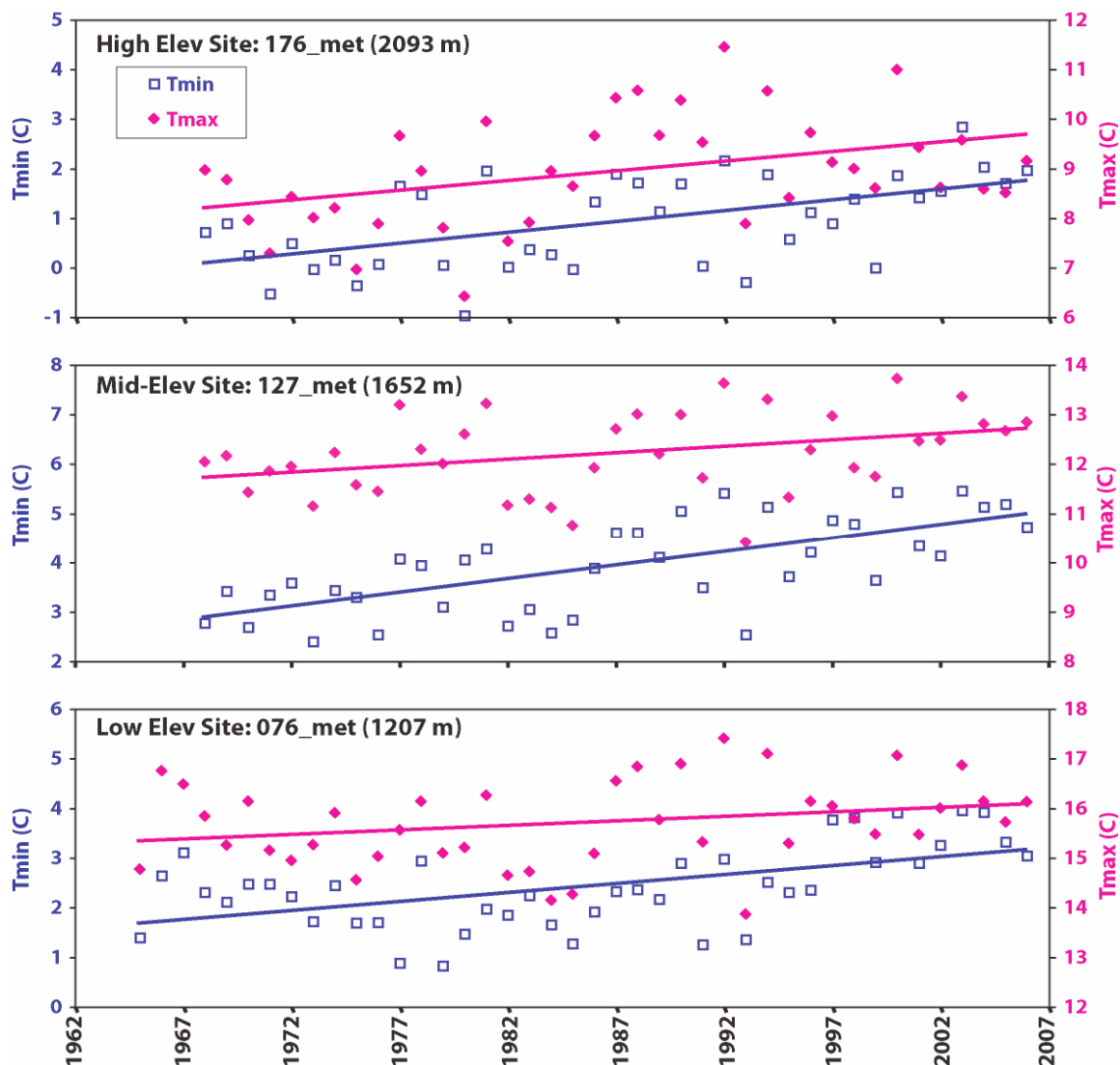


Figure 3.2: Water year maximum and minimum temperatures for high (Site *176_met*, 2093 m), mid- (Site *127_met*, 1652 m), and low elevation (Site *076_met*, 1207 m) meteorological sites. Pink diamonds shows maximum and blue squares shows minimum temperature. Trend lines are indicated for each site, showing an increase in both minimum and maximum temperature at all sites.

At mid-elevation (*127_met*) the increase in minimum daily temperature is large and shows a strong trend in all seasons (significant at the 95% level). The only significant change (at the 90% level) in seasonal maximum daily temperature at site

Table 3.3: Trends (in °C per decade) in maximum and minimum temperature based on least square linear fitting and Mann-Kendall test. Bold numbers indicate significance level greater than 90%; Blue, bold-Italic numbers, significance level greater than 95%. Critical shifts⁵ caused by trends are highlighted in yellow.

340Annual (Water Year) Trends						
Site ID	T _{min} I			T _{max} I		
	Mean	SD	Trend ± SE	Mean	SD	Trend ± SE
<i>176_met</i>	0.9	0.9	0.44 ± 0.78	8.9	1.1	0.39 ± 1.04
<i>127_met</i>	3.9	0.9	0.55 ± 0.69	12.2	0.8	0.26 ± 0.76
<i>076_met</i>	2.4	0.8	0.36 ± 0.71	15.7	0.9	0.18 ± 0.84
b) Fall (Oct – Dec) Trends						
<i>176_met</i>	-2.9	1.3	0.30 ± 1.29	3.8	1.6	0.43 ± 1.50
<i>127_met</i>	-0.2	1.4	0.41 ± 1.34	6.5	1.5	0.28 ± 1.48
<i>076_met</i>	-2.1	1.4	0.19 ± 1.41	9.4	1.4	0.00 ± 1.46
c) Winter (Jan – Mar) Trends						
<i>176_met</i>	-5.8	1.6	0.42 ± 1.55	0.3	1.7	0.51 ± 1.65
<i>127_met</i>	-3	1.4	0.43 ± 1.34	3.4	1.3	0.33 ± 1.31
<i>076_met</i>	-3.6	1.5	0.38 ± 1.47	6.5	1.6	0.27 ± 1.54
d) Spring (Apr – Jun) Trends						
<i>176_met</i>	2.1	1.4	0.48 ± 1.28	11.1	1.8	0.26 ± 1.80
<i>127_met</i>	5.5	1.4	0.57 ± 1.30	15.1	1.5	0.10 ± 1.49
<i>076_met</i>	4.8	1	0.44 ± 0.87	19.3	1.5	0.16 ± 1.53
e) Summer (Jul – Aug) Trends						
<i>176_met</i>	10.2	1.3	0.55 ± 1.10	20.3	1.2	0.37 ± 1.13
<i>127_met</i>	13.2	1.4	0.80 ± 1.13	23.6	1.3	0.33 ± 1.24
<i>076_met</i>	10.4	1.2	0.43 ± 1.08	27.5	1.3	0.29 ± 1.25

127met is the increase during summer. At high elevation (*176_met*) the increase in minimum daily temperature is significant in all seasons, and the increase in maximum daily temperature is significant in all but spring. At site *176_met* trends in increasing daily maximum and minimum temperature are strongest during fall and winter. Whereas

⁵ Critical shifts are identified if temperature trends crosses freezing point (0 °C) during the period of record.

springtime minimum temperature show an increasing trend maximum daily temperature do not show a significant trend. Summer increases in both minimum and maximum temperature are significant (at 90% level) at site *176_met*.

3.3. Precipitation

Data presented in **Table 3.4** illustrate the complexity of precipitation patterns in mountain basins, and the limitations of attempting to establish a precipitation lapse rate over mountainous areas with limited precipitation data when attempting to estimate basin-wide precipitation. Though there is a general increase in water year total precipitation with elevation (869 mm km^{-1} , a basin-wide increase of nearly a 4x), discontinuities are evident. Sites on the wetter, western side of the RCEW (*163_ppt*, *174_ppt*, *144_ppt*, *155_ppt*, *116_ppt*) ranging in elevation from 1491 – 2170 m show a wind-corrected precipitation range of 474 – 1124 mm, and a precipitation lapse rate of 971 mm km^{-1} but only a 2.4x increase over the considered gauges, while those on the drier, rain-shadowed eastern side (*167_ppt*, *147_ppt*, *127_ppt*, *076_ppt*, *057_ppt*) ranging in elevation from 1188 – 2003 m show a range of 239 – 806 mm, with a smaller lapse rate of 696 mm km^{-1} , but a larger 3.4x increase over the considered gauges (**Table 3.4**).

Water year precipitation data are subject to considerable interannual variability, as evidenced by the high standard deviations in the annual mean (**Table 3.4**) and the only significant temporal trend in water year precipitation data is a decrease at site *144_ppt* ($-45 \text{ mm/decade} \pm 220$) which is attributed to logging in the late 1990's. Seasonal precipitation data and trend analysis are presented for 3 of the eleven measurement sites, representing high elevation (*176e_ppt*), mid-elevation (*127_ppt*) and low elevation

Table 3.4: Annual and seasonal precipitation for the period 1963-2006.

Gauge ID	Elevation (m)	Annual		Fall		Winter		Spring		Summer	
		Mean (mm)	SD (mm)	Mean (%)	SD (%)	Mean (%)	SD (%)	Mean (%)	SD (%)	Mean (%)	SD (%)
<i>163_ppt</i>	2170	1124	263	32.88	9.09	38.88	7.72	21.94	7.00	6.31	3.70
<i>174_ppt</i>	2074	967	230	32.43	8.96	38.18	7.86	22.47	7.18	6.91	3.91
<i>176e_ppt</i>	2056	996	270	33.17	9.50	39.31	8.78	21.01	7.29	6.51	3.47
<i>167_ppt</i>	2003	806	213	32.58	9.94	37.74	9.18	22.30	8.09	7.38	3.99
<i>147_ppt</i>	1872	518	148	32.86	8.69	36.54	8.13	23.27	7.64	7.34	4.38
<i>144_ppt</i>	1815	881	226	32.60	9.39	36.03	8.78	23.17	7.94	8.19	4.73
<i>155_ppt</i>	1654	704	193	30.95	9.67	31.89	8.23	27.50	9.77	9.65	5.55
<i>127_ppt</i>	1652	351	98	28.37	9.65	29.42	8.33	31.13	10.69	11.08	5.45
<i>116_ppt</i>	1459	474	129	31.34	9.29	32.57	8.38	27.13	8.94	8.97	4.82
<i>076_ppt</i>	1207	279	77	28.74	9.47	29.62	9.80	30.08	11.49	11.57	7.22
<i>057_ppt</i>	1188	239	68	27.19	9.82	27.36	9.71	32.12	12.27	13.32	8.28

(076_ppt) showing the range of precipitation over the RCEW (**Figure 3.3**). The data indicate no significant trends during fall or winter, and only one site (174_ppt) has an increasing trend (significant at the 90% level) in spring.

3.4. Snowfall

At RCEW 60 – 75% of the water year precipitation occurs during fall and winter, regardless of elevation. Historically most of that precipitation has fallen as snow, melted during spring, and provided water for streamflow during spring and summer. The rain/snow proportions of water year precipitation are critical to the timing of streamflow in the RCEW.

Hanson (2001) reported that, in the RCEW, the proportion of snowfall in the annual precipitation total varied from around 20% at the lowest elevations to more than 75% at the highest. This was a monthly estimate based on the *ad hoc* assumption by Cooley et al. (1988) that precipitation in any month in which the mean temperature was $\leq 1^{\circ}\text{C}$ would be considered snow. Similar air-temperature based methods have been used by many investigations (e.g. Hanson et al. 1979; Lapp et al. 2005; Hamlet et al. 2005), but the temperature thresholds used are variable and seem to be site and season dependent. Knowles et al. (2006) used increased snow depth as an indicator of snowfall, but these data are also limited, particularly during storms.

Actual observations of precipitation phase are rare, but since 2001 phase determination has been available at many of the precipitation sites within the RCEW. The approach is based on concurrent measurement of precipitation, snow depth and dew point temperature during precipitation events. Olsen (2003) recommends wet-bulb

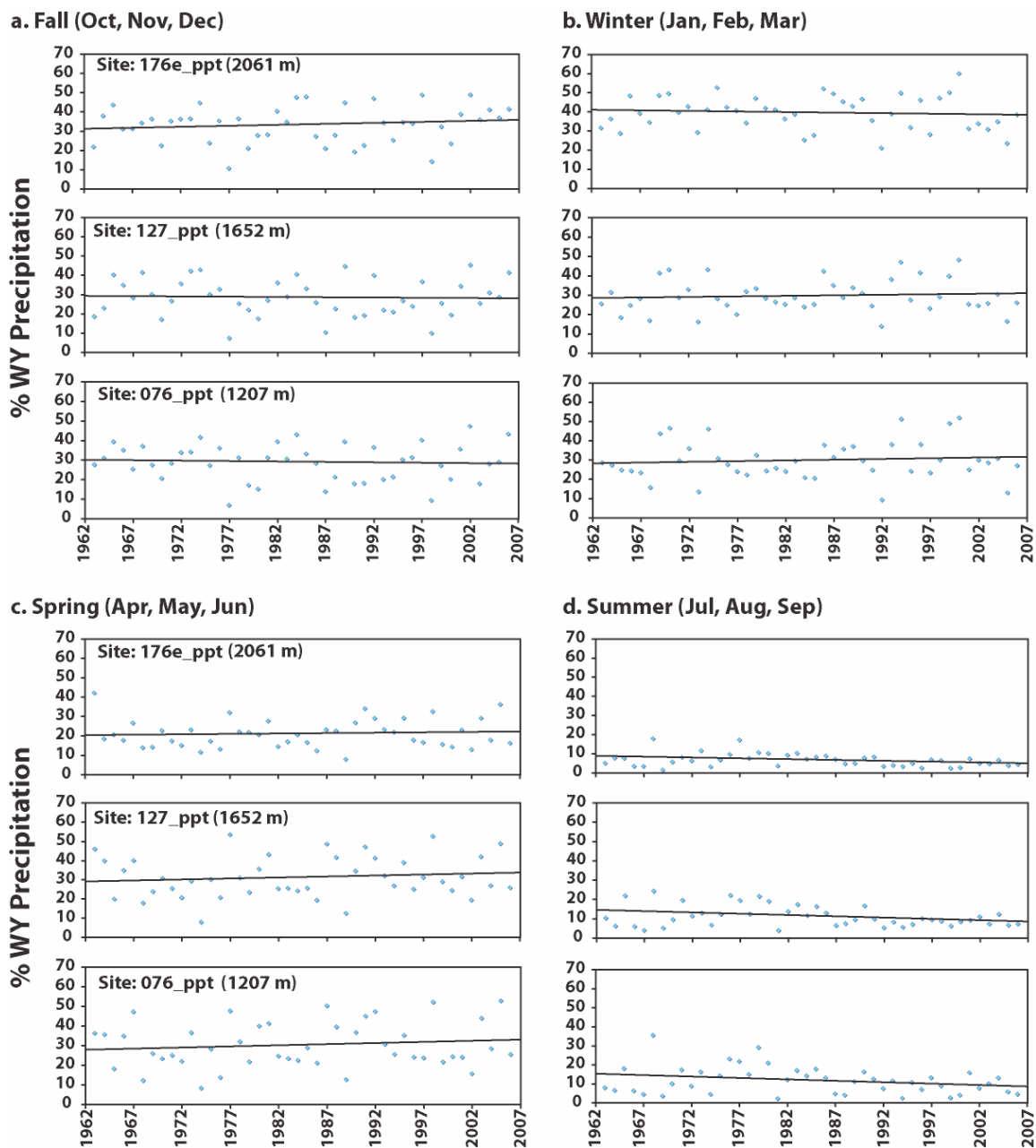


Figure 3.3: Seasonal precipitation as percentage of total water year (WY) precipitation at the high, mid- and low elevation measurement sites. Trend lines are indicated for each over the period of record.

Temperature as a determinate of air mass potential for rain or snow, but suggests near-surface dew point temperature as the most reliable predictor of precipitation phase for a specific location. This approach has been used reliably for analysis of rain-on-snow events (Marks et al. 1998, 2001b), and for time-series simulations of the seasonal snowcover at a variety of scales and a number of locations across the western U.S. (Marks et al. 1999, 2001b, 2002; Marks and Winstral 2001; Garen and Marks 2005). If the dew point temperature is above 0°C, precipitation is assumed to be rain, if it is <0°C, snow, and if close to 0°C, mixed rain and snow. A detailed discussion of the use of dew point temperature to determine precipitation phase using 2004-2006 transect data from the RCEW is presented by Marks and Winstral (2008).

For the analysis presented here, concurrent measurements of humidity (dew point temperature) and precipitation were available from the three long-term meteorological sites back to the early 1980's, so dew point temperature is known for every storm from then to the present. Daily maximum and minimum temperature data were used to estimate storm dew point temperatures for the early part of the RCEW data record. Hourly temperature estimates for the pre-hourly data period were simulated for the three long-term met stations (*176_met*, *127_met*, *076_met*). A sinusoidal diurnal cycle between maximum and minimum temperature with a temperature maximum offset from noon was derived for each month from the 1986 – 1995 hourly temperature data. These monthly cycles were then used to derive hourly temperatures for the early period of record. Monthly storm-period (events > 1 mm) dew point temperature deficit ($T_a - T_{dpt}$) was estimated from the 1986 – 1995 hourly temperature and humidity data. These were then used to estimate storm dew point temperatures for the 1962-1982 portion of the

RCEW precipitation data set. Because it best matched recent observations, and to avoid the “mixed phase” issue, it was assumed that if the dew point temperature was $\leq 0^{\circ}\text{C}$, the precipitation fell as snow.

Figure 3.4 presents snow as a fraction of total water year precipitation for the high (*176e_ppt*), mid- (*127_ppt*) and low (*076_ppt*) elevation sites. Site *176e_ppt* is snow-dominated, with a relatively constant mean water year value of nearly 70% snow over the period of record. Sites *127_ppt* *076_ppt* are rain-dominated, with mean water year values over the period of record of 40% and 30% snow, respectively. These values have changed 4-5% per decade over the period of record.

Temporal trend analysis for fall, winter and spring seasons clarifies that while snow is decreasing at all elevations, the strongest trends are at the lower elevations (**Table 3.5**). Snowfall shows a significant decreasing trend at the low elevation site (*076_ppt*) in all seasons. The mid-elevation site (*127_ppt*) shows significant decreasing trends only in fall and spring. The only significant seasonal trend for the high elevation site (*176e_ppt*) is a decrease in snow during fall. During winter, the percentage snow at both the high and mid-elevation sites are relatively unchanged.

3.5. Snow Measurements

Data from the RCEW bi-weekly snow courses listed in **Table 3.1** from 1964 – 2006 (43 water years) snow seasons were analyzed for temporal trends in mean April 1 and May 1 SWE (**Table 3.6**) and timing and depth of peak SWE (**Table 3.7**). All snow courses show a decreasing trend in both April 1 and May 1 SWE. The least significant

trends occur at the highest elevation courses, and the most significant at the low elevation courses. Note that the very large decreasing trend at snow course *144_sc* is likely due to

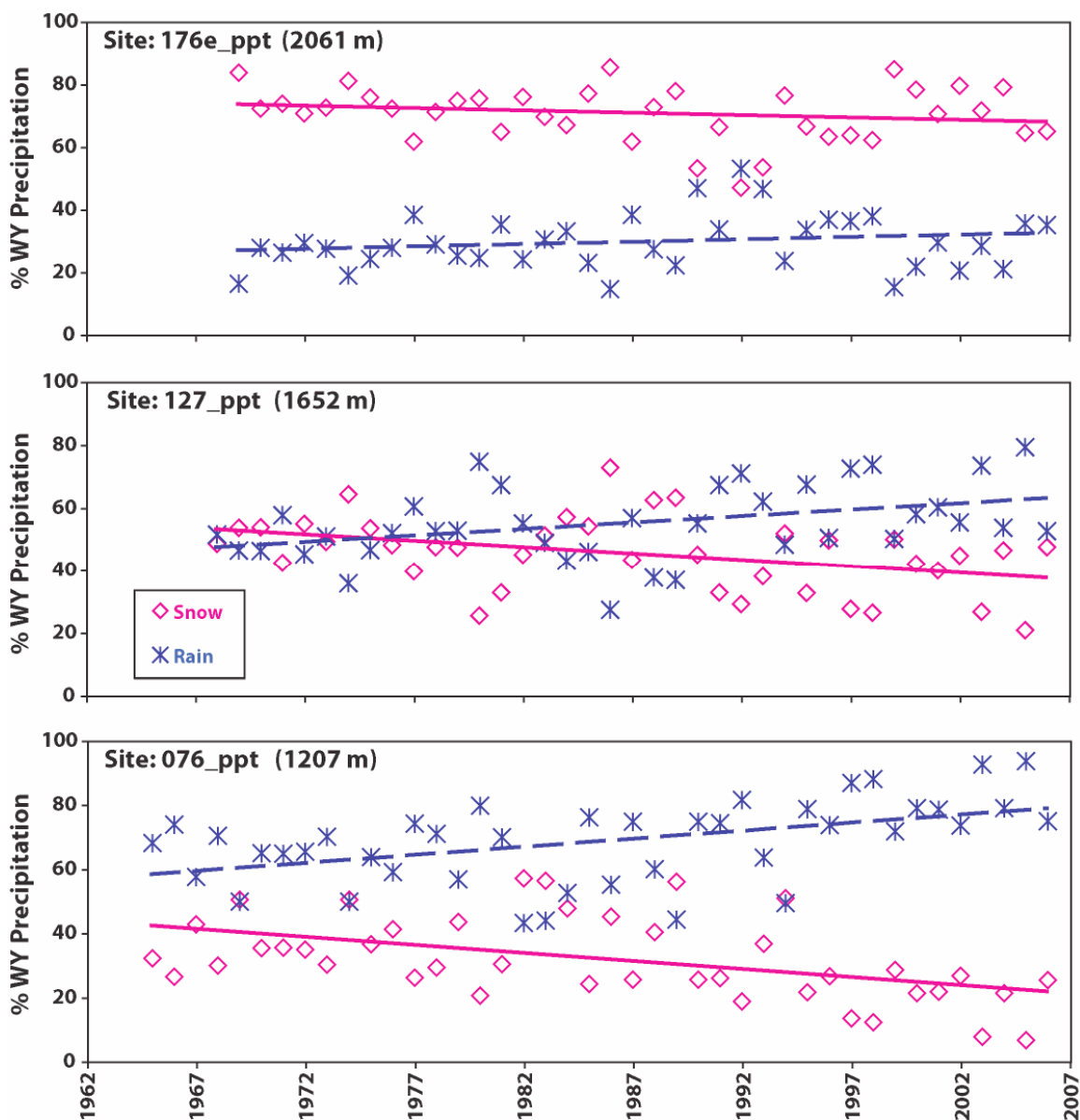


Figure 3.4: Rain and snow fraction (percentage) of water year total precipitation at high (*176e_ppt*), mid- (*127_ppt*) and low (*076_ppt*) elevation measurement sites. Pink diamonds show snow, blue stars show rain. Trend lines indicated for each over the period of record showing a decrease in snow and an increase in rain at all elevations.

Table 3.5: Trends (in % per decade) in fraction (%) of precipitation falling as snow. Blue, bold-italic numbers: significance level greater than 95%. Critical shifts⁶ caused by trends are highlighted in yellow.

a) Annual				
Site				
Identification	Mean (%)	SD (%)	Trend \pm SE	
<i>176e_ppt</i>	67.4	10.3	<i>-1.52 \pm 8.65</i>	
<i>127_ppt</i>	45.1	10.8	<i>-4.10 \pm 10.97</i>	
<i>076_ppt</i>	31.7	10.5	<i>-5.02 \pm 11.49</i>	
b) Fall				
<i>176e_ppt</i>	83.5	13.2	<i>-7.41 \pm 10.40</i>	
<i>127_ppt</i>	56.1	16.2	<i>-5.85 \pm 15.97</i>	
<i>076_ppt</i>	41.6	17.4	<i>-7.56 \pm 14.96</i>	
c) Winter				
<i>176e_ppt</i>	87.3	11.6	<i>-1.00 \pm 11.69</i>	
<i>127_ppt</i>	67.7	17.2	<i>-0.38 \pm 17.38</i>	
<i>076_ppt</i>	53.3	20.7	<i>-7.37 \pm 18.84</i>	
d) Spring				
<i>176e_ppt</i>	42.1	16.4	<i>-1.16 \pm 16.54</i>	
<i>127_ppt</i>	24.3	15.1	<i>-3.40 \pm 14.74</i>	
<i>076_ppt</i>	14.8	13.8	<i>-2.56 \pm 13.57</i>	

deforestation that occurred at the site in the mid-1990's. This affects the decreasing trend in depth of SWE, making it larger than it expected, but should not affect trends toward earlier timing of peak SWE (**Table 3.6**). Example trends for May 1 SWE are presented for high elevation (*163c_sc*, 2125 m), mid-elevation (*176_sc*, 2056 m) and low (*155_sc*, 1743 m) elevation snow courses.

⁶ Critical shifts are identified if annual of seasonal precipitation regime changes from snow dominated to rain dominated during the period of records.

Table 3.6: Trends (in mm per decade) in April 1 and May 1 SWE based on least square linear fitting and Mann-Kendall test for the water year period 1964-2006. Bold numbers indicate significance level greater than 90%; Blue, bold-italic numbers a significance level greater than 95%. The large, significant trend at *144_sc* caused by site modification (deforestation) is highlighted in yellow.

Site ID	1-Apr			1-May		
	Mean (mm)	SD (mm)	Trend \pm SE	Mean (mm)	SD (mm)	Trend \pm SE
<i>163_sc</i>	701.3	200.4	-22.1 \pm 201.8	686.2	241.1	-18.8 \pm 243.6
<i>163b_sc</i>	640.3	209.7	-35.6 \pm 209.1	501.8	288.2	-57.2 \pm 285.5
<i>163c_sc</i>	662.9	218.5	-32.2 \pm 218.8	532.8	289.4	-53.6 \pm 287.5
<i>174_sc</i>	636.5	210.5	-44.0 \pm 208.0	490.6	283.7	-70.5 \pm 277.2
<i>176_sc</i>	542.1	202.5	-53.5 \pm 196.8	377.4	266.1	-92.8 \pm 249.9
<i>144_sc</i>	205.3	162.6	-97.1 \pm 125.9	42.4	112.2	-34.9 \pm 107.2
<i>155_sc</i>	162.6	116.8	-32.2 \pm 113.1	13.4	54.8	-12.7 \pm 53.7

May 1 trends are strongest at the high and mid-elevation courses, while at the low elevation course (*155_sc*), no snow has been measured on May 1 since 1984 and therefore the decreasing trend is weak (**Figure 3.5**). At this elevation, melt now occurs primarily in March and the April 1 trend is relatively strong (**Table 3.6**).

All snow courses indicate a trend toward earlier peak SWE and less depth of SWE at peak (**Table 3.7**). Low elevation courses (*144_sc*, 1815 m; *155_sc*, 1743 m) show the strongest trend toward earlier peak SWE, with a shift of 7 – 10 days earlier per decade, or 28 – 40 days earlier over the period of record. Mid- to low elevation courses (*174_sc*, 2073 m; *176_sc*, 2056 m; *144_sc*, 1815 m) show the strongest trend in reduced depth of peak SWE, with a shift of 50 – 85 mm less per decade. The lowest elevation course (*155_sc*, 1743 m) shows a similar trend in depth of peak SWE, but it is not significant at

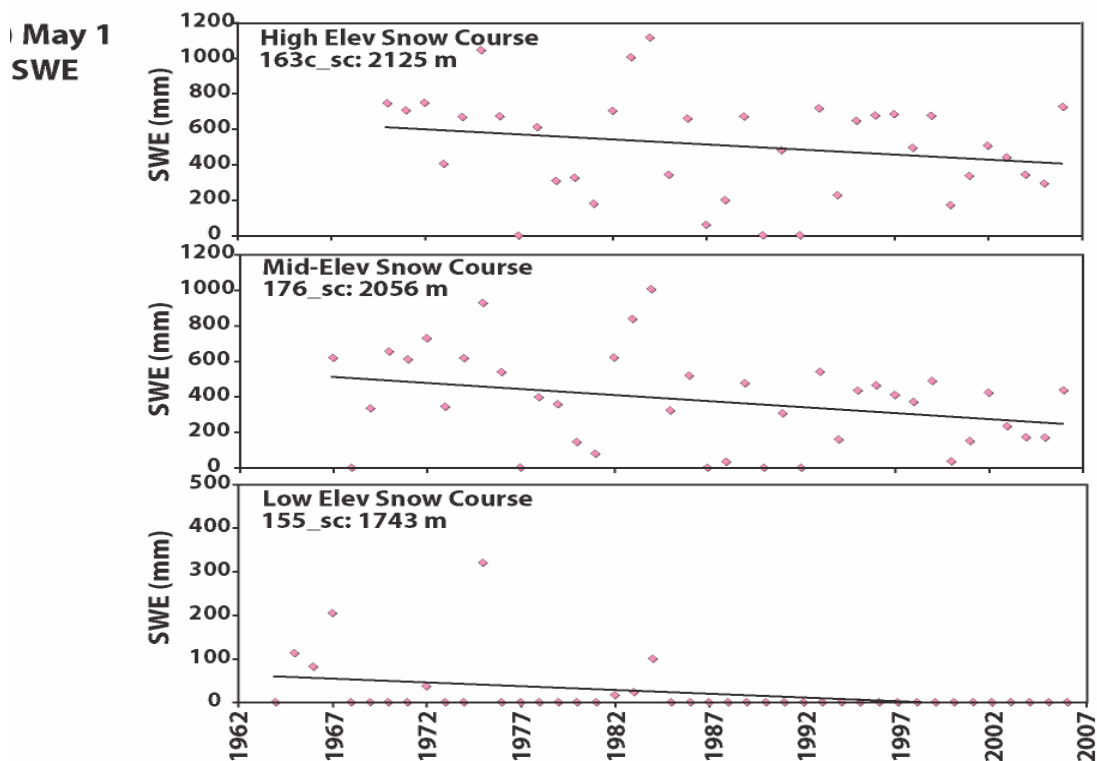


Figure 3.5: May 1st SWE (mm) for high elevation (*163c_sc*, 2125 m), mid-elevation (*176_sc*, 2056 m) and low elevation (*155_sc*, 1743 m) snow courses. Trend lines are indicated for period of record showing a consistent decrease at all elevations, with a strong decrease at the low elevation snow course (*155_sc*) in both months.

The 90% level. High elevation courses (*163_sc*, 2162 m; *163b_sc*, 2147 m; *163c_sc*, 2125 m) show similar trends in both timing and depth of peak SWE, but these are not significant at the 90% level.

The snow pillow (site *176_sp*) results support the observed trends at the nearby snow course, (*176_sc*), and provide supplemental information about the timing of snowpack initiation and melt out. Since 1983 at *176sc* and *176sp*, mean dates of peak SWE were March 31 and March 29, depths of peak SWE were 573 mm 564 mm, and the

Table 3.7: Trends in timing (days per decade) and depth (mm per decade) of peak SWE accumulation based on least square linear fitting and Mann-Kendall test for water year period 1964-2006. Bold numbers indicate a significance level greater than 90%; Blue, bold-italic numbers a significance level greater than 95%.

Site ID	Timing of Peak SWE			Depth of Peak SWE (mm)		
	Mean Date	SD (days)	Trend \pm SE	Mean (mm)	SD (mm)	Trend \pm SE
<i>163_sc</i>	15-Apr	15	-1.3 \pm 15.1	757	211	-18.3 \pm 214
<i>163b_sc</i>	7-Apr	15	-2.2 \pm 15.1	681	222	-37 \pm 225
<i>163c_sc</i>	7-Apr	16	-1.6 \pm 16.2	695	225	-31.8 \pm 228
<i>174_sc</i>	6-Apr	15	-1.8 \pm 15.6	665	218	-50.8 \pm 220
<i>176_sc</i>	31-Mar	15	-3.1 \pm 15.2	573	210	-55.6 \pm 212
<i>144_sc</i>	11-Mar	24	<i>-10.2 \pm 23.9</i>	272	147	-84 \pm 143
<i>155_sc</i>	28-Feb	21	<i>-6.8 \pm 21.4</i>	254	99	-8.5 \pm 100

trends toward earlier peak SWE were -3.1 and -2.5 days per decade, respectively. Over the period from 1983 -2006, the date of snow cover initiation at *176sp* is delayed by 7.8 (\pm 13.7) days per decade (significant at the 95% level). Trends are indicated toward earlier melt-out (3.5 days per decade), and a reduced depth of peak SWE (-82 mm per decade), but these are not significant at the 90% level. The date of snow pillow peak SWE appears to be only slightly earlier (2.5 days per decade) over the period of record.

3.6. Soil Freezing

The presence of frozen soil has a significant hydrologic impact by reducing or eliminating infiltration, which may increase surface runoff, erosion and the potential for flooding, and a biological impact by holding surface soil moisture in place during winter, reducing deep drainage and evaporative losses and allowing the growing season to begin (Seyfried et al. 1990; Seyfried and Flerchinger 1994; Seyfried and Murdock 1997; Shanley and Chalmers 1999; Gray et al. 2001). To evaluate changes in soil freezing, data

from three of the four soil temperature measurement sites listed in **Table 3.1** – *127_stm* (1652 m), *098_stm* (1259 m) and *076_stm* (1207 m) – were used to determine the number of days with frozen soil in each year of record. Data from the high elevation site *176_stm* (2097 m) were not used because the length of record is much shorter (14 water years) than at the other sites. A soil *freeze day* was defined as a day when the noon soil temperature at 10 cm was at or below freezing.

Table 3.8 and **Figure 3.6** present the number of *soil freeze days* at the mid- (*127_stm*, 1652 m), low slope (*098_stm*, 1259 m) and valley-bottom (*076_stm*, 1207 m) sites. Only hourly, recorded soil temperature data were used, so the data record was limited to 1986 – 2006, 21 water years.

To take advantage of new technology, new profiles were installed in 1990 at the *098_stm* and *127_stm* sites, and in 1994 at the *076_stm* site. Seyfried et al. (2001a) presents details of data recording and soil temperature instrumentation at the RCEW. Dates of profile changes are indicated on **Figure 3.6**. All three sites show strong trends toward fewer *freeze days*. However, **Figure 3.6** indicates a sharp discontinuity associated with the 1994 profile change at site *076_stm*, leaving the trend analysis in doubt for the valley-bottom site.

Table 3.8: Trends (in number of days per decade) in soil *freeze days* at mid-elevation, low slope, and valley-bottom sites. Bold numbers indicate significance level greater than 90%; Blue, bold-italic numbers significance level greater than 95%.

Site ID	Mean (days)	SD (days)	Trend \pm SE
<i>127_stm</i>	48.1	26.2	<i>-25.5 \pm 21.4</i>
<i>098_stm</i>	51.7	21.3	<i>-13.0 \pm 20.3</i>
<i>076_stm</i>	46.9	31.1	<i>-33.1 \pm 23.9</i>

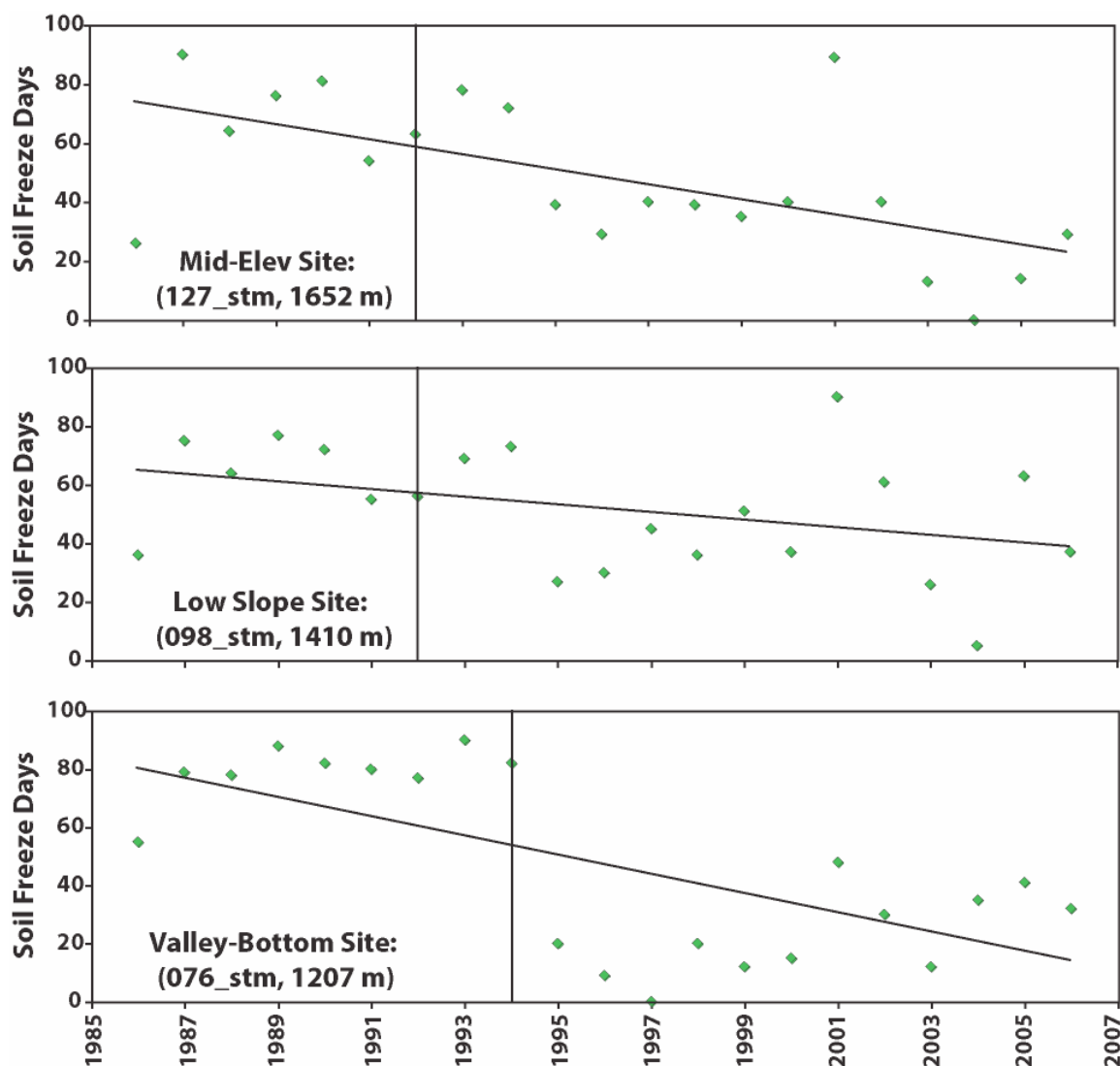


Figure 3.6: Number of *soil freeze* days for mid-elevation (*127_stm*, 1652 m), low slope (*098_stm*, 1410 m) and valley-bottom (*076_stm*, 1207 m) sites. Vertical line shows the timing of temperature profile change. Note the discontinuity after the instrument change at the valley-bottom site (*076_stm*). Trend lines are indicated for each over the period of record showing a consistent decrease in the number of soil freeze days at all sites (though the trend at the valley-bottom site is clearly biased by the profile change discontinuity).

3.7. Plant Water Stress

As discussed by Seyfried et al. (2001c), within the RCEW soil water storage follows an annual cycle with its peak during late winter or early spring when spring rain

and snowmelt provide water to replenish soil water storage. During the growing season, evaporative demand greatly exceeds precipitation. Soil water storage declines rapidly due to plant-water extraction and evaporation until soil water storage reaches a stable minimum in late summer each year. This late summer soil water condition, with vegetation present but no apparent transpiration, is regarded as the limit of what the vegetation can extract from the soil.

To assess the potential impact of climate warming, reduced summer precipitation and earlier snowmelt on the *plant-water stress* experienced by the native vegetation, we estimated the length of time the vegetation was under water stress each year. In order to make comparisons across sites, which have different soils, we used a constant fraction (45%) of the average total plant-available soil water, which is defined as the difference between the annual maximum soil water storage and the summer minimum described above. This resulted in *plant-water stress* index values of 8 cm H₂O at high elevation site *176_stm*, 7 cm H₂O at mid-elevation site *127_stm* and 3.5 cm H₂O at low slope site *098_stm*. In the absence of summer precipitation, the earlier in the growing season the *plant-water stress* value is reached, the longer soils are dry and the native vegetation will have to persist under water-stress.

Table 3.9 presents the period of record (1977 – 2006, 30 water years) mean onset date of *plant-water stress*, along with associated trends for the high (*176_stm*), mid- (*127_stm*) and low slope (*098_stm*) soil measurement sites. Data from the valley-bottom site (*076_stm*) were not used for this analysis because reliable soil water data were not available until after 1987. The high elevation site (*176_stm*) shows a very strong trend (nearly 8 days per decade earlier) and the mid-elevation sites shows a strong trend (nearly

5 days per decade earlier) toward earlier onset of *plant-water stress*, indicating that the length of *plant-water stress* has been extended by 3 weeks or more at higher elevations within the RCEW over the period of record. The low slope site shows almost no change over the period of record.

Table 3.9: Trends (in days per decade) in timing of plant water stress for high (*176_stm*), mid- (*127_stm*) and low slope (*098_stm*) soil measurement sites for 1976 – 2006 (31 water years) period of record. Plant water stress is defined as 45% of average peak *plant-available water* or “field capacity” in the top meter of soil at each site. Blue, bold-italic numbers indicate significance level greater than 95%.

Site ID	Mean (date)	SD (days)	Trend \pm SE
<i>176_stm</i>	4-Jul	13.6	<i>-7.5 \pm 12.2</i>
<i>127_stm</i>	12-Jun	21.5	<i>-4.6 \pm 21.6</i>
<i>098_stm</i>	8-Jun	23.5	-1.0 \pm 24.1

3.8. Streamflow

Streamflow data from three weirs, Reynolds Mtn. East (RME), Tollgate (TG), and the RCEW basin outlet were analyzed by water year and by season over the 1964 – 2006 period of record. At all three weirs, most of the flow water year flow occurs from March – June. During these months, nearly 90% of streamflow occurs at the RME headwater weir (*166_sf*), 82% at the mid-elevation TG weir (*116_sf*) and 70% at the RCEW outlet weir (*036_sf*) (**Figure 3.7**). Due to the large interannual variability in precipitation, water year runoff volume variability is great, with standard deviations of at least 50% of the annual mean at all sites, and no significant temporal trends in annual runoff volume emerged for the period of record (**Table 3.10a**).

Trend analysis of monthly streamflow as a fraction of annual total indicates a shift to earlier flows at RME (*166_sf*) and TG (*116_sf*) weirs, with increases in March and

April and decreases in June flows (**Table 3.10**). Temporal trends at RCEW outlet (*036_sf*) weir are less conclusive, with an increase in May flows as the only significant change. Spring and summer diversions to irrigation below *116_sf* probably confound trend analysis at the RCEW outlet weir.

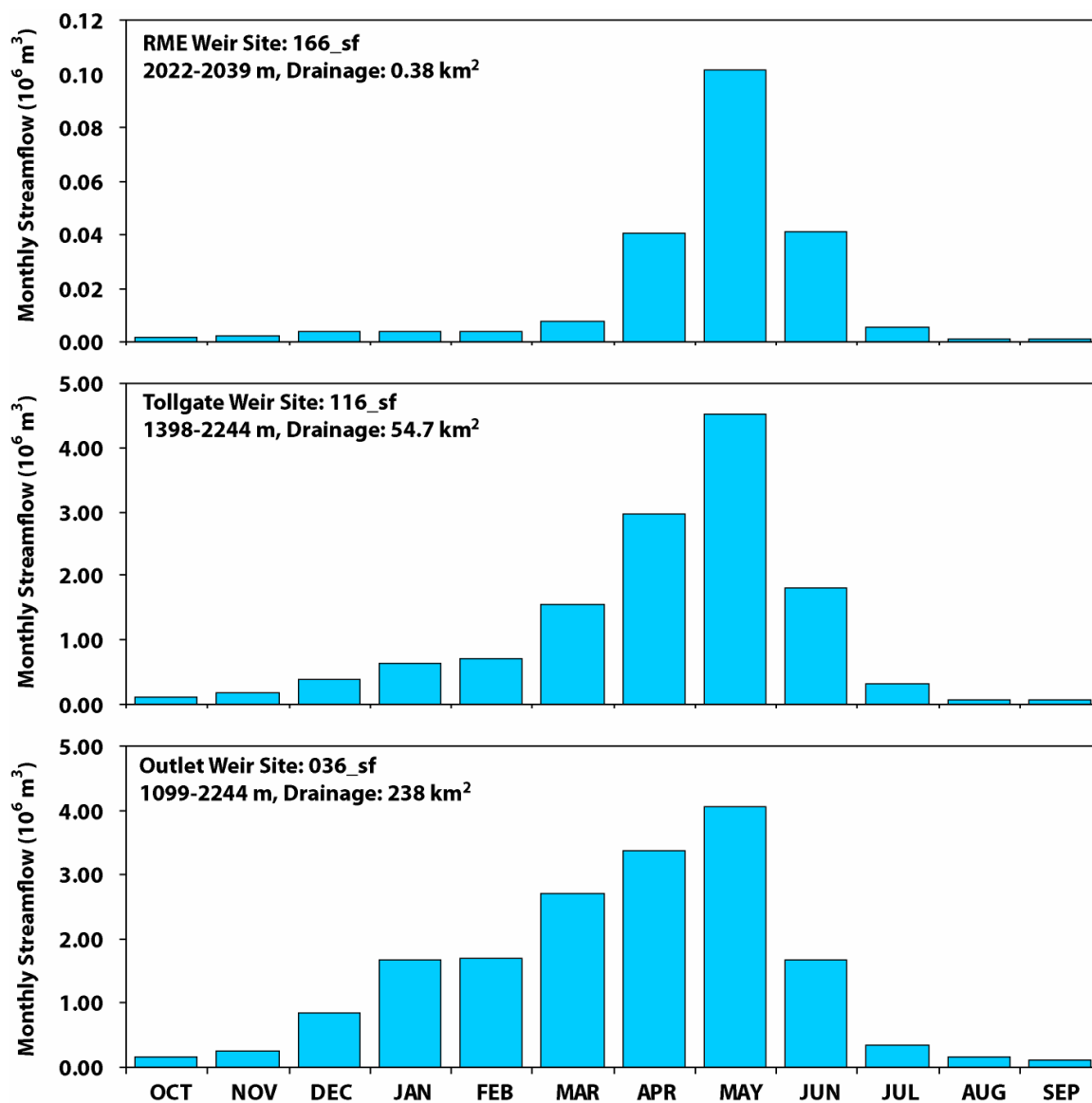


Figure 3.7: Average monthly streamflow at the RME headwater catchment weir (*166_sf*), the Tollgate mid-elevation weir (*116_sf*) and the RCEW outlet weir (*036_sf*).

Table 3.10: a) Trends (in 10^6 m^3 per decade) in streamflow ($10^6 \text{ m}^3 \text{ WY}^{-1}$) based on least square linear fitting and Mann-Kendall test for the period record. B-e) Trends (in % per decade) in monthly distribution of streamflow as % of total water year streamflow over the Mar – Jun for the period of record. Bold numbers indicate significance level greater than 90%; Blue, bold-Italic numbers a significance level greater than 95%.

341 Water Year			
Weir ID	Mean ($10^6 \text{ m}^3 \text{ WY}^{-1}$)	SD	Trend \pm SE
<i>166_sf</i>	0.21	0.10	-0.0005 \pm 0.1
<i>116_sf</i>	13.4	7.52	-0.066 \pm 7.6
<i>036_sf</i>	17.1	12.4	-0.175 \pm 12.3

b) March			
Weir ID	Mean (%)	SD	Trend \pm SE
<i>166_sf</i>	4.1	4.2	<i>0.4 \pm 4.2</i>
<i>116_sf</i>	11.0	5.0	0.2 \pm 5.0
<i>036_sf</i>	14.9	7.5	-0.4 \pm 7.6

c) April			
Weir ID	Mean (%)	SD	Trend \pm SE
<i>166_sf</i>	22.8	13.5	<i>3.2 \pm 13.0</i>
<i>116_sf</i>	24.3	9.4	<i>2.7 \pm 8.9</i>
<i>036_sf</i>	19.6	7.7	0.8 \pm 7.7

d) May			
Weir ID	Mean (%)	SD	Trend \pm SE
<i>166_sf</i>	45.6	11.3	-0.3 \pm 11.5
<i>116_sf</i>	33.9	7.9	0.7 \pm 8.0
<i>036_sf</i>	24.0	10.4	<i>3.1 \pm 9.8</i>

e) June			
Weir ID	Mean (%)	SD	Trend \pm SE
<i>166_sf</i>	16.6	10.5	<i>-2.7 \pm 10.0</i>
<i>116_sf</i>	12.5	6.2	<i>-1.5 \pm 6.0</i>
<i>036_sf</i>	10.3	6.0	-0.2 \pm 6.0

Precipitation-runoff relationships at the annual scale integrate the covariance in annual precipitation and runoff thereby removing much of the confounding effect of interannual variability in precipitation from the analysis. Basin mean annual precipitation was estimated for each water year, using a simple isohyetal relationship based on the average annual value from gauges within each elevation band. Annual precipitation –

runoff relationships were developed for the periods of record up to and following the year 1985 (**Figure 3.8**) to identify the aggregate effect of the temperature difference on annual hydrologic response.

For the period before 1985 the runoff response at the RME headwater (*166_sf*) and larger Tollgate (*116_sf*) catchments are strongly linear and quite similar in slope (0.86 ± 0.07 and 0.89 ± 0.09 , respectively) and threshold precipitation to runoff (355 ± 84 mm and 334 ± 68 mm, respectively) (**Table 3.11**). The RCEW outlet (*036_sf*) has a much lower runoff response rate (0.39 ± 0.05) than the smaller non-agricultural catchments but a similar threshold precipitation depth to runoff (300 ± 63 mm). The runoff response prediction intervals prior to 1985 decreased with increasing catchment size (**Figure 3.8**, **Table 3.11**) as reflected by the decreasing standard error of the estimate for RME (91mm), Tollgate (58 mm) and RCEW (27 mm) . For the period following 1985, there were insignificant changes in the runoff response from the pre- 1985 period at the lower Tollgate and RCEW weirs, and precipitation threshold to response at all sites. However, the runoff response at RME increased significantly to 0.98 ± 0.04 for the period 1986-2006.

4. Discussion

The data and trend analyses over the 1965 – 2006 (42 water years) period of record show both maximum and minimum temperature are increasing at all elevations, but minimum temperature is increasing more rapidly. Annually, the temperature trends are significant at all elevations and indicate increases in minimum temperature of 1.7 –

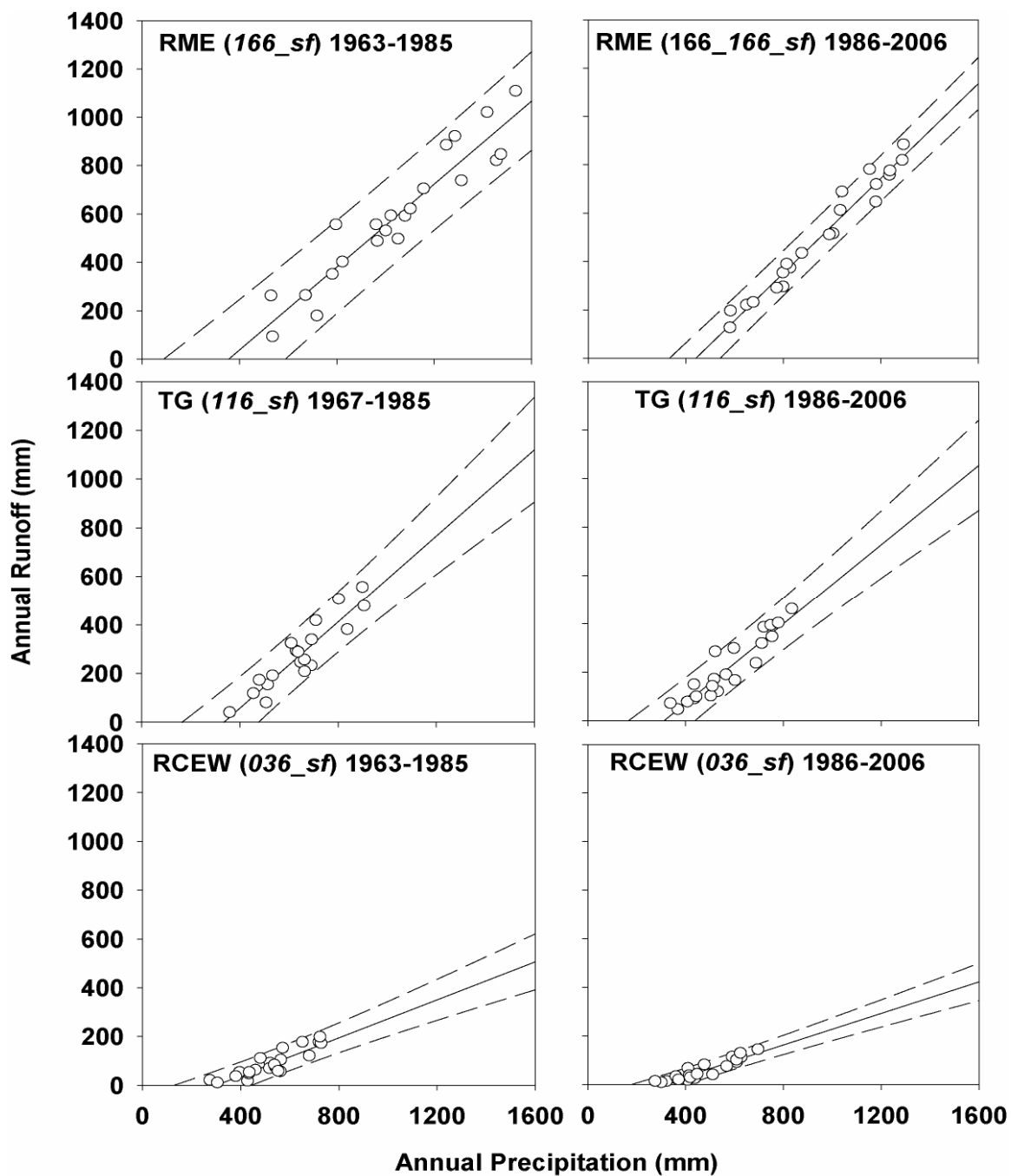


Figure 3.8: Annual Precipitation – Runoff relationship for RME (*166_sf*), Tollgate (*116_sf*) and the RCEW outlet (*036_sf*), for period prior to and after 1985. Annual values, slope and +/- one standard error are plotted.

Table 3.11: Annual Precipitation – Runoff relationship for RME (*I66_sf*), Tollgate (*I16_sf*) and the RCEW outlet (*O36_sf*), for period prior to and after 1985. Slope, precipitation threshold (P_0), R^2 and standard error are presented.

	Slope (-)	P_0 (mm)	R^2	std error of estimate (mm)
RME				
1963-1985	0.86 ± 0.067	355 ± 84	0.89	91
1986-2006	0.98 ± 0.042	441 ± 42	0.97	44
TG				
1967-1985	0.89 ± 0.091	334 ± 68	0.85	58
1986-2006	0.82 ± 0.075	311 ± 54	0.86	49
RCEW				
1963-1985	0.39 ± 0.046	300 ± 63	0.78	27
1986-2006	0.32 ± 0.030	302 ± 45	0.85	16

2.5°C, and 0.8 – 1.7°C for maximum temperature over the period of record. However, the most important differences in hydrology by elevation within the watershed are observed at the seasonal time scale.

Seasonally, increasing trends in average daily maximum temperature are significant for the high elevation site in fall (>90%) and winter (>95%) and summer (>90%) and for the mid (>90%) and low (>95%) elevation sites in summer only. Trends in minimum temperature increases are significant in all seasons at all sites, with the exception of fall for the low elevation site. Increases in fall and winter minimum temperature tend to be larger and more significant at the high and mid-elevation sites, and larger and more significant at the mid- and low elevations sites in spring and summer. Mean conditions over the period of record indicate that all elevations experience diurnal freezes during fall and winter. Fall, winter and spring mean daily minimum temperatures

are cooler at the low elevation site than at the mid-elevation site, primarily because strong temperature inversions occur in the valley bottom during winter. Generally, the mid-elevation site is just above the inversion level, and does not experience this effect.

At high and mid-elevations, several temperature thresholds (highlighted in yellow in **Table 3.3**) appear to have been crossed during the period of record. Annually (water year), the mean minimum daily temperature at high elevation for the period of record is 0.9°C , with strong (>95%) increasing trend of 0.44°C per decade (**Table 3.3a**). This suggests that at the beginning of the period of record, the mean daily minimum at this site was at or below 0°C , while at the end it is nearly 2°C . The mean winter daily maximum temperature at high elevation for the period of record is 0.3°C , with a strong (>95%) increasing trend of 0.51°C per decade (**Table 3.3b**). This suggests that at the beginning of the period of record, the mean winter maximum daily temperature was close to -1°C , and that by the end it is around 1.4°C . The increase in the water year mean minimum daily temperature suggests a shift at high elevation from one dominated by an annual freeze – thaw diurnal cycle, to one where, on average, the diurnal cycle is above freezing. The increase in winter maximum daily temperature suggests a shift from winter conditions where the entire diurnal cycle is sub-freezing to one that generally has a diurnal freeze – thaw.

The mean fall minimum daily temperature at mid-elevation for the period of record is -0.2°C , with a strong (>95%) increasing trend of 0.41°C per decade (**Table 3.3c**). This suggests that at the beginning of the period of record, mean fall minimum daily temperature was about -1°C , and that by the end of the period of record was close to 0.7°C . This indicates a fall shift at mid-elevation from a freeze – thaw diurnal cycle to an

above-freezing diurnal cycle. These trends indicate that freezing temperatures at mid-elevations are now limited to winter, and temperatures at high elevations are becoming more like those at mid-elevation at the beginning of the period of record. Like much of the interior northwestern U.S, elevations within the RCEW are limited and do not extend much beyond the elevation of the high elevation measurement site (*176_met*). In more alpine regions colder conditions are able to shift to higher elevation areas, while in the RCEW there is no higher elevation land area to shift to, so there is no longer a season where the entire diurnal cycle is below freezing.

Precipitation phase (snow vs. rain) is strongly affected by warming climate. The percent snow in the water year precipitation has decreased at all elevations over the period of record (1965 – 2006, 42 water years). The decreasing trend is most significant (>95%) at mid- and low elevations. The data presented in **Table 3.5** (highlighted in yellow) indicate that some critical hydro-climatic thresholds have been crossed. At high elevation, the snow fraction is only slightly reduced over the period of record. However, at mid-elevation, the snow fraction has decreased from 54% to 37% over the period of record, while at low elevation, it has decreased 42% to 21% over the period of record (**Table 3.5a**). Both changes indicate that mid- and low elevations have shifted from a regime of mixed snow and rain to one that is dominated by rain.

During fall, there has been a large decrease (significance >95%) in snowfall at all elevations (**Table 3.5b**). At high elevation the decline is large (from 99% to 67%) indicating that during fall high elevations have shifted from a totally snow dominated system to one that, while still snow dominated, has a significant rain component. At mid-elevation the decline is from 69% to 44% snow and at low elevation the decline is from

58% to 25% snow, indicating that both sites have shifted from a snow-dominated rain-snow mix to one that is rain-dominated.

During winter, the only significant (>95%) decreasing trend in snowfall occurred at low elevation, which showed a decline from 69% to 37% snow (**Table 3.5c**). This indicates that even during winter at low elevations there has been a shift from a snow-dominated to a rain-dominated system. In spring, significant (>95%) decreasing trends occur at both mid- and low elevations. Again, the elevational trend is evident, as the decrease in snow fraction is greatest at lowest elevation, and least at mid- and high elevation.

Snow water equivalent (SWE) is also strongly affected by warming climate. Marks et al. (2001a) points out the SWE timing and depth differences between the low and mid elevation snow courses (*176_sc, 144_sc, 155_sc*) and the high elevation snow courses (*163_sc, 163b_sc, 163c_sc, 174_sc*). While the snow regimes are different between these, the impact they represent to the hydrology of the RCEW is also distinct. Over the period of record (1964 – 2006, 43 water years), both April 1 and May 1 SWE are decreasing, as is the depth and timing of peak SWE at all measurement sites. As with the snow fraction, the decreasing trends are largest and most significant at the low elevations. The hydrologic importance of these trends is in the hypsometry of the RCEW, where only 2% or about 5 km² the land area is above 2060 m, while 24% or about 57 km² of the RCEW is between 1700 – 2060 m. The loss or redistribution of 100mm of high elevation (above 2060 m) SWE represents less than 1% of the mean water year streamflow from the RCEW, while the same 100mm loss or seasonal

redistribution of SWE from 1700 – 2060 m seasonal snowcover represents more than 14% of water year streamflow from RCEW.

Though at higher elevations it is colder and more snow falls, because it represents a small area, its hydrologic impact on the RCEW is not as important as the mid- to low elevation snowcover. The snowcover at snow measurement sites above 2060 m (*163_sc*, *163b_sc*, *163c_sc*, *174_sc*) show a relatively small response to climate warming, without a significant trend toward earlier peak SWE or reduced April 1 SWE. However, sites between 1700 and 2060 m (*176_sc*, *144_sc*, *155_sc*) show a strong response to warming with a significant (>95%) trend toward earlier peak SWE, and a significant (>95%) trend toward reduced April 1 SWE. The data indicate that the only high elevation snow course with a significant (>90%) decreasing trend in April 1 SWE is *163c_sc*, which shows a 21% decrease from 732 to 594 mm SWE. The mid- and low elevation courses show significant decreasing trends of 43% (657 to 427 mm SWE) for *176_sc*, and 85% (231 to 93 mm SWE) for *155_sc* (**Figure 3.5, Table 3.6**). The data indicate that the only significant changes in the timing of peak SWE occur at low elevations, with data from *144_sc* showing that the date of peak SWE has shifted to 44 days earlier, and data from *155_sc* showing a shift to 30 days earlier (**Table 3.7**) over the period of record. At the end of the record, both courses now tend to peak near the middle of February, indicating that while these two snow courses initially represented different snow environments, they now essentially represent the lower extent of the seasonal snowcover within the RCEW.

Though the record is shorter (1983 – 2006, 24 water years), the hourly snow pillow data provide a more detailed perspective on how climate warming has affected the seasonal snowcover. Data from the snow pillow on the date and depth of peak SWE are

similar to the *176_sc* snow course located adjacent to the pillow. The snow pillow provides data on the dates of snowcover initiation and melt-out, which cannot be derived from the snow course data. Though the data indicate that snowcover initiation is later and melt-out earlier (a shorter snow season), the only significant (>95%) trend for these dates is in the timing of snowcover initiation. The data indicate that this date occurs 20 days later than it did at the beginning of the period of record. This is consistent with trends in increasing fall temperatures and decreases in fall snowfall.

The number of soil *freeze days* shows a significant decreasing trend (>95%) at both sites with viable data (*127_stm*, *098_stm*) over the 21 water years of record (**Table 3.8, Figure 3.6**). It is important to note that deep snow accumulation at these sites is very rare and much more commonly characterized as intermittent and thin. The insulating effect of a snowcover is well documented and generally results in much warmer soils. However, the same insulating property can work to extend soil-freezing events where snow cover is shallow and intermittent because snow events are generally associated with freezing conditions and a snow cover reduces incoming solar energy and helps maintain freezing conditions. Most frozen-soil runoff events occur in the presence of a shallow snow cover that prevents rapid soil thawing (Seyfried et al. 1990). The lack of snow deposition and warmer temperatures suggests that potential frozen-soil runoff events will migrate to higher elevations and become less dramatic as the land area affected decreases. However, if cold conditions allow soil freezing and the formation of an early season semi-continuous snowcover down to lower elevations, the likelihood of a later rain-on-snow frozen-soil runoff event would be increased.

The decrease in *soil freeze* days at mid-elevation (*127_stm*) is largest at nearly 25 days per decade, or a decrease in *freeze days* of more than 50 days over the period of record. The decrease in *soil freeze days* should increase infiltration of rainfall at lower elevations within the RCEW, but may also increase direct evaporation from the soil during winter. Decreasing trends in the date of the onset of *plant-water stress* are significant (>95%) at the high (*176_stm*) and mid-elevation (*127_stm*) sites, but not at the low slope site. Trends are largest at the high elevation site, where the date of *plant-water stress* onset has moved forward by nearly three weeks over the period of record. The lack of change at low slope areas (*098_stm*) is expected, as at lower elevations within the RCEW there is limited precipitation, almost no snowfall, and this has changed little over the past 45 years. The impact of climate warming on native plants will be strongest in locations where the hydrology has been altered.

The observed shifts in *plant-water stress* (**Table 3.9**) also reflect trends in snow cover discussed above. At high elevation (*176_stm*), the native vegetation is entirely covered by snow most winters, so that there is no transpiration or soil evaporation until after snowmelt, a time of relatively high evaporative demand (May). The documented earlier melt-out date over the period of record, therefore results in earlier transpiration and hence earlier and longer *plant water stress* (summer precipitation was always negligible and is now less than before). At the low slope site (*098_stm*), no change in *plant water stress* was observed even though there has been an increase in air temperature. This is also consistent with snow accumulation patterns. At the low slope site, snow rarely covered the vegetation and generally melted in winter, prior to significant evaporative demand, so that precipitation phase has little effect on soil water

availability. The effect of the temperature increase on evaporative demand is probably overwhelmed by large year-to-year variations in precipitation. Results at mid-elevation (*127_stm*) are, predictably, intermediate, as snow cover of the vegetation is more common and melt out slightly later at mid-elevation than at the low slope areas. These data indicate that the impact of climate warming on vegetation in this region will be most pronounced at higher elevations that experience continuous, relatively deep (>40 cm) snow cover.

Both mean water year and seasonal precipitation volume are unchanged at all measurement sites over the period of record (**Figure 3.3**). The only significant trends indicated by the data are a general decrease in summer precipitation at all sites. However, these summer trends, while significant, are small (about 1% decrease per decade). Though the shift in other seasons is not significant at the 90% level, the decrease in summer precipitation represents a re-distribution of water year precipitation to fall and spring at mid- to high elevations, and to winter and spring at lower elevations.

Whereas mean water year streamflow, like precipitation, is unchanged as over the period of record; seasonal streamflow, like snowmelt, has shifted toward earlier flow. Late winter and early spring flows have increased, while late spring and summer flows have decreased. There is a strong elevational gradient to this shift. The high elevation, headwater weir shows significant (>95%) March and April flow increases, while the mid-elevation weir shows significant (>95%) April flow increases. The outlet weir, however, shows a significant (>95%) May flow increase. All three weirs show decreases in June flow, with very significant (>95%) decreases at headwater weir, significant decreases (>90%) at the mid-elevation weir, and non significant (<90%) change at the outlet weir.

The accuracy of estimated values for mean annual precipitation over RME, Tollgate and the entire RCEW, used in the rainfall – runoff analysis are suspect because precipitation is highly variable over the RCEW and, as shown in **Table 3.4**, that variability is not a simple function of elevation. However, this analysis is presented as an example of how climate warming may alter basin hydrology at an annual time-scale. A more detailed, and better verified estimates of mean basin precipitation, SWE, surface water input and streamflow, at multiple time-scales, for selected snow seasons over the smaller RME catchment is presented in Chapter 4.

The rainfall – runoff analysis presented here indicates that predictability of annual runoff depth from the developed precipitation-runoff curves for the two-decade period since 1985 is better than for the two decades preceding 1985. Whereas decreases in the variance from the predicted relationship occur at all sites between the pre- and post-1985 periods, the 50% reduction in standard error of the estimate at the high elevation catchment is the most striking change, and may drive a reduction in variance over larger nested watersheds (**Figure 3.8, Table 3.11**). The contemporaneous decrease in duration of snowcover, increase in annual runoff response and decrease in predictive variability of annual runoff from the RME catchment suggests that as high elevation drainages cross temperature thresholds controlling snow accumulation and melt, the runoff season will become temporally compressed and as a result may be more predictable. Any gains in runoff from high elevation snowcovers are likely to depend on the increase in plant water stress days within the catchment as the period of runoff is advanced. Such gains are likely to be offset as warming continues further reducing the spatial variability of soil

water input, due to decreased redistribution of snow and as vegetation communities respond to warming.

5. Conclusions

In agreement with other studies of temperature trends in the western U.S. and Canada (e.g. Trenberth et al. 2007), temperatures have significantly warmed at all elevations within the RCEW with trends indicating minimum temperature warming is greater (+1.7 to +2.5°C) than maximum temperatures (+0.8 to +1.7°C). Trends in the data indicate that important thermal thresholds have been crossed during the period of record.

At high elevation, the mean water year diurnal cycle is shifting from freeze – thaw to above freezing, and the winter diurnal cycle from below freezing to a daily freeze – thaw. Although this change has not been accompanied by significant changes in phase of precipitation or depth and timing of peak SWE, snow pillow data indicate that initiation of the seasonal snowcover occurs later and melt-out occurs earlier, resulting in a snow season that is at least a month shorter than it was at the beginning of the record. This change in timing of snow cover is followed directly by a three-week increase in the duration of plant water stress. The earlier melt also drives increases in March and April runoff that are balanced by decreases in May and June runoff.

At mid-elevations, the fall diurnal cycle is shifting from freeze – thaw to above freezing. These changes have affected the proportion of snow in water year precipitation, the timing of snowmelt and streamflow, the number of *soil freeze* days and the length of time native plants are subjected to water stress.

The data also indicate a decrease in SWE at all elevations, with the largest and most significant decreases at mid- and low elevations. This elevational gradient is important to the hydro-climatology of the RCEW because so much more area exists at mid- and low elevations than at high elevations. Dates of peak SWE occur earlier at all elevations. At low elevations, the date of peak SWE has shifted to mid-February.

At lower elevations where, in the absence of a snowcover, soil freezing is possible, the number of *soil freeze* days has significantly decreased. While this may increase infiltration of rainfall and reduce flooding, it also will likely increase the rate of soil dry down. The onset of plant-water stress is occurring earlier at mid- and high elevations, with the largest shift at high elevations where hydrology has been most significantly altered. This will increase the time native plants are under water stress and put ecosystems at risk.

The data indicate that, while there is large year-to-year variability, water year (annual) streamflow and precipitation have not changed over the period of record. However, as other studies have shown (e.g. Regonda et al. 2005; Mote et al. 2005), there has been a seasonal shift in streamflow, with increases in winter and early spring, and decreases in late spring and summer. This shift is stronger at high elevation, and delayed at mid- and low elevations. Fall, winter and spring precipitation volume has not changed, but the proportion of snow has significantly declined at all elevations. This has caused critical shifts in precipitation regimes such that while high elevations are still snow dominated, more of a rain – snow mix now exists, and mid- and low elevations have changed from mixed rain and snow to rain dominated.

Together these results indicate that the hydro-climatology of the RCEW and similar regions of the interior northwestern U.S. have already been affected by climate warming. Snowfall and the seasonal snowcover have been significantly affected. Changes snow deposition and melt have altered patterns of soil temperature and moisture, and streamflow. In the short term, these trends will likely have a significant impact on land and water management practices. If they were to continue for the next 50-100 years, as suggested by the IPCC report (2007), the RCEW will be very different hydro-climatically.

6. References

- Aguado, E., Cayan, D. R., Riddle, L., and Roos, M. (1992). "Climate fluctuations and the timing of west coast streamflow." *J. Clim.*, 5(12), 1468-1483.
- Akinremi, O. O., McGinn, S. M., and Cutforth, H. W. (1999). "Precipitation trends on the Canadian prairies." *J. Clim.*, 12(10), 2996-3003.
- Bindoff, N. L., Willebrand, J., Artale, V., Cazenave, A., Gregory, J., Gulev, S., Hanawa, K., Le Quere, C., Levitus, S., Nojiri, Y., Shum, C. K., Talley, L. D., and Unnikrishnan, A. (2007). "Observations: Oceanic climate change and sea level." *Climate change 2007: The physical science basis*. Contributions of working group I to the fourth assessment report of the Intergovernmental Panel on Climate Change, S. Solomon, D. Quin, M. Manning, Z. Chen, M. Marquis, K. B. Averyt, M. Tignor, and H. L. Miller, eds., Cambridge University Press, Cambridge, UK and New York, 385-432.
- Brunetti, M., Burrioni, L., Maugeri, M., and Nanni, T. (2000). "Trends of minimum and maximum daily temperatures in Italy from 1865 to 1996." *Theor. Appl. Climatol.*, 66, 49-60.
- Cayan, D. R., Kammerdiener, S. A., Dettinger, M. D., Caprio, J. M., and Peterson, D. H. (2001). "Changes in the onset of spring in the Western United States." *Bull. Am. Meteorol. Soc.*, 82(3), 399-415.
- Cooley, K. R., Hanson, C. L., and Johnson, C.W. (1988). "Precipitation erosivity index estimates in cold climates." *Trans. ASAE*, 31, 1445-1450.

- Dettinger, M. D., and Cayan, D. R. (1995). "Large-scale atmospheric forcing of recent trends toward early snowmelt runoff in California." *J. Clim.*, 8, 606-623.
- Dettinger, M. D., Cayan, D. R., Diaz, H. F., and Meko, D. M. (1998). "North-south precipitation patterns in Western North America on interannual-to-decadal timescales." *J. Clim.*, 11(12), 3095-3111.
- Easterling, D. R., Evans, J. L., Groisman, P. Y., Karl, T. R., Kunkel, K. E., and Ambenje, P. (2000). "Observed variability and trends in extreme climate events: a brief overview." *Bull. Am. Meteorol. Soc.*, 81(3), 417-425.
- Flerchinger, G. N., Marks, D., Hardegree, S.P., Nayak, A., Winstral, A.H., Seyfried, M.S., Pierson F.P., and Clark, P.E. (2007). "45 Years of Climate and Hydrologic Research Conducted at the Reynolds Creek Experimental Watershed.", *Environmental and Water Resources: Milestones in Engineering History*. Rogers J. R. Ed. Sponsored by ASCE, Environmental and Water Resources Institute, and National History & Heritage Committee. ASCE, Reston, VA, 135-143.
- Garbrecht, J., Van Liew, M., and Brown, G. O. (2004). "Trends in precipitation, streamflow, and evaporation in the Great Plains of the United States." *J. Hydrol. Eng.*, 9(5), 360-367.
- Garen, D. C., and Marks, D. (2005). "Spatially distributed energy balance snowmelt modeling in a mountainous river basin: Estimation of meteorological inputs and verification of model results." *J. Hydrol.*, 315(1-4), 126-153.
- Gray, D., Toth, B., Pomeroy, J., Zhao L., and Granger, R. (2001). "Estimating areal snowmelt infiltration into frozen soils." *Hydrolog. Process.*, 15(16), 3095-3111.
- Groisman, P. Y., and Easterling, D. R. (1994). "Variability and trends of total precipitation and snowfall over the United States and Canada." *J. Clim.*, 7(1), 184-205.
- Hamlet, A. F., Mote, P. W., Clark, M. P., and Lettenmaier, D. P. (2005). "Effects of temperature and precipitation variability on snowpack trends in the Western United States." *J. Clim.*, 18, 4545-4561.
- Hamon, W. R. (1973). "Computing actual precipitation: Distribution of precipitation in mountainous areas." *WMO Rep. No. 362*, World Meteorological Organization, Geneva, 1, 159-173.
- Hanson, C. L. (2001). "Long-term precipitation database, Reynolds Creek Experimental Watershed, Idaho, United States." *Water Resour. Res.*, 37(11), 2831-2834.

- Hanson, C. L., Johnson, G. L., and Rango, A. (1999). "Comparison of precipitation catch between nine measuring systems." *J. Hydrol. Eng.*, 4(1), 70-75.
- Hanson, C. L., Marks, D., and Van Vactor, S. S. (2001). "Long-term climate database, Reynolds Creek Experimental Watershed, Idaho, United States." *Water Resour. Res.*, 37(11), 2839-2841.
- Hanson, C. L., Morris, R. P., and Coon, D. L. (1979). "A note on the Dual-gage and Wyoming shield precipitation measurement systems." *Water Resour. Res.*, 15(4), 956-960.
- Hanson, C. L., Pierson, F. B., and Johnson, G. L. (2004). "Dual-gauge system for measuring precipitation: Historical development and use." *J. Hydrol. Eng.*, 350-359.
- Hirsch, R.M., and Slack, J.R. (1984). "Nonparametric trend test for seasonal data with serial dependence." *Water Resour. Res.*, 20(6), 727-732.
- Hu, Q., Woodruff, C. M., and Mudrick, S. E. (1998). "Interdecadal variations of annual precipitation in the Central United States." *Bull. Am. Meteorol. Soc.*, 79(2), 221-229.
- Huntington, T. G., Hodgkins, G. A., Keim, B. D. and Dudley R. W. (2004). "Changes in the proportion of precipitation occurring as snow in New England (1949-2000)." *J. Clim.*, 17(13), 2626-2636.
- Hurrell, J. W. (1995). "Decadal trends in the North Atlantic Oscillation: Regional temperatures and precipitation." *Science*, 269(5224), 676-679.
- Hurrell, J. W., and Van Loon, H. (1997). "Decadal variations in climate associated with the North Atlantic Oscillation." *Clim. Change*, 36(3-4), 301-326.
- IPCC (2007). *Climate change 2007, The physical science basis*, Cambridge University Press, Cambridge, U.K.
- Karl, T. R., Jones, P. D., Knight, R. W., Kukla, G., Plummer, N., Razuvayev, V., Gallo, K. P., Lindseay, J., Charlson, R., and Peterson, T. C. (1993). "A new prospective on recent global warming: Asymmetric trends of daily maximum and minimum temperature." *Bull. Am. Meteorol. Soc.*, 74(6), 1007-1023.
- Karl, T. R., and Knight, R. W. (1998). "Secular trends of precipitation amount, frequency, and intensity in the United States." *Bull. Am. Meteorol. Soc.*, 79(2), 231-241.

- Karl, T. R., Kukla, G., and Gavin, J. (1984). "Decreasing diurnal temperature range in the United States and Canada from 1941 through 1980." *J. Clim. Appl. Meteorol.*, 23(11), 1489-1504.
- Knowles, N., Dettinger, M. D., and Cayan, D. R. (2006). "Trends in snowfall versus rainfall in the Western United States." *J. Clim.*, 19(18), 4545-4559.
- Lapp, S., Byrne, J., Townshend, I., and Kienzle, S. (2005). "Climate warming impacts on snowpack accumulation in an alpine watershed." *Int. J. Climatol.*, 25, 521-536.
- Lemke, P., Ren, J., Alley, R.B., Allison, I., Carrasco, J., Flato, G., Fujii, Y., Kasere, G., Mote, P., Thomas R.H., and Zhang, T. (2007). "Observations: Changes in snow and frozen ground." *Climate change 2007: The physical science basis*. Contributions of working group I to the fourth assessment report of the Intergovernmental Panel on Climate Change, S. Solomon, D. Quin, M. Manning, Z. Chen, M. Marquis, K. B. Averyt, M. Tignor, and H. L. Miller, eds., Cambridge University Press, Cambridge, UK and New York, 337-383.
- Leipprand, A., and Gerten, D. (2006). "Global effects of doubled atmospheric CO₂ content on evapotranspiration, soil moisture and runoff under potential natural vegetation." *Hydrolog. Sciences*, 51(1), 171-185.
- Lettenmaier, D. P., Wood, E. F., and Wallis J. R. (1994). "Hydro-climatological trends in the Continental United States, 1948-88." *J. Clim.*, 7(4), 586-607.
- Leung, L. R., and Ghan, S. J. (1999). "Pacific Northwest climate sensitivity simulated by a regional climate model driven by a GCM. Part II: 2xCO₂ simulations." *J. Clim.*, 12, 2031-2053.
- Manabe, S., Milly, P. C. D., and Wetherald, R. (2004). "Simulated long-term changes in river discharge and soil moisture due to global warming." *Hydrolog. Sciences*, 49(4), 625-642.
- Marks, D. (2001). "Introduction to special section: Reynolds Creek Experimental Watershed." *Water Resour. Res.*, 37(11), 2817.
- Marks, D., Cooley, K. R., Robertson, D. C., and Winstral, A. (2001a). "Long-term snow database, Reynolds Creek Experimental Watershed, Idaho, United States." *Water Resour. Res.*, 37(11), 2835-2838.
- Marks, D., Domingo, J., Susong, D., Link, T., and Garen, D. (1999). "A spatially distributed energy balance snowmelt model for application in mountain basins." *Hydrolog. Process.*, 13(12-13), 1935-1959.

- Marks D, and Dozier J. (1992). "Climate and energy exchange at the snow surface in the alpine region of the Sierra Nevada: 2. Snowcover energy balance." *Water Resour. Res.* 28(11): 3043–3054.
- Marks, D., Kimball, J., Tingey, D., and Link, T. (1998). "The sensitivity of snowmelt processes to climate conditions and forest cover during rain-on-snow: A case study of the 1996 Pacific Northwest flood." *Hydrolog. Process.*, 12(10-11), 1569-1587.
- Marks, D., Link, T., Winstral, A., and Garen, D. (2001b). "Simulating snowmelt processes during rain-on-snow over a semi-arid mountain basin." *Ann. Glaciol.*, 32(1), 195-202.
- Marks, D., Seyfried, M., Flerchinger G., and Winstral, A. (2008). "Research data collection at the Reynolds Creek Experimental Watershed" *J. Service Climatol.*, (to appear).
- Marks, D., and Winstral, A. (2001). "Comparison of snow deposition, the snow cover energy balance, and snowmelt at two sites in a semiarid mountain basin." *J. Hydrometeorol.*, 2(3), 213-227.
- Marks, D., and Winstral, A. (2008). "Finding the rain/snow transition elevation during storm events in a mountain basin." *Hydrolog. Process.*, (to appear).
- Marks, D., Winstral, A., and Seyfried, M. (2002). "Simulation of terrain and forest shelter effects on patterns of snow deposition, snowmelt and runoff over a semi-arid mountain catchment." *Hydrolog. Process.*, 16(18), 3605-3626.
- McCabe, G. J., and Clark, M. P. (2005). "Trends and variability in snowmelt runoff in the Western United States." *J. Hydrometeorol.*, 6, 476-482.
- Mote, P. W. (2003a). "Trends in snow water equivalent in the Pacific Northwest and their climatic causes." *Geophys. Res. Lett.*, 30(12), 1601, doi:10.1029/2003GL017258, 2003.
- Mote, P. W. (2003b). "Twentieth-century fluctuations and trends in temperature, precipitation, and mountain snowpack in the Georgia Basin-Puget Sound region." *Can. Water Resour. J.*, 28(4), 567-585.
- Mote, P. W. (2006). "Climate-driven variability and trends in mountain snowpack in Western North America." *J. Clim.*, 19(23), 6209-6220.
- Mote, P. W., Hamlet, A. F., Clark, M. P., and Lettenmaier, D. P. (2005). "Declining mountain snowpack in western North America." *Bull. Am. Meteorol. Soc.*, 86, 39-49.

- Olsen, A. (2003). "Snow or rain? – a matter of wet-bulb temperature." ISSN 1650-6553 Nr 48(http://www.geo.uu.se/luva/exarb/2003/Arvid_Olsen.pdf).
- Pierson, F. B., Slaughter, C. W., and Cram, Z. K. (2001). "Long-term stream discharge and suspended-sediment database, Reynolds Creek Experimental Watershed, Idaho, United States." *Water Resour. Res.*, 37(11), 2857-2861.
- Quintana-Gomez, R. A. (1999). "Trends of maximum and minimum temperatures in Northern South America." *J. Clim.*, 12, 2104-2112.
- Randall, D. A., Wood, R. A., Bony, S., Colman, R., Fichet, T., Fyfe, J., Kattsov, V., Pitman, A., Shukla, J., Srinivasan, J., Stouffer, R. J., Sumi, A., and Taylor, K. E. (2007). "Climate models and their evaluation." *Climate change 2007: The physical science basis*. Contributions of working group I to the fourth assessment report of the Intergovernmental Panel on Climate Change, S. Solomon, D. Qin, M. Manning, Z. Chen, M. Marquis, K. B. Averyt, M. Tignor, and H. L. Miller, eds., Cambridge University Press, Cambridge, UK and New York, 589-662.
- Regonda, S. K., Rajgopalan, B., Clark, M., and Pitlick, J. (2005). "Seasonal cycle shifts in hydroclimatology over the Western United States." *J. Clim.*, 18, 372-384.
- Robins, J. S., Kelly, L. L. and Hamon, W.R. (1965). "Reynolds Creek in southwest Idaho: an outdoor hydrologic laboratory." *Water Resour. Res.*, 1, 407-413.
- Serreze, M. C., Clark, M. P., Armstrong, R. L., McGinnis, D. A., and Pulwarty, R. S. (1999). "Characteristics of the Western United States snowpack from snowpack telemetry (SNOTEL) data." *Water Resour. Res.*, 35, 2145-2160.
- Seyfried, M., and Flerchinger, G. N. (1994). "Influence of frozen soil on rangeland erosion." *Variability in rangeland water erosion processes*, Blackburn, W., Schuman, G. and Pierson, F., eds., Soil Science Society of America, Special Publication 38, 67-82.
- Seyfried, M., Flerchinger, G. N., Murdock, M. D., and Hanson, C. L. (2001a). "Long-term soil temperature database, Reynolds Creek Experimental Watershed, Idaho, United States." *Water Resour. Res.*, 37(11), 2843-2846.
- Seyfried, M., Hanson, C. L., Murdock, M. D., and Van-Vactor, S. S. (2001b). "Long-term lysimeter database, Reynolds Creek Experimental Watershed, Idaho, United States." *Water Resour. Res.*, 37(11), 2853-2856.
- Seyfried, M., Murdock, M. D., Hanson, C. L., and Flerchinger, G. N. (2001c). "Long-term soil water content database, Reynolds Creek Experimental Watershed, Idaho, United States." *Water Resour. Res.*, 37(11), 2847-2851.

- Seyfried, M., and Murdock, M. (1997). "Use of air permeability to estimate infiltrability of frozen soil." *J. Hydrol.*, 202, 95-107.
- Seyfried, M., Wilcox, B., and Cooley, K. (1990). "Environmental conditions and processes associated with runoff from frozen soils at Reynolds Creek watershed." *Proceedings International Symposium: Frozen Soil Impacts on Agricultural, Range, and Forest Lands*, USACE Cold Regions Research and Engineering Laboratory, 90-1, 125-134.
- Shanley, J., and Chalmers, A. (1999). "The effect of frozen soil on snowmelt runoff at Sleepers River, Vermont." *Hydrolog. Process.*, 13(12-13), 1843-1857.
- Slaughter, C. W., Marks, D., Flerchinger, G. N., Van Vactor, S. S., and Burgess, M. D. (2001). "Thirty-five years of research data collection at Reynolds Creek Experimental Watershed, Idaho, United States." *Water Resour. Res.*, 37(11), 2819-2823.
- Stewart, I. T., Cayan, D. R., and Dettinger, M. D. (2004). "Changes in snowmelt runoff timing in Western North America under a 'Business as usual' climate change scenario." *Clim. Change*, 62, 217-232.
- Stewart, I. T., Cayan, D. R., and Dettinger, M. D. (2005). "Changes towards earlier streamflow timing across Western North America." *J. Clim.*, 18, 1136-1155.
- Trenberth, K. E., Jones, P. D., Ambenje, P., Bojariu, R., Easterling, D., Tank, A. K., Parker, D., Rahimzadeh, F., Renwick, J. A., Rusticucci, M., Soden, B., and Zhai, P. (2007). "Observations: Surface and atmospheric climate change." *Climate change 2007: The physical science basis*. Contributions of working group I to the fourth assessment report of the Intergovernmental Panel on Climate Change, S. Solomon, D. Qin, M. Manning, Z. Chen, M. Marquis, K. B. Averyt, M. Tignor, and H. L. Miller, eds., Cambridge University Press, Cambridge, UK and New York, 235-336.
- Winstral, A., and Marks, D. (2002). "Simulating wind fields and snow redistribution using terrain-based parameters to model snow accumulation and melt over a semi-arid mountain catchment." *Hydrolog. Process.*, 16(18), 3585-3603.
- Yang, D., Goodison, B. E., Metcalfe, J. R., Louie, P., Elomaa, E., Hanson, C., Golubev, V., Gunther, T., Milkovic, J. and Lapin, M. (2001). "Compatibility evaluation of national precipitation gage measurements." *J. Geophys. Res.*, 106(D2), 1481-1491.
- Yang, D., Goodison, B. E., Metcalfe, J. R., Louie, P., Leavesley, G., Emerson, D., Hanson, C. L., Golubev, V. S., Elomaa, E., Gunther, T., Pangburn, T., Kang, E., and Milkovic, J. (1999). "Quantification of precipitation measurement

discontinuity induced by wind shields on national gauges.” *Water Resour. Res.*, 35(2), 491-508.

Yue, S., Pilon, P., and Cavandias, G. (2002). “Power of the Mann–Kendall and Spearman’s rho tests for detecting monotonic trends in hydrological series.” *J. Hydrol.*, 259(1-4), 254-271.

CHAPTER 4

SENSITIVITY OF SNOWCOVER TO CLIMATE WARMING IN A SEMI-ARID MOUNTAIN CATCHMENT⁷

Abstract

Changes in mid-elevation snowcover and duration have been well documented but the complex interaction among topography, energy balance and snowpack occurrence complicate the prediction of future changes. In this study, sensitivity of seasonal snowcover to climate warming is assessed for the range of precipitation and temperature conditions typical of a mountain catchment, in Idaho, USA. A spatially distributed energy and mass balance snow model, *Isnobal*, is used to continuously simulate snow accumulation and melt for five years and then for climates adjusted by +/- 2°C. Model output of snow water equivalent (SWE) for the base condition compares well to field measurements for all years (Nash-Sutcliffe model efficiency coefficient of 0.81 to 0.97). Simulations from the adjusted climate scenarios indicate that colder conditions increase snow to rain fraction and snow water equivalent and thereby delay surface water input (SWI) to soil and streams until late spring and early summer. Warming scenarios showed the converse, with advances in the date of peak SWE from the base case of up to 2 ½ months, and associated decreases of about 50 % in SWE. This analysis indicates that climate warming of 2°C will result in a critical hydrologic shift across the region, as mean winter maximum and minimum temperatures cross thresholds determining predominant precipitation phase. As early winter precipitation shifts from snow to rain

⁷ Coauthored by A. Nayak, D. Marks, D.G. Chandler, and A. Winstral.

and snowpack water storage is reduced, the snowpack becomes more susceptible to melt from mid winter and spring rain on snow events. The related advance of the SWI timing from spring to a mid-winter peak, with reduced SWI in spring or early summer, indicates earlier and drier summer conditions with the greatest relative change for wet years.

1. Introduction

Precipitation in the mountainous western US is winter dominated and a significant fraction of the annual total falls as snow. High elevation mountain snowcovers play an important role in the regional hydrologic cycle, storing winter precipitation as snow and releasing melt water during spring and summer when water demand is at its peak. Water from snow melt contributes 50-80% of soil moisture and total streamflow in the western U.S. (Stewart et al. 2004; Marks et al. 2001b). The magnitude and timing of water released from melting seasonal snowcovers are critical for regional ecosystem and water management strategies.

Over the last 50 years, mean surface temperature in the western US has increased by 1-3 °C (Trenberth et al. 2007). A number of studies have shown substantial changes in snow deposition and melt patterns such as decrease in the snow fraction of precipitation (Aguado et al. 1992; Dettinger and Cayan 1995; Huntington et al. 2004; Regonda et al. 2005; Knowles et al. 2006; Chapter 3), decrease in total snow accumulation (Mote 2003a&b, 2006; Mote et al. 2005; Chapter 3), earlier timing of snowmelt runoff and earlier peak streamflow (Aguado et al.1992; Dettinger and Cayan 1995; Cayan et al. 2001; Regonda et al. 2005; Stewart et al. 2004, 2005; Chapter 3). Trends in patterns of snow deposition and melt are expected to continue at a similar or accelerated rate if

climate continues to warm as predicted (Meehl et al. 2007). Alterations to the hydrologic regime driven by global warming may require proactive adjustments to water management strategies in the western USA.

Weather patterns over the western US are strongly influenced by natural oceanic circulations such as Pacific decadal oscillation (PDO) and El-Nino southern oscillation (ENSO) (Hurrell 1995; Hurrell and Van Loon 1997; Dettinger et al. 1998) which results in great variability in precipitation (wet and dry cycles) and climate conditions (warm and cold phases) over the region. This regional variability in climate and precipitation results in year-to-year differences in the distribution and timing of snowcover development and melt. The studies cited above are focused on long-term changes in snow accumulation and melt and do not specifically address the complexities introduced by the inter-annual climate and precipitation variability. Moreover, they report large-scale hydrologic cycle changes and are primarily based on data collected at low and mid elevation sites with limited data from high elevation sites.

Given the influence the mountain snowcover has on the regional hydrological cycle it is important to understand the sensitivity of mountain snowcovers to warming climate conditions. This will require simulation of the development and depletion of the seasonal snowcover across complex mountain terrain, under varying climate conditions. The mountains of the western U.S. display tremendous heterogeneity in patterns of snow deposition and melt caused by variations in vegetation canopy, topography and elevation over short distances (Luce et al. 1998; Marks et al. 2002; Winstral and Marks 2002; Winstral et al. 2002). Winstral and others (e.g. Winstral and Marks 2002; Winstral et al. 2002, 2008a&b) showed that it is possible to use a generalized wind field to accurately

simulate the redistribution of snow in complex terrain, and Marks et al. (2002) showed that this method can be coupled to an energy balance snow model to improve simulation of complex patterns of snow distribution, melt and surface water input (SWI) to soils in mountain basins. Surface water input (SWI) is defined as the input of melt-water or rain to the soil surface.

In the western U.S., water management strategies are based on the assumption that regional climate is relatively stable, within the natural range of variability, and that a predictive relationship between temperature, snowcover, snowmelt and streamflow can be developed. However, in view of observed and predicted changes in temperature, climate, snowfall and precipitation in the western U.S. (see Chapter 3), the reliability of seasonal snow cover as a storage reservoir for late spring and summer runoff is in question. How temperature forcing affects runoff is particularly important for extremely wet and dry years, during which reservoirs must be managed for either flood or drought, respectively.

The objectives of this research are to use a snow distribution, energy and mass balance model to: (1) investigate how a range of natural climate and precipitation variability alters patterns of snow deposition, melt, and the delivery of water to the soil and stream in a mountain basins; (2) evaluate the sensitivity of the seasonal snowcover to colder and warmer average temperatures for snow seasons with cold and wet, cold and dry, warm and wet and warm and dry base conditions; (3) understand how climate-altered snowcover affects delivery of water to soil and streamflow of mountain basins near the transitional snow line.

2. The Study Site

This study was conducted within the Reynolds Mountain East (RME) experimental catchment, a small headwater sub-basin located on the southern rim of the Reynolds Creek Experimental Watershed (RCEW), in Owyhee Mountains of southwest Idaho. The majority of precipitation falls during the cold season (fall, winter and spring) as snow, but recent research indicates significant trends to more rain and less snow (Nayak et al. 2008). As is typical of the mountain west, the depth of water storage increases with elevation and is greatest snowpack of headwater catchments.

RME is a perennial headwater catchment with drainage area of 0.38 km² and elevation range of 2022-2139 m (**Figure 4.1**). Within this basin, precipitation is measured at three locations, meteorological and snow depth data are collected at seven stations, temperature, humidity and wind profiles collected at two tower stations, and stream discharge is measured at the catchment outflow. For this study, precipitation, snow and meteorological data are used from the two long-term stations, one located on a wind-exposed ridge (site *176_met*, elevation 2097 m, hereafter referred to as the *ridge site*) and other located in area sheltered by grove of aspen trees (site *176e_met*, elevation 2061 m, hereafter referred to as the *grove site*). Extensive analysis of long-term precipitation, snow and meteorological records from *ridge* and *grove* sites has documented topographic and vegetation interactions with wind and provided reliable estimates of snow deposition across RME (Marks and Winstral 2001; Marks et al. 2001a, 2002; Winstral et al. 2002; Winstral and Marks 2002). Dominant plant communities in the basin are mixed sagebrush, aspen and fir. About 30% of the basin is forested and 70% is mixed sagebrush (Winstral and Marks 2002; Marks et al. 2002).

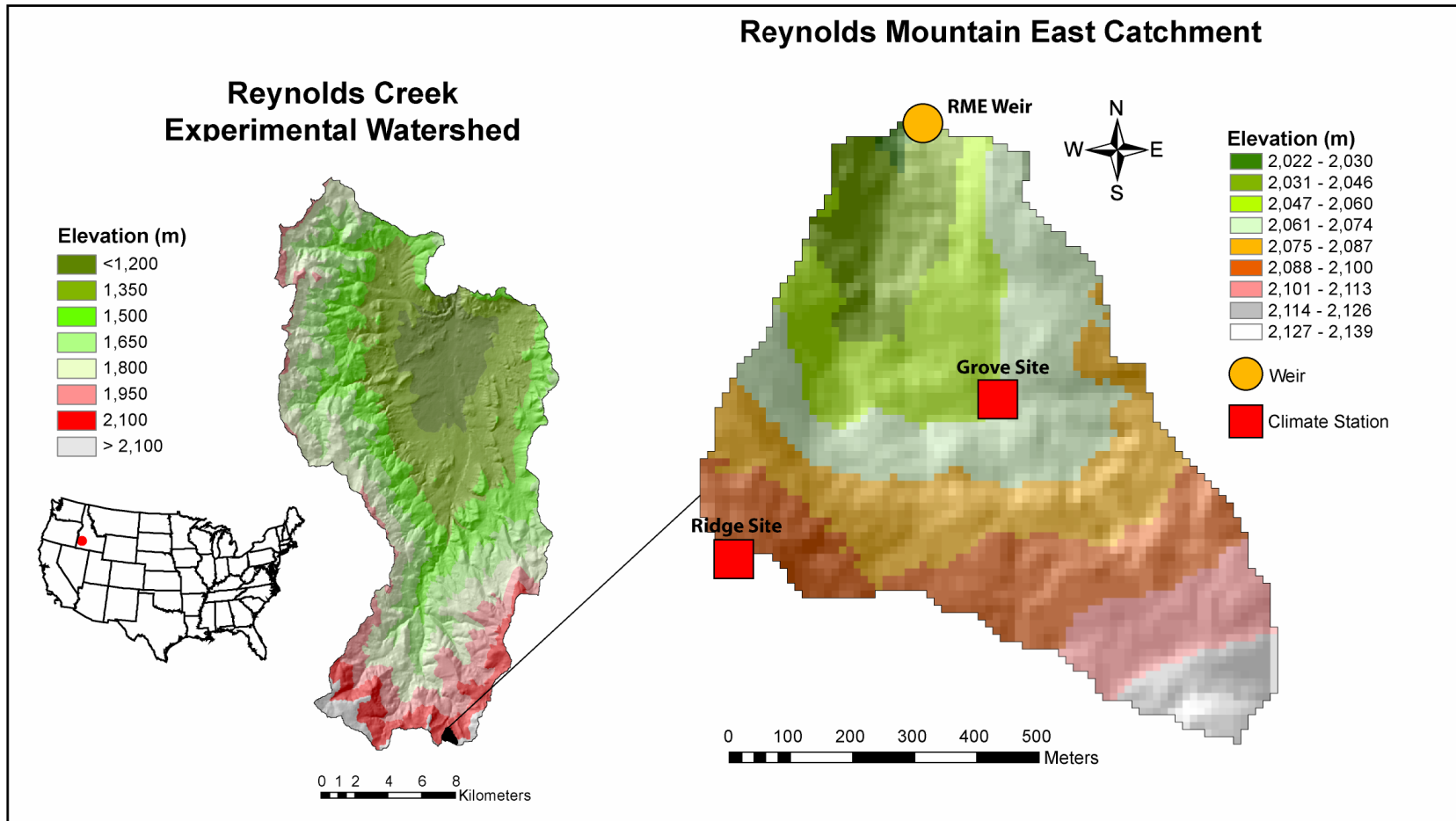


Figure 4.1: The Reynolds Mountain East (RME) catchment, within the Reynolds Creek Experimental Watershed (RCEW). Locations of the outlet weir, ridge and grove measurement sites are indicated.

For RME, as shown in Chapter 3, over the past 45 years, increasing trends in minimum and maximum temperature ($+0.44^{\circ}\text{C}$ and $+0.39^{\circ}\text{C decade}^{-1}$). They also show a modest ($-1.52\% \text{ decade}^{-1}$) decrease in the RME snow fraction of precipitation, decreases in peak SWE ($-56 \text{ mm decade}^{-1}$), and earlier date of peak SWE ($-3.1 \text{ days decade}^{-1}$). These trends are accompanied by a streamflow shift to March and April ($+2.8\% \text{ decade}^{-1}$) from June ($-2.7\% \text{ decade}^{-1}$) with no change in annual precipitation or stream discharge volume. These trends indicate a temperature increase of about 2°C , with about a 7% reduction in the precipitation snow fraction over the 45 years (1962-2006) of analysis.

3. The Study Snow Seasons

Three wet (1984, 1986, and 2006) and two dry (1987 and 2001) snow seasons were selected to represent the range of precipitation and temperature that have occurred naturally in the RME (Chapter 3). These years also satisfy the *Isnobal* model requirement for hourly meteorological forcing data, which is available for RME since 1984. A brief summary of climate conditions during the selected snow seasons is presented in **Table 4.1**. Dew point temperature is used to approximate precipitation temperature and divide precipitation into rain or snow, based on the criteria used in Marks et al. (1999). Bi-weekly division of precipitation as rain and snow is presented in **Figure 4.2**.

The 1984 *snow season* was cold and wet. Average air temperatures were nearly 1°C below normal and precipitation was 153 % of the long-term average *snow season* wind corrected precipitation at *grove site*. Average Nov-May and dew point temperatures near lowest of the five snow seasons analyzed. Although 307 mm (25%) of the total

Table 4.1: Summary of conditions during selected *snow seasons*.

Snow Season	1984	1986	1987	2001	2006
Precipitation (mm):					
<i>grove site</i> ^a	1428 (153%)	1179 (126%)	603 (65%)	707 (76%)	1188 (127%)
<i>ridge site</i>	625	528	364	516	796
Distributed Basin Total	1221	981	532	674	1148
Distributed Basin Rain ^b	307 (25%)	115 (12%)	165 (31%)	157 (23%)	346 (30%)
Air Temperature (°C):					
Seasonal ^c	0.6 (-0.8)	2.4 (+1.0)	2.9 (+1.5)	1.4 (-0)	1.9 (+0.5)
Nov-May	-2.9	-2.1	-1.9	-3.3	-2.2
Dew Point Temperature (°C):					
Seasonal	-4.2	-4.8	-4.9	-4.2	-4.5
Storm ^d	-4.4	-4.3	-3.9	-4.1	-3.5
Wind Speed (m s ⁻¹):					
<i>grove site</i>	2.5	2.8	2.3	2.5	2.0
<i>ridge site</i>	5.2	5.2	4.0	5.9	5.5
Streamflow (mm): ^e	1040 (187%)	800 (142%)	213 (38%)	283 (50%)	762 (136%)

^a Percentages in parenthesis are of the long-term average *snow season* wind corrected precipitation at *grove site*.

^b Percentages in parenthesis show rainfall as fraction of total *snow season* precipitation.

^c Values in parenthesis show departure from long-term average *snow season* temperature.

^d Average dew point temperatures during Nov-May precipitation events.

^e Values in parenthesis are percentages of the long-term average *snow season* streamflow at RME weir.

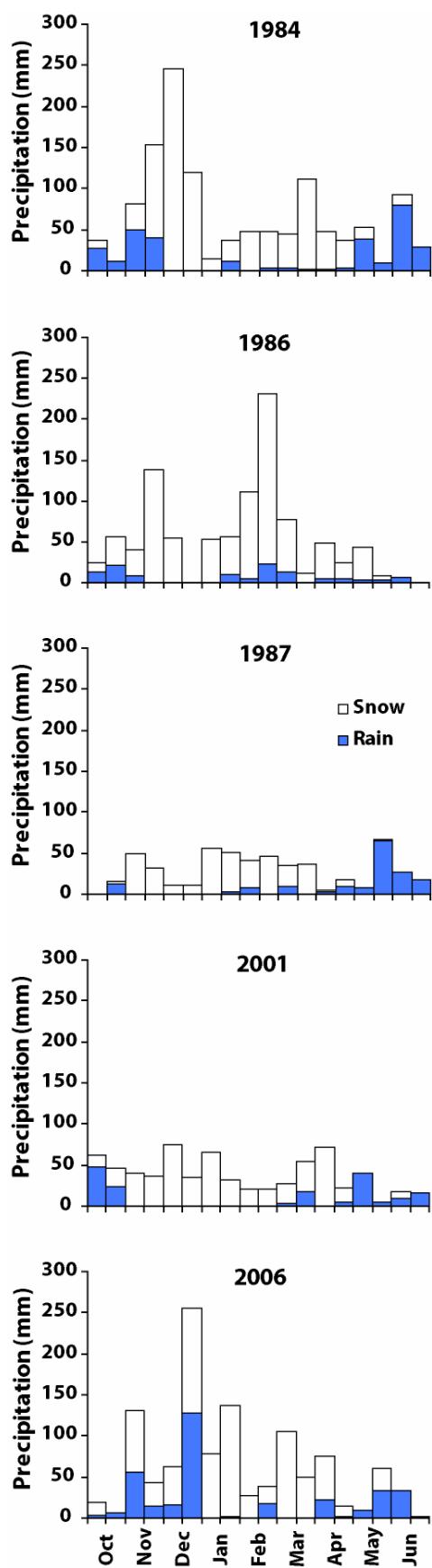


Figure 4.2: Bi-weekly basin total precipitation (snow and rain) for the five selected *snow seasons*.

seasonal precipitation was rain, most of this fell in fall, prior to or during early snowcover development and in late spring, during melt-out (**Figure 4.2**). Snowcover was initiated with a very large influx of snow during fall and early winter, and sustained by substantial snowfall during late winter and early spring.

The 1986 *snow season* was cool and wet. Average air temperatures were nearly 1°C above normal, though average Nov-May and dew point temperatures were low. Precipitation was 126 % of the long-term average wind corrected seasonal precipitation, only 12% (115 mm) of which was rain. The season was characterized by a very cold and snowy late fall, winter and early spring, with much higher temperatures in late spring. Though a substantial snowcover had developed during fall and early winter, a large input of snow occurred during late winter and early spring.

The 1987 *snow season* was warm and very dry with air temperature 1.5°C above normal, and the lowest seasonal humidity of the 5 snow seasons analyzed. Average Nov-May and storm temperatures were the warmest of all years analyzed. Seasonal precipitation was only 65% of wind corrected long term average, 31% (165 mm) of which was rain. If not for the 118 mm of rain in May and June, which fell after snow melt was complete, 1987 *snow season* would have been substantially drier.

The 2001 *snow season* was cool and dry with air temperatures close to normal, low humidity and the lowest average Nov-May temperatures of the years analyzed. Precipitation was 76% of long term wind corrected average. Only 23% (157 mm) of total precipitation was rain, most of which fell near the beginning or end of the snow season.

The 2006 *snow season* was warm and wet with air temperature 0.5°C above normal, high Nov-May temperatures and the highest storm dew points of the five *snow*

seasons analyzed. Precipitation was 127% of long term wind corrected average. 30% (346 mm) of total precipitation was rain and many rain-on-snow events occurred in the initial stages of snow cover development and throughout the season. The precipitation pattern is similar to 1984, with a large input of precipitation in fall and early winter. The significant difference, however, is that a substantial portion of this precipitation fell as rain. While rain-on-snow (ROS) events do occur in the RCEW, historically they have been infrequent, and most precipitation that fell as rain either occurred before snow cover initiation or after melt-out. As discussed in Chapter 3, rain is now a larger proportion of precipitation than in the past, and ROS is more frequent. In the selected *snow seasons*, 2006 is an example of this trend, where many mixed, rain and ROS events occurred throughout the *snow season*.

4. The Modeling Approach

The first objective is to investigate how a range of natural climate and precipitation variability alters patterns of snow deposition, melt, and the delivery of water to the soil and stream in a mountain basin. This is performed for the study snow seasons at RME with the *Isnobal* model and results are referred to as the base condition.

Isnobal is designed to run over a digital elevation model (DEM) grid and solves the snow cover energy and mass balance over each grid-cell. In general the energy balance of a snow cover can be given as:

$$\Delta Q = R_n + H + L_v E + G + M$$

where ΔQ is change in snow-cover energy, and R_n , H , $L_v E$, G and M are net radiative, sensible, latent, conductive and advective (from addition of precipitation mass) energy

fluxes. *Isnobal* represents the snow cover as a two-layer system: a surface fixed-thickness active layer and a lower layer. The model solves for the temperature and specific mass of each layer. Melt is computed in either layer when the *cold content* is greater than 0.0. Runoff from the base of the snow cover is predicted when the accumulated liquid water content exceeds a specific threshold. In addition to the state variables listed in **Table 4.2**, the model predicts energy and mass fluxes to and from the snow cover. Downward fluxes from the bottom of the snow cover and rain in the absence of snow are considered surface water input (SWI). Marks et al. (1999) present a detailed description of the equations solved and a discussion of the structure of the model.

Table 4.2: State variables predicted and forcing variables required by the *Isnobal* snow model.

State Variables:	Forcing Variables:
Snow Depth (m)	Net Solar Radiation (W m^{-2})
Snow Density (kg m^{-3})	Incoming Thermal Radiation (W m^{-2})
Snow Surface Layer Temperature ($^{\circ}\text{C}$)	Air Temperature ($^{\circ}\text{C}$)
Average Snow Cover Temperature ($^{\circ}\text{C}$)	Vapor Pressure (Pa)
Average Snow Liquid Water Content (%)	Wind Speed (m s^{-1})
	Soil Temp ($^{\circ}\text{C}$)
	Precipitation Mass (mm)
	Precipitation Temperature ($^{\circ}\text{C}$)

The model has been extensively tested and verified across mountainous regions of the western US and Canada (Marks et al. 1999; Link and Marks 1999a&b), to simulate snow cover processes and properties during rain-on-snow (ROS) (Marks et al. 1998, 2001a), and to simulate the interaction of topography and vegetation with the seasonal snow cover (Marks et al. 2002). When coupled to a wind-field and snow redistribution

model, *Isnobal* accurately predicted patterns of snow water equivalent (SWE) and snow covered area (SCA), including wind scour and deposition (drifting) (Winstral et al. 2002; Winstral and Marks 2002; Marks et al. 2002; Winstral et al. 2008a&b).

For this experiment, *Isnobal* is coupled with a wind field and snow redistribution model (Winstral and Marks 2002) to simulate hourly snow cover development and melt. The wind field and snow redistribution model (Winstral and Marks 2002) uses shelter or exposure parameters derived using upwind topography and vegetation to develop distributed time-series of snow accumulation rates and wind speeds. A 10x10 m grid cell DEM is used as a base for model simulations along with a 10x10 m grid vegetation coverage map to account for canopy effects. Continuous model simulations were done at an hourly time step for five *snow seasons* (1984, 1986, 1987, 2001, and 2006). A *snow season* is defined as the 9-month period from October 1 to June 30. Hence, the 1984 *snow season* runs from October 1, 1983, to June 30, 1984. Distributed surfaces of forcing meteorological variables (**Table 4.2**) are generated using the data collected at *ridge* and *grove sites*. Redistribution of precipitation by wind is a function of precipitation phase, which was decided on the basis of dew point temperature (T_{dp}) (Marks and Winstral 2008). As precipitation phase is adjusted for altered temperature model scenarios, Alter-shielded gauge-catch at the *ridge site* is adjusted by a best-fit regression developed from base-condition averages of T_{dp} and wind speed (u_s) at the *ridge site*, and the ratio of precipitation at the *grove* and *ridge sites* ($P_{pt(grove/ridge)}$) for the selected *snow seasons*:

$$P_{pt(grove/ridge)} = 1.76 \quad u_s \geq 10 \text{ m s}^{-1} \text{ or } T_{dp} \geq -2.7^\circ\text{C}$$

$$P_{pt(grove/ridge)} = 0.311 + 0.2183 * u_s - 0.0864 * T_{dp} \quad u_s < 10 \text{ m s}^{-1} \text{ and } T_{dp} < -2.7^\circ\text{C}$$

In the case of change in precipitation phase to mixed (from all snow or rain), alter-shielded precipitation gauge catch is adjusted using the weighted average ratio depending on the fraction of snow and rain. For pure rain events, wind-corrected gauge catch at the *grove site* is uniformly distributed across the RME catchment.

Model performance for the base condition was evaluated by comparison of model values of SWE and SWI to equivalent field data. Model simulated daily SWE at the *grove site* grid cell to measured SWE at the *grove site* snow pillow. Verifying SWI is less direct. The model calculates surface water input (SWI), which is the delivery of liquid water, including snowmelt and rain, to the soil surface at each grid cell. Though SWI is indirectly related to stream discharge, most of the fall and early winter SWI is utilized for recharge of soil and ground water storage. The exception to this is the occurrence of large ROS events when the soil is either frozen or saturated, as occurred in 2006. To remove uncertainty from SWI losses to soil moisture storage, in our evaluation of model performance for SWI, we compare cumulative predicted basin average SWI to cumulative stream discharge for the period from peak SWE to the end of the *snow season*.

SWE and SWI were evaluated using three standard tests: (1) The root mean square difference (RMSD), (2) the mean bias difference (MBD) and (3) the Nash-Sutcliffe model efficiency (ME) (Nash and Sutcliffe 1970). The three tests are calculated as

$$RMSD = \frac{1}{n} \sqrt{\sum_{i=1}^n (x_{sim(i)} - x_{obs(i)})^2}$$

$$MBD = \frac{1}{n} \sum_{i=1}^n (x_{sim(i)} - x_{obs(i)})$$

$$ME = 1 - \left[\frac{\sum_{i=1}^n (x_{sim(i)} - x_{obs(i)})^2}{\sum_{i=1}^n (x_{obs(i)} - \bar{x}_{obs})^2} \right]$$

5. Experimental Design

The second objective of this research is to investigate the sensitivity of the seasonal snowcover to expected changes in temperature and humidity expected under climate warming for each of the base conditions. Potential significant effects include direct effects on sensible heat flux between the atmosphere and the snowcover, temperature influences on humidity by altering the water-holding capacity, and thermal radiation from the atmosphere (see Brutsaert 1975, 1982; Marks and Dozier 1979, 1992).

Forcing data scenarios were developed from the base-level data, by adjusting temperatures $+2^{\circ}\text{C}$ and -2°C , which was approximately the magnitude of change presented in Chapter 3. To insure consistent precipitation events, and temperature – humidity coherence in forcing data for the scenarios, we kept the relative humidity constant. Temperature – humidity coherence means that precipitation could only occur when humidity was at, or close to saturation. The most objective way to insure this is to keep the relative humidity unchanged and to re-calculate the absolute humidity for the scenarios. This approach had the effect of increasing the T_{dp} for the $+2^{\circ}\text{C}$ scenarios, and decreasing T_{dp} for the -2°C scenarios in a way that was similar to trends in precipitation phase noted in Chapter 3.

For each temperature scenario, precipitation event timing and volume were held constant, but adjusted temperature and humidity resulted in changes in precipitation phase and the magnitude of redistribution. Changes in precipitation phase altered snow albedo, which is a function of temperature and density of snowfall (Marks et al. 1999), resulting in lower snow albedo for warm or mixed rain/snow events. ROS causes in accelerated grain growth, further lowering snow albedo (Marks et al. 1998).

6. Results and Discussion

In this section results of the modeling experiment are presented. In section **6.1** results of the base-condition simulations are summarized and validated. Section **6.2** compares basin average SWE and cumulative SWI results between the base and scenario simulations. Section **6.3** presents spatial results for the base and scenario simulations, evaluating changes in snow distribution for two of the five selected *snow seasons*. Finally, section **6.4** presents a detailed analysis of how warming or cooling may affect extreme events such as drought or flooding.

6.1. Base-Condition Simulations

Simulation results for base-conditions for each of the selected *snow seasons* illustrates the differences in key hydrologic cycle parameters during wet and dry, cold and warm *snow seasons*. **Figure 4.3a** compares measured snow pillow and snow course SWE at the *grove site* to the simulated value from the grid cell that contains the *grove site* for all five selected *snow seasons*. The *Isnobal* model reliably simulates both the accumulation and ablation of SWE at the *grove site*, and even handles mixed precipitation and rain-on-snow (ROS) events. Simulated basin average SWE for each of

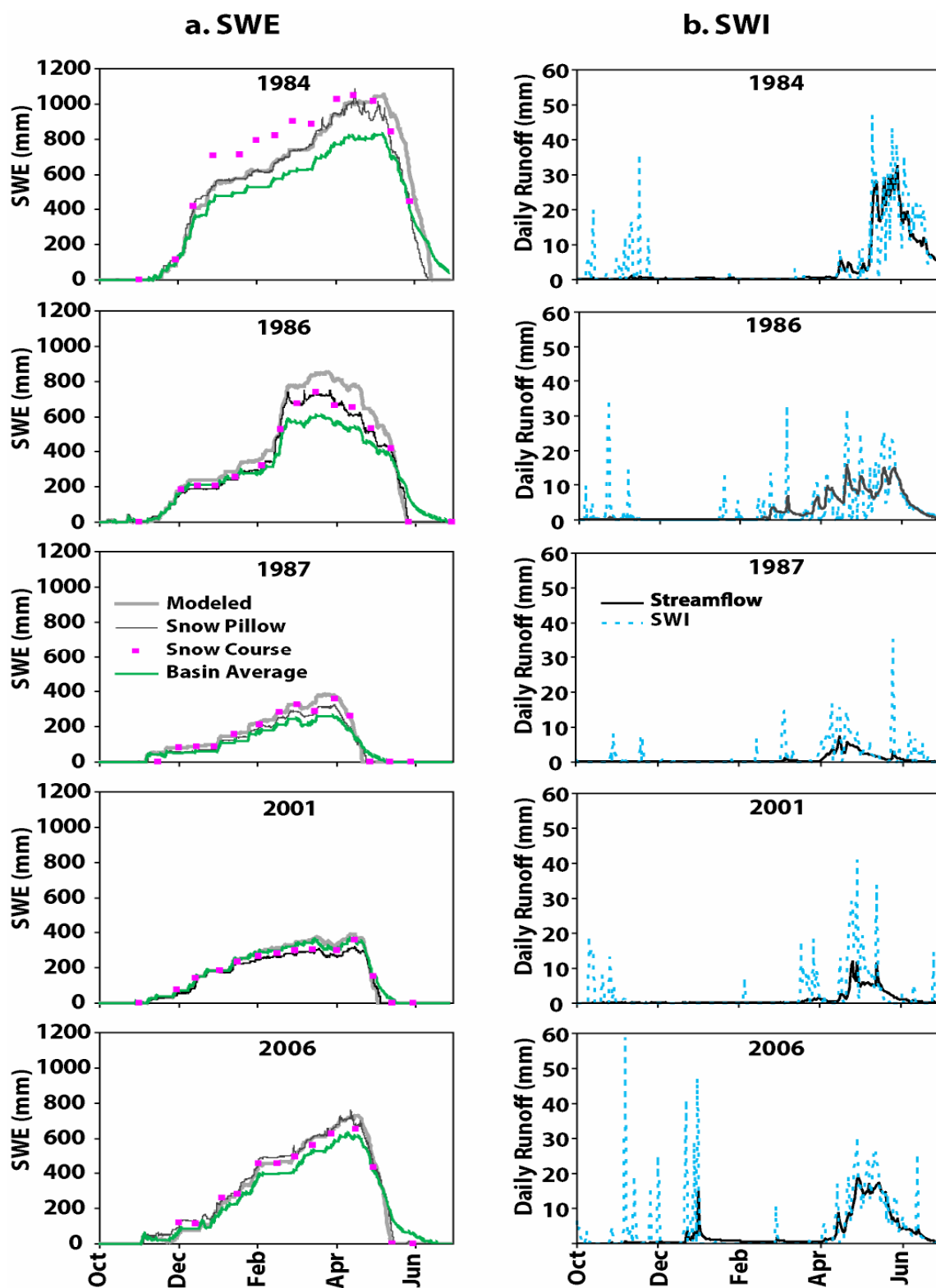


Figure 4.3: Base-condition simulation results for each of the selected *snow seasons*. a) *Grove site* snow pillow and snow course results are compared to SWE from the *grove site* simulation grid cell, and to simulated basin average SWE. b) daily total simulated surface water input (SWI) compared to measured streamflow.

the selected *snow seasons* is also presented. Both measured and simulated SWE at the *grove site*, which is a sheltered clearing surrounded by trees (similar in many ways to NRCS SNOTEL sites), is generally greater than basin average SWE at RME.

Figure 4.3a also shows that basin average SWE continues for several weeks after melt-out at the *grove site*, indicating that drift areas continue to hold snow even after the snowcover over most of the rest of the catchment has melted. These simulation results are in agreement with those presented by Winstral and Marks (2002) and Marks et al. (2002) who showed that within RME, snow deposition and melt patterns are controlled by the distribution of terrain and vegetation shelter and exposure zones, with sheltered areas holding more snow and melting later than exposed areas which hold less snow and melt earlier.

Comparing point measurements to spatially derived values is not straight-forward. While the *grove site* snow course and the snow pillow are in the same general area, they are located 3-5 m apart and do not measure the same snowcover. In some years, the snow course SWE is nearly identical to snow pillow SWE, but in others, particularly during cold, wet snow seasons, like 1984, it tends to track well during snowcover development and melt-out, but be larger during mid-season. During cold conditions, snow deposition is highly variable, while warmer conditions tend to have more uniform snow distribution. Simulated SWE is based on mean snow deposition conditions over a 10x10m area, and does not account for within-grid-cell variability. It is also difficult to specify the exact area represented by the selected grid-cell, because the positional accuracy of the DEM is no better than +/- 5m, so location of the model grid-cell representing the *grove site* is only approximate.

1984 *snow season* was cold and wet with April 1 SWE measured at the *grove site* 178% (945 mm) and stream discharge from the basin 187% (1040 mm) of long-term (1962-2006) seasonal average (October 1 to June 30). During the cold, wet 1984 *snow season*, a small drift occurred in the snow course track during mid-winter. This resulted in a 14-18% difference between snow course and snow pillow SWE from January to mid-March. During this time, simulated SWE closely matched the snow pillow, suggesting that the simulation conditions within the *grove site* grid-cell did not recognize or account for the snow course drift. During the cool, wet 1986 *snow season*, snow course and snow pillow SWE are in good agreement, with April 1 SWE at the *grove site* was 125% (669 mm) and seasonal stream discharge from the basin was 152% (800 mm) of long-term seasonal average. Simulated SWE matches observations during snowcover development and melt-out, but over-estimates measured SWE by 6-10% from mid-February to early April. Measured dew point temperatures during the 1986 snow season are questionable, due to instrument calibration issues. The data indicate that the mid-February storm was all snow, while the drop in snow pillow SWE (**Figure 4.3a**) suggests it was a mixed rain/snow event. In 1987 the temperature/humidity sensor was replaced with a more robust design.

During the 1987, 2001 and 2006 snow seasons, simulated SWE generally matches both snow course and snow pillow SWE. **Figure 4.3a**, however, shows that simulated SWE better matches snow course SWE during the 1987 and 2001 snow seasons. 1987 April 1 SWE was 57 % (305 mm) and seasonal stream discharge only 40 % (213 mm) of the long-term seasonal average. 2001 April 1 SWE was 50% (264 mm) and seasonal stream discharge 54% (283 mm) of the long-term seasonal average. In 2006, April 1

SWE was 128% (681 mm) of the average and total seasonal stream discharge was about 145% (762 mm) of the average.

Comparison of daily total SWI and stream discharge is presented in **Figure 4.3b** for each of the simulation years. SWI generated during October-December in most years is due to rain or warm conditions following snow events, resulting in melt of a shallow snowcover. In most years SWI virtually ceases once the snowcover develops, beginning again only when snowmelt starts in spring. The effect of mixed or rain-on-snow (ROS) precipitation events can be seen in SWI spikes in late fall, winter, and increase in stream discharge before initiation of snowmelt. **Figure 4.3b** indicates that much of the SWI generated during the fall and winter contributes to recharge of groundwater and soil water storage. This is particularly evident during the 2006 *snow season*, when a substantial volume of SWI was generated during fall and early winter with little subsequent streamflow. However, during spring snowmelt, SWI shows good relationship to stream discharge. Correlation between SWI and stream discharge is weaker for dry *snow seasons* because a much larger fraction on SWI is required to bring the soils to field capacity prior to initiation of streamflow.

Model performance was evaluated for both SWE and SWI. Results of the performance tests are presented in **Table 4.3** below. Model efficiency (ME) for predicted snow season daily SWE is good in all years, but is slightly less in the 1987 and 2001 drought years. In general predicted SWE is slightly higher in most years, with RMS differences between predicted SWE and total precipitation of 6% for 1984, 7% for 1986, 7% for 1987, 6% for 2001 and 3% for 2006. Model efficiency (ME) for predicted cumulative daily SWI during melt-out is very good during the 1984, 1986 and 2006 snow

seasons. For 1984 and 1986, predicted SWI has little bias, with RMS differences between predicted SWI and measured *snow season* streamflow of 4% for both 1984 and 1986. Both MB and RMS differences are large (+11% and 12% respectively) for the warm, and very rainy 2006. The larger differences in 2006 occur in spite of the fact that it was a substantial *snow season* (135% of average), because the previous 6 *snow seasons* were dry (2000, 67%; 2001, 55%; 2002, 97%; 2003, 74%; 2004, 90%; 2005, 76%), so that much of the generated SWI was utilized for soil and ground water recharge.

Table 4.3: Root mean square difference (RMSD), (2) mean bias difference (MBD) and (3) Nash-Sutcliffe model efficiency (ME) for daily simulated vs. measured SWE at the *grove site* from the start of snowcover to the end of the *snow season*, and cumulative simulated basin SWI vs. measured streamflow from peak SWE to the end of the *snow season* for each of the simulation years.

Snow Seasons	RMSD	MBD	ME
Daily SWE (mm)			
1984	84	30	0.93
1986	78	58	0.90
1987	40	33	0.82
2001	43	32	0.81
2006	36	-20	0.97
Cumulative Daily SWI (mm)			
1984	38	9	0.98
1986	28	-17	0.99
1987	95	78	-2.30
2001	148	124	-4.68
2006	90	80	0.84

For the 1987 and 2001 drought years, however, model efficiency (ME) for predicted cumulative daily SWI from during melt-out is poor, with a strong bias toward more simulated SWI than measured streamflow (+37% for 1987, +44% for 2001), and

RMS differences of 45% for 1987 and 52% for 2001. Clearly, much of the SWI generated during drought years is utilized for recharge of soil and ground water storage. The very large RMS and bias differences in 2001 occurred because the proceeding *snow season* was also dry (66% of average), whereas the year proceeding 1987 was 141% of average.

Comparison of cumulative seasonal SWI and stream discharge on July 1 is presented in **Figure 4.4**, which shows that for the cold, wet years measured stream discharge was a significant fraction of simulated SWI (90% in 1984, 87% in 1986). This was because the preceding twelve water years (1975 – 1986) were very wet. Only 3 years were below average (1977, 1979, and 1981), and the three wettest years on record were 1982 (148%), 1983 (143%), and 1984 (154%). For the 1984 and 1986 snow seasons, there was a small soil and ground water storage deficit, and SWI was converted almost directly to streamflow.

However, for the warm, wet 2006 *snow season*, this fraction was reduced (67% in 2006), because that year was preceded by 6 dry years, and much of the early season SWI went to soil and ground water recharge. In the 1987 and 2001 dry years, stream discharge was only 44% and 42% of simulated SWI respectively. During dry years, it generally takes a larger percentage of SWI to bring the soils to saturation prior to the initiation of streamflow. Conditions during 1987 and 2001 were both dry, but circumstances were quite different. Though conditions prior to 1987 were wet, the 1987 snow season was very warm, was the second driest year on record and without the 118 mm of rain (nearly 25% of *snow season* precipitation) that fell after melt-out, would have been the driest on record. Most of this late spring rain went to again recharge the soil and

groundwater, rather than being translated into streamflow. The 2001 *snow season* was cool and not as dry as 1987, and produced more streamflow though as a percentage of SWI it was less. 2001 was the second of a pair of very dry years (2000 was just 66% of average) so the soil and groundwater deficit was larger and consumed a larger percentage of SWI.

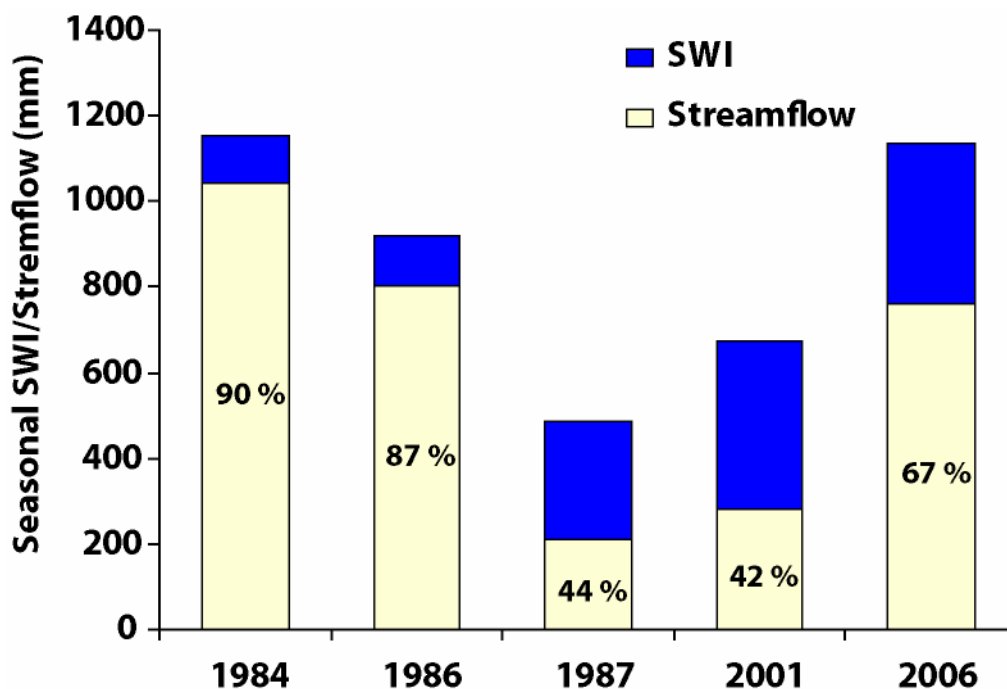


Figure 4.4: Base-condition total *snow season* SWI and streamflow for each of the selected *snow seasons*. Note that in cold wet years streamflow is nearly equal to SWI, while in warm, wet years it is less, and in dry years it is substantially less.

In all five simulated snow seasons, snowcover was initiated in November. For all years, except 1986, peak SWE occurs in late April – early May. SWE peaked in March in 1986 due to a very large mid-March snow event, with very little precipitation after

that. In cold wet years (1984, 1986) SWI peaks in late May – early June, while in dry years (1987, 2001) SWI peaks in April. The warm and wet 2006 *snow season* is anomalous, in that SWI occurs throughout the snow season, with dual peaks – one in December, one in May.

6.2. Base, -2°C, and +2°C Scenario Simulations:

Basin Average Results

Basin average SWE for selected dates, date of 50% SWI, cumulative SWI at the time of peak SWE and precipitation and rainfall total for base, -2°C and +2°C scenarios for each of the simulation years are presented in **Tables 4.4-4.8**. **Figure 4.5a** presents daily basin average SWE for the base, -2°C and +2°C simulations for each of the selected *snow seasons*. As expected the -2°C scenarios show greater SWE and the +2°C scenarios show less SWE when compared to base simulations. It is noteworthy that with the exception of the 2006 *snow season*, the decrease in simulated SWE with the +2°C scenarios is much greater than the increase with the -2°C scenarios.

Because precipitation mass is forced to be nearly constant in base and altered temperature scenario simulations, the primary influence of decreasing the temperature on precipitation is a change of phase from rain into snow. In cold, wet years, there was not much rain for the base simulation, so colder temperatures added only a small amount of additional SWE. In dry years, there was little precipitation, and while the rain proportion was substantial (31% for 1987; 23% for 2001) the depth was small (165 mm for 1987; 157 mm for 2001) and most rain fell before snowcover development , or after the

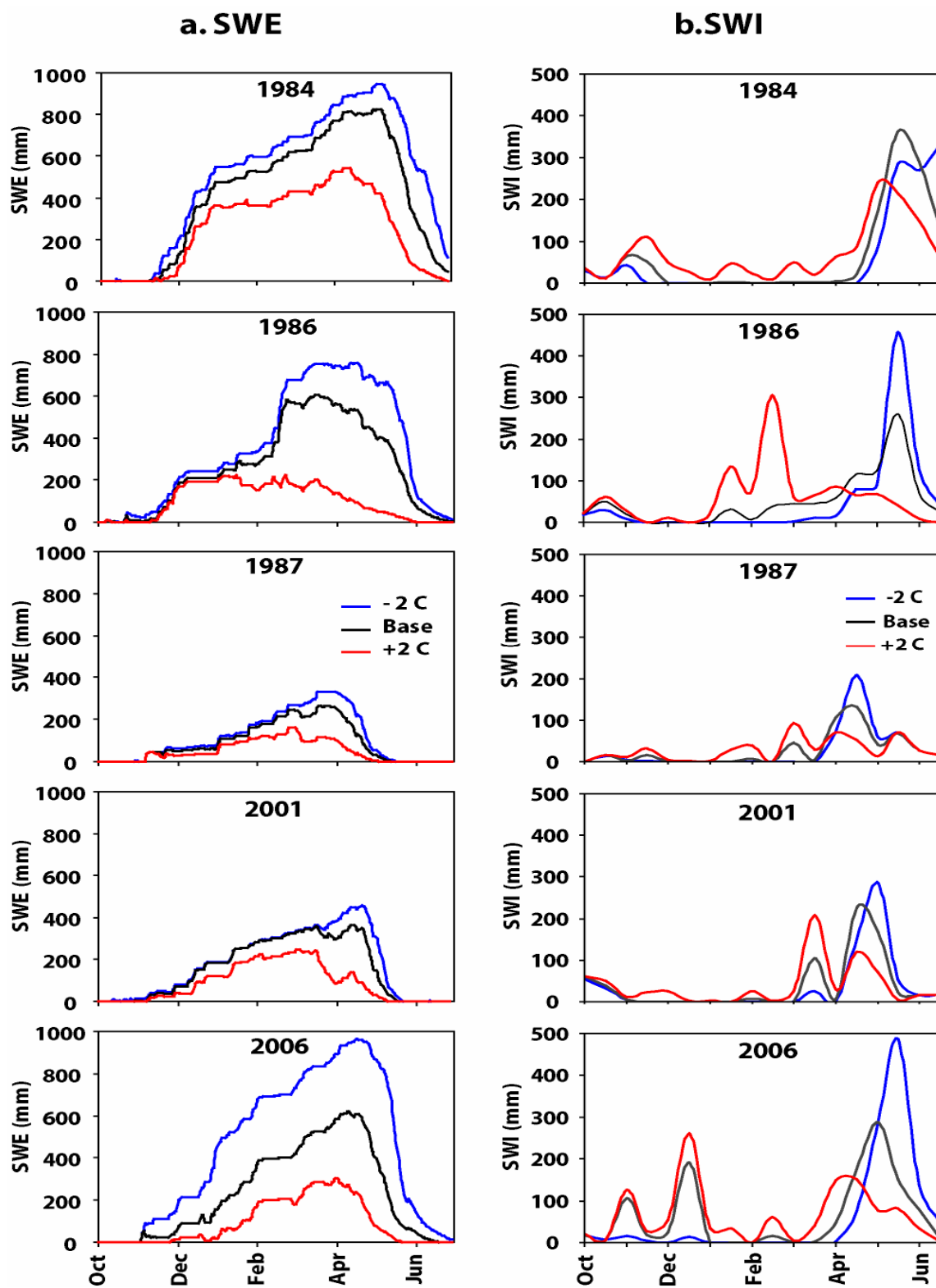


Figure 4.5: a) Daily basin-average SWE for the base, -2°C , and $+2^{\circ}\text{C}$ simulations for each of the selected *snow seasons*. b) Bi-weekly basin-total SWI hydrographs for the base, -2°C , and $+2^{\circ}\text{C}$ simulations for each of the selected *snow seasons*.

snow melted. For the dry years, simulated colder temperatures had almost no effect until spring, when peak SWE showed a relative increase over base conditions and snowcover persisted a few days later. The 2006 *snow season*, however, was wet and warm, with 30% (346 mm) of *snow season* precipitation falling as rain, so colder temperatures added a substantial amount of SWE.

In **Tables 4.4-4.8** the 200 mm SWI value is approximately $\frac{1}{2}$ that required to recharge the soil – groundwater system so that streamflow can be initiated (see **Table 3.11**; Chapter 3). The date of 50% SWI indicates timing of the delivery of water to the soil, and the percentage of total seasonal SWI at peak SWE shows how coupled SWI is to SWE. Cold, wet or dry conditions (1984, 1987, 2001) tend to delay recharge until spring, and 50% SWI until after peak SWE. Warm, wet conditions (1986, 2006) tends to earlier recharge of the soil – groundwater system, and date of 50% SWI. All of the selected years show a strong relationship between SWE and SWI, with the colder years (1984, 1986, and 1987) indicating that only about 20% of SWI had been produced by the date of peak SWE, and the warmer years (2001 and 2006) indicating about 35%. Cold scenarios delay SWI production and recharge, and increase the significance of peak SWE. Warmer scenarios cause SWI production and recharge to occur much earlier, and significantly reduce the relationship between SWE and SWI.

For the 1984 *snow season* (**Table 4.4**), the cold scenario does not change the date of peak SWE, increases it by only 14% (119 mm), shifts the date of 200 mm SWI to 18 days later, the date of 50% SWI to 9 days later, reduces the percent of SWI occurring prior to peak SWE to only 8%, and reduces the rain fraction to only 12% of total precipitation. The warm scenario reduces peak SWE by 34% (282 mm), and shifts the

date of peak SWE 23 days earlier. The rain fraction nearly doubles from 25% to 47%, the date of 200 mm SWI to nearly 5 months (163 days) earlier and 50% SWI 25 days earlier. Nearly 50% of the season SWI occurs prior to peak SWE, significantly reducing the relationship between SWE and SWI.

Table 4.4: 1984 *snow season* basin-average SWE for selected dates, date and depth of peak SWE, dates of 200 mm and 50% SWI, SWI occurring prior to peak SWE and precipitation and rain total. Percentages in parentheses (%) indicate the fraction of peak SWE, total SWI or the rain fraction of total precipitation. Positive or negative numbers in parentheses (+/-) indicate date advance or retreat from base conditions.

	-2.0 °C	Base Case	+2.0 °C
Peak SWE:			
Depth (mm):	945	826	544
Date:	5-May	5-May	12-Apr (-23)
Seasonal SWE, mm (%):			
23 Dec	444 (47%)	373 (45%)	281 (52%)
1 Mar	693 (73%)	621 (75%)	430 (79%)
16 Mar	746 (79%)	672 (81%)	443 (81%)
1 Apr	846 (90%)	770 (93%)	527 (97%)
16 Apr	889 (94%)	801 (97%)	501 (92%)
1 May	933 (99%)	822 (99%)	450 (83%)
16 May	879 (93%)	694 (84%)	282 (52%)
1 Jun	581 (61%)	325 (39%)	79 (15%)
Date of 200 mm SWI:	19-May (+18)	1-May	19-Nov (-163)
Date of 50% SWI:	4-Jun (+9)	26-May	1-May (-25)
SWI @ Peak SWE:	86 (8%)	216 (20%)	500 (47%)
Precipitation, mm:	1202	1221	1294
Rain, mm (%):	149 (12%)	307 (25%)	604 (47%)

The 1986 *snow season* (**Table 4.5**) was not as cold as 1984, and had more storm events that were either mixed rain – snow, or very close to that the dew point criterion for

determining precipitation phase. Because of these conditions, the cold scenario caused a larger divergence from base conditions than in 1984. Nearly all the season rain was converted to snow. This, delayed the date of peak SWE by 30 days, while increasing it by 26% (155 mm), delaying the date of 200 mm SWI by nearly 2 months, and 50% SWI by 23 days, reducing the proportion of SWI that occurred prior to peak SWE from 22% to

Table 4.5: 1986 *snow season* basin-average SWE for selected dates, date and depth of peak SWE, dates of 200 mm and 50% SWI, SWI occurring prior to peak SWE, and precipitation and rain totals. Percentages in parentheses (%) indicate the fraction of peak SWE, total SWI or the rain fraction of total precipitation. Positive or negative numbers in parentheses (+/-) indicate date advance or retreat from base conditions.

	-2.0 °C	Base Case	+2.0 °C
Peak SWE:			
Depth (mm):	759	604	225
Date:	15-Apr (+30)	16-Mar	21-Feb (-23)
Seasonal SWE, mm (%):			
23 Dec	241 (32%)	212 (35%)	193 (86%)
1 Mar	677 (89%)	566 (94%)	173 (77%)
16 Mar	754 (99%)	604 (100%)	201 (89%)
1 Apr	744 (98%)	563 (93%)	139 (61%)
16 Apr	758 (100%)	535 (88%)	96 (43%)
1 May	683 (90%)	425 (70%)	56 (25%)
16 May	607 (80%)	329 (54%)	34 (15%)
1 Jun	152 (20%)	82 (14%)	2 (1%)
16 Jun	49 (20%)	23 (4%)	0
Date of 50% SWI:	25-May (+23)	2-May	19-Feb (-73)
Date of 200 mm SWI:	2-May (+56)	7-Mar	18-Jan (-48)
SWI @ Peak SWE:	88 (10%)	215 (22%)	556 (61%)
Precipitation, mm:	977	981	1079
Rain, mm (%):	28 (3%)	115 (12%)	497 (46%)

10%, and reducing the rain fraction to only 3% of total precipitation. However, the warm scenario had an even stronger affect. Peak SWE was reduced by 63% (379 mm), and the date of peak SWE is shifted 23 days earlier to mid- February. The date of 200 mm SWI is a 1½ months (48 days) earlier, and 50% SWI is 2½ months (73 days) earlier, 61% of SWI occurs prior to peak SWE and the rain fraction nearly quadruples, from 12% to 46%. Melt-out dates are slightly extended by the cold scenario but reduced by nearly a month by the warm scenario.

For the warm and dry 1987 *snow season* (**Table 4.6**), the cold scenario does not change the date of peak SWE, increases it by 26% (68 mm), delays the date of 200 mm SWI by 9 days, the date of 50% SWI by only 5 days, decreased the proportion of SWI occurring prior to peak SWE from 19% to 5%, and only slightly reduces the rain fraction to 21% of total precipitation. The warm scenario shifts the date of peak SWE to 25 days earlier, and reduces peak SWE by 39% (102 mm). The date of 200 mm SWI occurs 40 days earlier, the date of 50% SWI 28 days earlier, the proportion of SWI that occurs prior to 50% SWE increases from 19% to 28%, and the rain fraction increases, from 31% to 43%.

For the cool, dry 2001 *snow season* (**Table 4.7**), the cold scenario delays the date of peak SWE 7 days, increases it by 26% (94 mm), delays the date of 200 mm SWI by a month (29 days), 50% SWI by 9 days, reduces the proportion of SWI occurring prior to the date of 50% SWE from 33% to 18%, and reduces the rain fraction by half to 12% of total precipitation. The warm scenario shifts the date of peak SWE to 41 days earlier, and reduces peak SWE by 32% (116 mm). The date of 200 mm and 50% SWI are shifted to

Table 4.6: 1987 *snow season* basin-average SWE for selected dates, date and depth of peak SWE, dates of 200 mm and 50% SWI, SWI occurring prior to peak SWE, and precipitation and rain totals. Percentages in parentheses (%) indicate the fraction of peak SWE, total SWI or the rain fraction of total precipitation. Positive or negative numbers in parentheses (+/-) indicate date advance or retreat from base conditions.

	-2.0 °C	Base Case	+2.0 °C
Peak SWE:			
Depth (mm):	331	263	161
Date:	23-Mar	23-Mar	26-Feb (-25)
Seasonal SWE, mm (%):			
23 Dec	74 (22%)	60 (23%)	36 (22%)
1 Mar	268 (81%)	243 (92%)	159 (99%)
16 Mar	295 (89%)	227 (86%)	97 (60%)
1 Apr	328 (99%)	253 (96%)	103 (64%)
16 Apr	230 (69%)	134 (51%)	36 (22%)
1 May	53 (16%)	31 (12%)	4 (2.5%)
16 May	3	0	0
1 Jun	0	0	0
Date of 50% SWI:	26-Apr (+5)	21-Apr	24-Mar (-28)
Date of 200 mm SWI:	24-Apr (+9)	15-Apr	6-Mar (-40)
SWI @ Peak SWE:	23 (5%)	92 (19%)	136 (28%)
Precipitation, mm:	528	532	543
Rain, mm (%):	110 (21%)	165 (31%)	235 (43%)

nearly a month (25 and 29 days, respectively) earlier, and the rain fraction is increased from 25% to 44%. Because the warm scenario reduces SWE and shifts the date of peak SWE to mid-winter, the proportion of SWI occurring prior to peak SWE actually declines from 33% to 30%.

For the warm and wet 2006 *snow season* (**Table 4.8**), which received nearly the same precipitation as 1984, but developed only 75% the peak SWE, the cold scenario converts most of the season rain to snow, delaying the date of peak SWE 6 days and

Table 4.7: 2001 *snow season* basin-average SWE for selected dates, date and depth of peak SWE, dates of 200 mm and 50% SWI, SWI occurring prior to peak SWE, and precipitation and rain totals. Percentages in parentheses (%) indicate the fraction of peak SWE, total SWI or the rain fraction of total precipitation. Positive or negative numbers in parentheses (+/-) indicate date advance or retreat from base conditions.

	-2.0 °C	Base Case	+2.0 °C
Peak SWE:			
Depth (mm):	456	362	246
Date:	21-Apr (+7)	14-Apr	4-Mar (-41)
Seasonal SWE, mm (%):			
23 Dec	185 (41%)	181 (50%)	118 (48%)
1 Mar	327 (72%)	323 (89%)	234 (95%)
16 Mar	361 (79%)	356 (98%)	244 (99%)
1 Apr	381 (84%)	296 (82%)	83 (34%)
16 Apr	449 (98%)	358 (99%)	114 (46%)
1 May	310 (68%)	150 (41%)	30 (12%)
16 May	39 (9%)	12 (3%)	0
1 Jun	0	0	0
Date of 50% SWI:	5-May (+9)	26-Apr	28-Mar (-29)
Date of 200 mm SWI:	27-Apr (+29)	29-Mar	4-Mar (-25)
SWI @ Peak SWE:	124 (18%)	224 (33%)	200 (30%)
Precipitation, mm:	677	685	697
Rain, mm (%):	81 (12%)	168 (25%)	304 (44%)

increasing it by 55% (340 mm). Because cold scenario converts the wet, rainy fall for the base condition to snow, the date of 200 mm SWI is delayed by nearly 5 months (137 days) from December 21 to May 7. However, the date of 50% SWI is only delayed 19 days, the proportion of SWI occurring prior to peak SWE reduced from 35% to 5%, and the rain fraction from 30% to 12% of total precipitation. The warm scenario reduces peak SWE by 52% (320 mm), and shifts the date of peak SWE 10 days earlier. The date of 200 mm SWI is shifted nearly a month (20 days) earlier, occurring in mid-fall. The date

of 50% SWI is shifted 2 months earlier (61 days) earlier, the proportion of SWI occurring prior to peak SWE from 35% to 59%, and the rain fraction nearly doubles, from 30% to 56%. Melt-out dates are extended by the cold scenario by about 2 weeks, but reduced by nearly a month in the warm scenario.

Table 4.8: 2006 *snow season* basin-average SWE for selected dates, date and depth of peak SWE, dates of 200 mm and 50% SWI, SWI occurring prior to peak SWE, and precipitation and rain totals. Percentages in parentheses (%) indicate the fraction of peak SWE, total SWI or the rain fraction of total precipitation. Positive or negative numbers in parentheses (+/-) indicate date advance or retreat from base conditions.

	-2.0 °C	Base Case	+2.0 °C
Peak SWE:			
Depth (mm):	962	622	306
Date:	17-Apr (+6)	11-Apr	1-Apr (-10)
Seasonal SWE, mm (%):			
23 Dec	286 (30%)	94 (15%)	10 (3%)
1 Mar	731 (76%)	417 (67%)	178 (58%)
16 Mar	836 (87%)	525 (84%)	285 (93%)
1 Apr	895 (93%)	583 (94%)	306 (100%)
16 Apr	961 (100%)	606 (97%)	236 (77%)
1 May	869 (90%)	408 (66%)	81 (26%)
16 May	550 (57%)	131 (21%)	18 (6%)
1 Jun	148 (15%)	48 (8%)	0
Date of 50% SWI:	18-May (+19)	29-Apr	27-Feb (-61)
Date of 200 mm SWI:	7-May (+137)	21-Dec	1-Dec (-20)
SWI @ Peak SWE:	62 (5%)	397 (35%)	669 (59%)
Precipitation, mm:	1132	1148	1159
Rain, mm (%):	131 (12%)	346 (30%)	644 (56%)

Figures 4.5b presents bi-weekly basin-total SWI for the base, -2°C and +2°C simulations for each of the selected *snow seasons*, plotted as SWI hydrographs. In

general the cold scenario shifts SWI to later and the warm scenario to earlier in the year. As discussed above, in wet years (1984, 1986, and 2006) SWI is translated almost directly to streamflow, but in dry years (1987 and 2001) SWI is utilized for soil and ground water recharge and is not strongly correlated to streamflow.

In 1984 the cold scenario delays SWI to beyond the simulation period, with peak SWI occurring on July 1. The warm scenario shifts peak SWI to about a month earlier and generates some winter SWI. The general shape of the SWI hydrograph is similar for base and both scenario simulations. In 1986 the cold scenario doesn't shift the date of peak SWI, but increases its magnitude by substantially reducing winter SWI. The warm scenario strongly shifts the date of peak SWI to 2½ months earlier in mid-winter.

Two of the selected *snow seasons* (1984 and 2006) are very similar in both the timing (**Figure 4.2**) and basin total of precipitation volume (1221 and 1148 mm respectively) and basin total simulated surface water input (SWI) (1155 and 1139 mm respectively) (**Figure 4.4**). However, the development of the seasonal snowcover and basin average SWE (**Figure 4.3b**) and the seasonal distribution of SWI (**Figure 4.5b**) are quite different. Most of this was caused by air and dew point temperature differences, and the resulting changes in precipitation phase. **Figure 4.5a** indicates that if the 2006 *snow season* had been colder, the development of SWE in the RME basin would have been very similar to the base condition in 1984, and if the 1984 *snow season* had been warmer basin SWE would have been similar to the base condition in 2006. **Figure 4.5b** shows a similar relationship for SWI. If the 2006 *snow season* had been colder, the resulting SWI hydrograph would have been similar to the base condition in 1984, and if

the 1984 *snow season* had been warmer, the resulting SWI hydrograph would have been similar to the base condition in 2006.

6.3. Base, -2°C and +2°C Scenario Simulations: Spatial Distribution Results

At the RME basin, snow distribution and melt patterns exhibit tremendous spatial heterogeneity (Winstral and Marks 2002; Marks et al. 2002). Marks et al. (2002) divided the RME basin into four shelter classes: *drift*, *sheltered*, *exposed* and *all else*, based on exposure/shelter to the upwind topography and vegetation. They showed that though *drift* and *sheltered* classes represent only 9% and 22% of the total basin area respectively they generally hold about 50% of the basin SWE, and contribute about 50% of the total generated SWI. *Drift* and *sheltered* classes also melt later than the other two shelter classes and responsible for almost all of the late spring SWI.

Though the comprehensive analyses of how the distribution of SWE and SWI over the RME catchment varies between the *snow seasons*, and how these distributions are affected by the cold and warm scenarios, are beyond the scope of this paper, bi-weekly distributions of SCA (%) and SWE (mm) for the base, -2°C, and +2°C scenario simulations are presented in **Figures 4.6 and 4.7** to illustrate spatial heterogeneities in the development and ablation of the snowcover. Simulated patterns of SCA and SWE show great spatial variability under all selected *snow seasons* and scenarios. During wet *snow seasons* (1984, 1986, and 2006) SWE depths range from very shallow (0-250 mm) to very deep (2500-3000 mm, even greater than 3000 mm in 1984 *snow season*) at the time

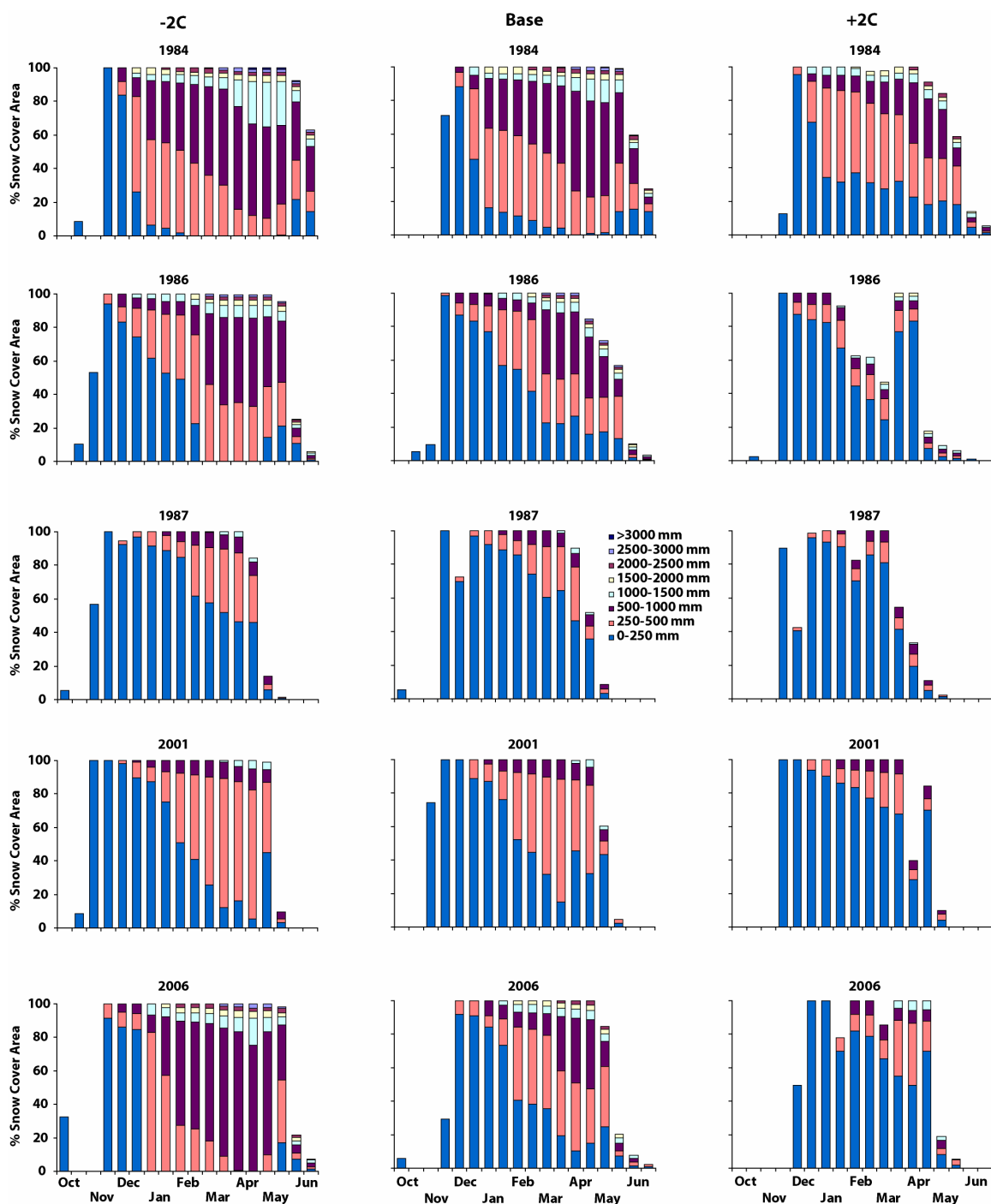


Figure 4.6: Bi-weekly basin area-normalized SCA (%), by SWE depth class for the base, -2°C , and $+2^{\circ}\text{C}$ simulations.

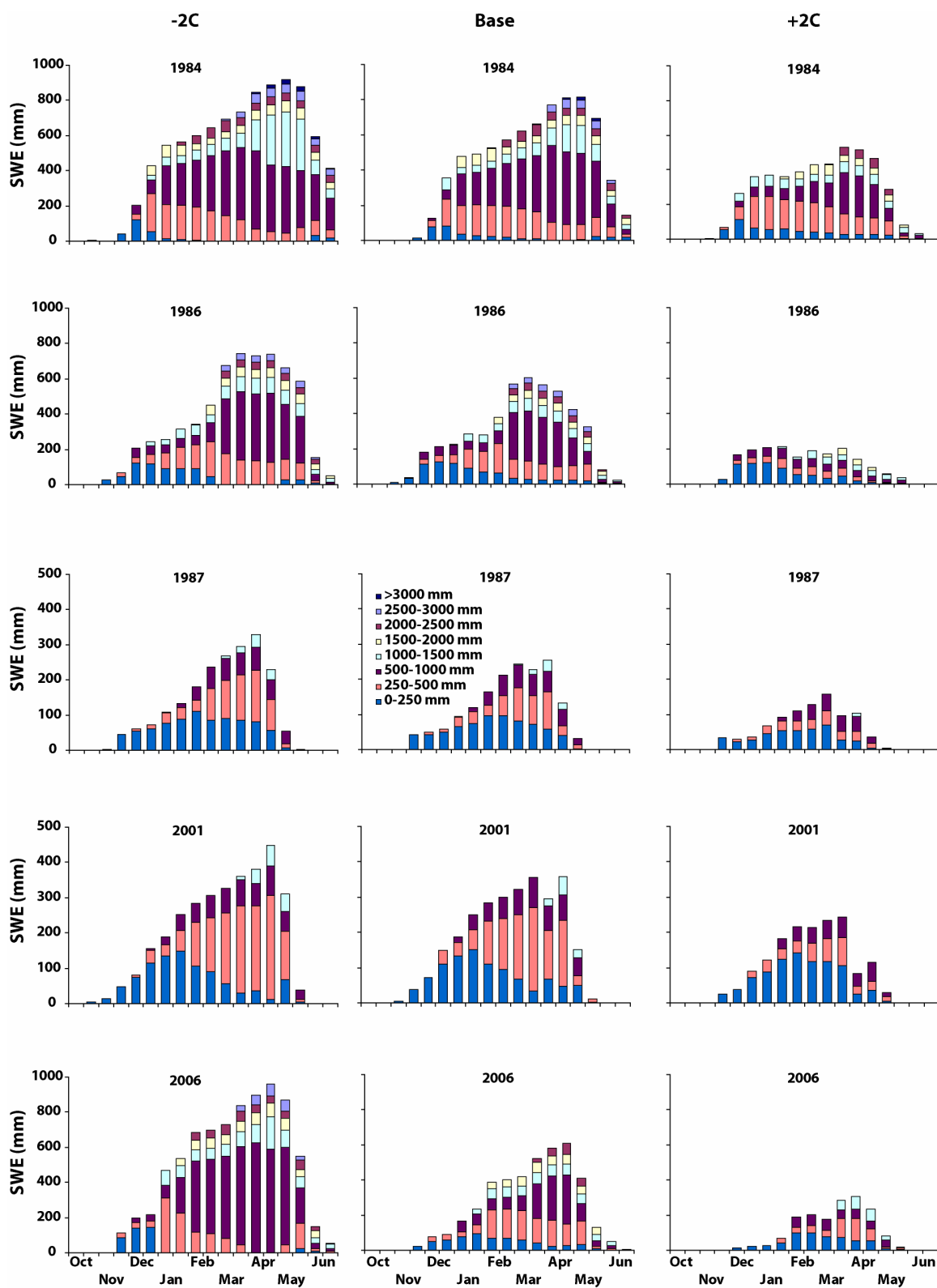


Figure 4.7: Bi-weekly basin average depth-normalized SWE (mm), by SWE depth class for the base, -2°C , and $+2^{\circ}\text{C}$ simulations. Note that the y-axis is scaled 0–1000 mm SWE for 1984, 1986, & 2006, and 0–500 mm SWE for 1987 & 2001 snow seasons.

of peak basin average SWE. During dry *snow seasons* (1987 and 2001) maximum SWE depth was in the range of 1000-1500 mm while some area of the basin was already snow free at the time of peak basin average SWE.

In all *snow seasons* higher ranges of SWE depths represent drift areas which continue to hold SWE during late spring. Lower ranges of SWE depths represent exposed conditions, where melt is initiated earlier (see also **Figure 4.8 and 4.9**). **Figure 4.6 and 4.7** show that both SCA and SWE increase with the cold scenario, and decrease as conditions get warmer. Though the precipitation mass and total seasonal SWI is essentially unchanged from base conditions for the scenario simulations, in all *snow seasons* the snowcover generally continues to develop in the cold scenario until the peak SWE is reached resulting in a sharp spring snowmelt pulse. Under the warm scenario frequent rain, ROS events and warm conditions cause reduced snowcover and a dampened spring snowmelt pulse (see **Figure 4.5b**).

Two snow seasons were selected as examples of how the spatial distribution of SWE varies under different temperature and moisture regimes. **Figure 4.8** presents spatial SWE images for selected dates from the warm, dry 1987 *snow season*, and **Figure 4.9** presents SWE images from the warm, wet 2006 *snow season*. The selected dates generally represent images of the development and depletion of the snowcover from the date of near-continuous snowcover to melt-out for the base condition.

Snowcover development during the warm and dry 1987 *snow season*, as shown in **Figure 4.8**, was well underway for the base condition, almost complete for the cold scenario, and just beginning for the warm scenario by early December. By February 1,

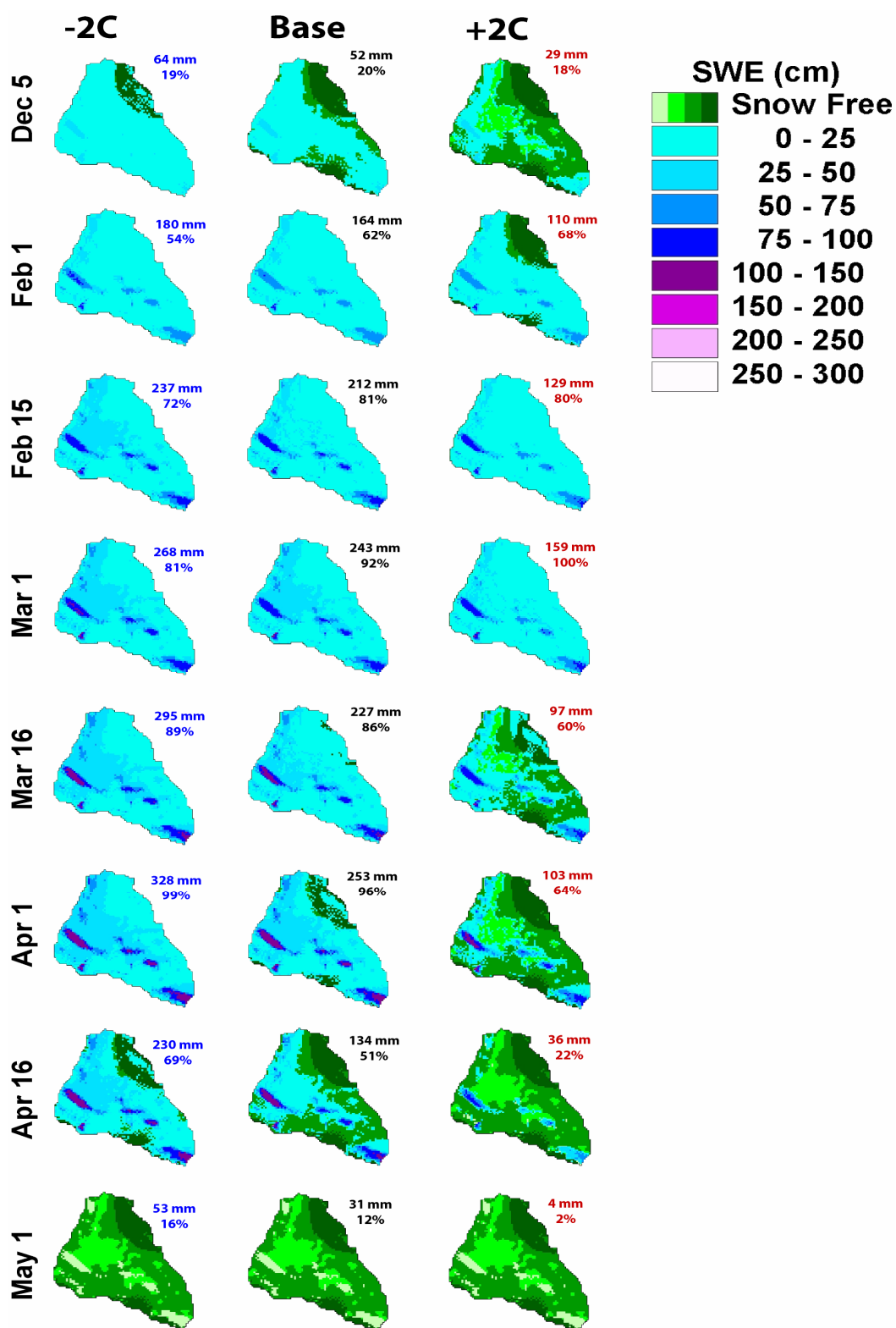


Figure 4.8: Spatial SWE images, 1987 snow season during snowcover development and ablation for base, -2°C , and $+2^{\circ}\text{C}$ simulations. Dec 5 through May 1 images presented. Average basin SWE and percent of peak SWE indicated for each image. Green colors indicate snow free areas.

the drift pattern was well developed in all three simulations, a continuous snowcover existed for both the base condition and cold scenario, but for the warm scenario the wind-exposed areas were still snow-free. By February 15 continuous snowcover was established for all three simulations, and by March 1 the warm scenario had reached peak SWE. During snowcover development, the warm scenario generates less than half the SWE generated by the base and cold scenario.

Snowcover depletion during the 1987 *snow season*, as shown by **Figure 4.8**, is already underway for the warm scenario by March 16, but peak SWE is not achieved until April 1 for the base condition and cold scenario. Even for this very dry year, on April 16 a substantial snowcover is still in place for the base condition and cold scenario. However, for the warm scenario only a few shallow drifts remain. By May 1 the warm scenario is essentially snow-free, but drifts remain for both the base condition and the cold scenario.

The snowcover during the warm and wet 2006 snow season, as shown by **Figure 4.9**, is well established in the cold scenario, almost continuous for the base condition and just beginning for the warm scenario by late December. The cold scenario has nearly three times the basin SWE of the base condition, and the warm scenario is essentially snow-free. By March 1 both the base condition and cold scenario have well established drifts that hold 4-5 times the basin average SWE. The warm scenario has nearly established a continuous snowcover, with shallow drifts. By March 16 all three simulations show a continuous, well-established snowcover, and by April 1 the warm scenario has reached peak SWE. Peak SWE for the warm scenario is only about half the base condition SWE, and only a third of the cold scenario SWE.

Snowcover depletion during the 2006 *snow season*, as shown by **Figure 4.9**, is already underway for the warm scenario by April 16, at the same time peak SWE is achieved for the base condition and cold scenario. By May 1 the warm scenario is nearly depleted with only shallow drifts holding SWE, depletion has begun for the base condition, and the cold scenario is still maintaining a substantial snowcover. Melt-out has occurred for the warm scenario by May 16, while the cold scenario still holds 57% of its peak SWE. By May 24 the base condition holds only shallow drifts, while the cold scenario maintains a nearly continuous snowcover with very deep drifts holding 10 times or more the basin SWE.

6.4. Base, -2°C, and +2°C Scenario Simulations: Rain-on-Snow Sensitivity

The work from Chapter 3 and the analysis in this chapter suggest that in mountainous regions of the northwestern US such as the RCEW the most important impact of climate warming will be precipitation phase change. The change in the rain/snow ratio to more rain and less snow is reducing SWE in the seasonal snowcover, by delaying snowcover initiation, and increasing mid-winter and early spring rain, which will lead to earlier snowcover depletion. This will result in increased winter streamflow, and reduced spring and summer streamflow. This shift will not be gradual but will be more like a step-function, because the change in phase from snow to mixed, or mixed to rain will result in a substantial change in how water is delivered to the soil in mountain basins such as RME. This is particularly true of events that occur at or just before peak SWE.

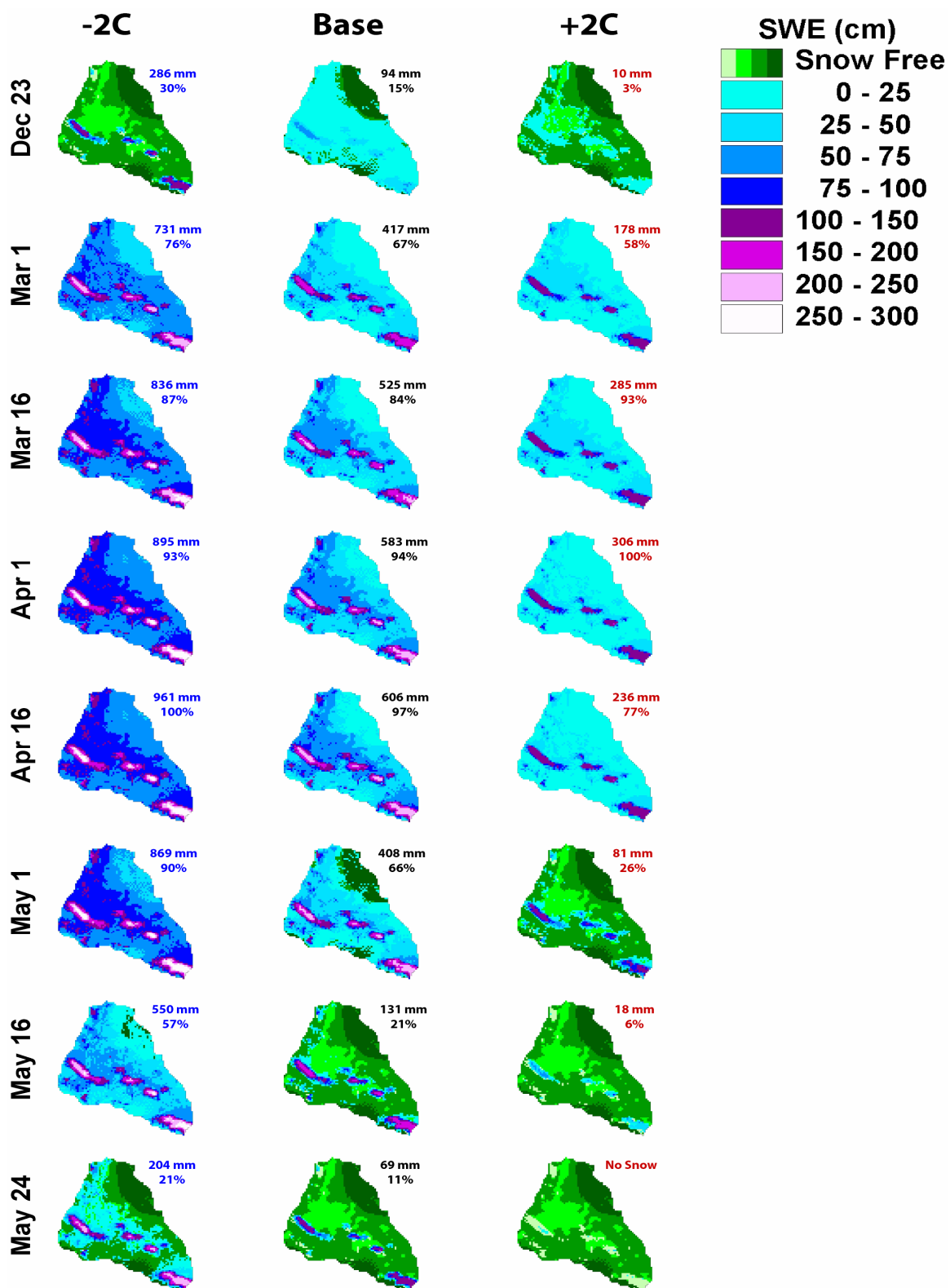


Figure 4.9: Spatial SWE images, 2006 snow season during snowcover development and ablation for base, -2°C , and $+2^{\circ}\text{C}$ simulations. Dec 23 through May 24 images presented. Average basin SWE and percent of peak SWE indicated for each image. Green colors indicate snow free areas.

In this paper we show the sensitivity of the seasonal snowcover to warming, and the impact that may have on the delivery of water to the soils and streams in the region. **Figure 4.5** shows how basin SWE would be affected by warmer or colder conditions, and how the SWI hydrograph will change as a result. Of the five-selected *snow seasons* only 1984 did not have a critical near-peak SWE precipitation event that under the scenario simulations resulted in sharp change in peak SWE and a substantial change to the SWI hydrograph. The most sensitive condition is an event that is mixed rain and snow in the base simulation. That sort of event is likely to become all snow under the cold scenario, and all rain under the warm scenario. Rain-on-snow (ROS) has tremendous thermodynamic potential because of the magnitude of possible condensation-induced heat transfer during the event (Marks et al. 1998, 2001a). Over the nearly 50 years of monitoring, all flood events within the RCEW have been associated with mid-winter or spring ROS events.

The 1986, 1987, 2001, and 2006 snow seasons all had such events. In the section below we will look in detail at the impact of climate warming on mixed rain/snow events that occurred a few days prior to peak SWE. The events selected are from the dry, warm 1987, and the wet, warm 2006 *snow seasons*. Because the 1987 snow season was warm (1.5°C above average) and dry (532 mm, 65% of average), it received little snow (peak SWE was 263 mm) and was sensitive to temperature increase. The warm, wet 2006 *snow season* was the most sensitive to warming, because it was already warm and most *snow season* precipitation was mixed. Under that condition, even a small change in temperature will have a large impact on SWE and the SWI hydrograph.

6.4.1. 1987 Mixed Rain-Snow, ROS
Event (3/5/1987-3/13/1987)

A mixed precipitation event occurred from March 5 – 13, 1987, ten days before peak SWE (see **Figure 4.10**). At the beginning of the storm, conditions were warm and almost all of the March 5 – 7 precipitation fell as rain as dew point temperatures were at or above 0°C. From March 8 – 13 conditions cooled, dew point temperatures fell below 0°C, with precipitation becoming mixed and finally turning to snow. Total basin precipitation during the storm period was 26 mm of which 38% (10 mm) was rain. Note that while this seems like a small event, during the dry conditions of the 1987 *snow season*, it represented 5% of total precipitation, and 6% of total rainfall.

This was one of the largest events of the 1987 *snow season*. Simulated SWE decreased from 232 mm to 208 mm during March 5 – 7 and thereafter increase to 219 mm by the end of storm period. Total SWI generated during the storm period was 37 mm (8% of the *snow season* total) of which 29 mm was generated during the first two days.

Under the cold scenario (**Figure 4.10a**), the storm become snow dominated, with no rain, causing an increase in SWE from 264 to 286 with negligible SWI. However, under the warm scenario, the rain-fraction of storm precipitation increased to 61% and resulted in a decrease in SWE from 127 to 93 mm with storm-total SWI of 61 mm. As shown in **Figure 4.10c**, energy flux is slightly more negative than the base condition under the cold scenario, but of much lower magnitude, and nearly in balance under the warm scenario.

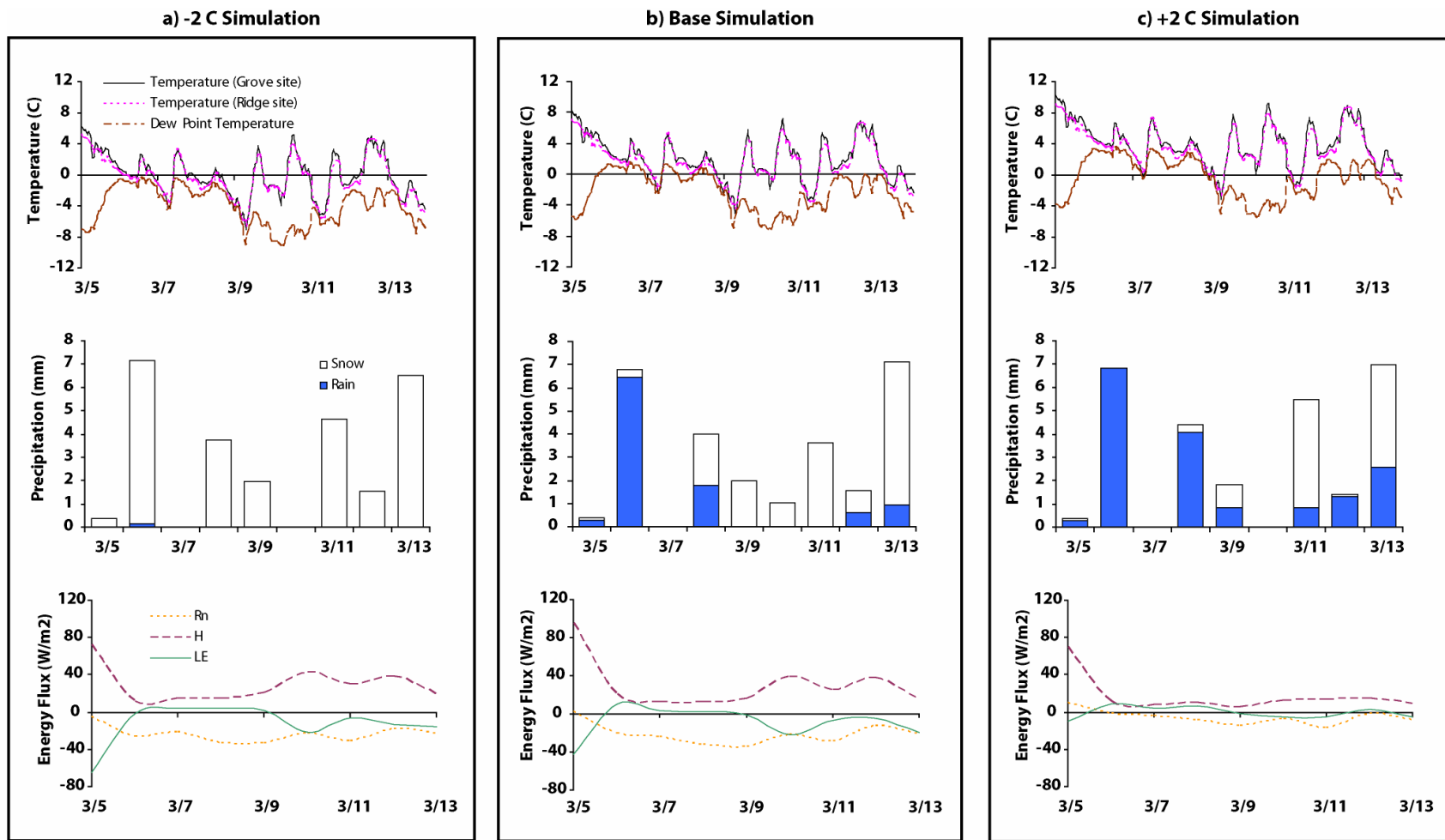


Figure 4.10: Weather, precipitation and energy flux conditions during the March 5 – 13, 1987 mixed precipitation event for a) base, b) -2°C, and c) +2°C simulations.

6.4.2. 2006 Mixed Rain-Snow, ROS
Event (4/3/2006-4/15/2006)

Between April 3 – 15, 2006, a mixed rain-snow event occurred, spanning the April 11 date of peak SWE (see **Figure 4.11**). Total basin precipitation during this storm-period was 62 mm of which about 37% (23 mm) was rain. This event accounted for about 6% of *snow season* precipitation, and 7% of *snow season* rainfall. The period from April 3 – 11 was moderate to cold, with 52 mm precipitation, only about 29% (15 mm) of which was rain. Basin average SWE increased from 583 mm to 622 mm (which was peak SWE for the 2006 snow season). During this initial period of the storm only 12 mm of SWI was generated. As the storm progressed, conditions become warmer. Between April 12 – 15, air temperature during both day and night was above freezing. Dew point temperatures were also above freezing until April 14, and nearly 85% of the precipitation (8 mm out of 9 mm) during this period fell as rain. SWE decreased to 595 mm and a total of 35 mm of SWI was generated over the period of the storm.

Cold scenario (**Figure 4.11a**) total storm period precipitation decreased to 60 mm, only 10% of which was rain. SWE increased gradually through the end of the storm period from 896 to 950 mm. Only 2 mm of SWI is simulated for the storm period and the event caused the date of peak SWE to shift from April 11 to April 17 under the cold scenario.

Under the warm scenario (**Figure 4.11c**), precipitation during the storm period becomes rain dominated. Total storm period precipitation increases to 66 mm with the reduction in wind redistribution, 89% (58 mm) of which was rain. SWE continuously

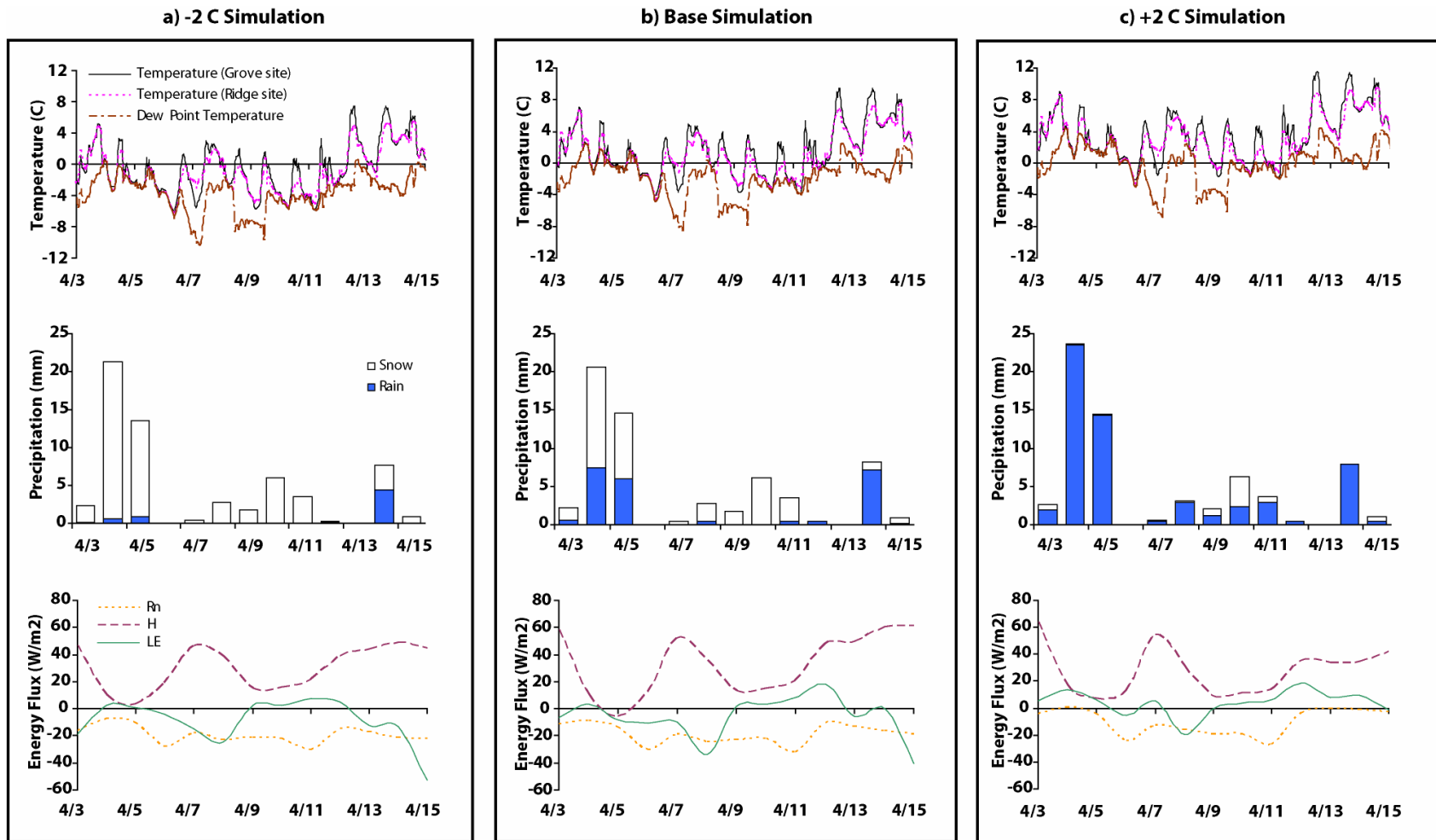


Figure 4.11: Weather, precipitation and energy flux conditions during the April 3 – 15, 2006 mixed precipitation event for a) base, b) -2°C, and c) +2°C simulations.

decreased from 293 to 226 mm, 147 mm of SWI was produced during the storm period and the event caused the date of peak SWE to shift from April 11 to April 1.

7. Summary and Conclusions

The five *snow seasons* selected for analysis represent a large range of variability in basin climate (temperature, humidity, wind and precipitation – rain and snow) ranging from wet to dry and warm to cold. Base-condition simulations over the RME catchment using these forcing data show an equally large range of variability for the development of the seasonal snowcover, snow distribution, timing and magnitude of peak SWE, SWI, and snowmelt.

Simulations using the -2°C and $+2^{\circ}\text{C}$ scenarios show critical changes in basin SWE associated with climate warming. In general, the seasonal snowcover is less sensitive to cold scenarios than warm. Cold scenario simulations resulted in an increase in basin SWE, a decrease in early SWI, a delay in soil and groundwater recharge required to initiate streamflow, and a concentration of SWI in late spring and early summer. In general, these shifts were small (a 14-26% increase in peak SWE, a delay in the date of 200 mm SWI by 9 – 56 days, and 50% SWI of 5 – 23 days), the proportion of SWI occurring prior to peak SWE by about $\frac{1}{2}$, and a SWI hydrograph not that different from the base condition. The one exception was the 2006 where the cold scenario simulation was substantially different from the base condition, with peak SWE increasing by 50%, a delay in the date of 200 mm SWI by 137 days, the date of 50% SWI shifting to 19 days later, and the proportion of SWI that occurred prior to peak SWE reduced from 35% to 5%.

The seasonal snowcover showed a much greater sensitivity to warm scenario simulations. In all *snow seasons*, warm scenario simulations produced about half the SWE produced by the base condition, shift of 10 – 41 days earlier for the date of peak SWE, 20 – 163 days earlier for the 200 mm SWI date, 28-73 days earlier for the 50% SWI date and an increase of 28 – 30% for dry years and 47 – 61% for wet years in the proportion of SWI occurring prior to peak SWE. The 1986 and 2006 snow seasons were particularly sensitive to warm scenario conditions. Storms during these *snow seasons* were close to the freezing temperature (0°C) so the warm scenario had the affect of decreasing peak SWE by 63% and 52%, and shifting the date of 50% SWI to 73 and 61 days earlier, and increasing the proportion of SWI that occurred prior to peak SWE to 61 and 59% respectively. Nearly half the base condition SWE deposited during the 1986 snow season resulted from a very large storm in February. For the warm scenario, most of this event became rain. Again 2006 was different from the other simulation years, with precipitation throughout the snow season being a mix of rain and snow. For both 1986 and 2006, the warm scenario simulations produce very different SWI hydrographs from the base condition with strong shifts to earlier timing for SWI.

If conditions are relatively cold, particularly during storms, SWE, the seasonal snowcover and the SWI hydrograph will be less affected by changes in temperature. However, if conditions are warm during storms, SWE, the seasonal snowcover and the SWI hydrograph will be strongly affected by temperature change. Hydrologically the most critical climate warming effect is change in precipitation phase, because that will have an immediate impact on the SWI hydrograph. As we see from the base, -2°C and +2°C scenario simulations, converting warm snow to cold snow or cold rain to warmer

rain has a relatively small impact on SWI hydrographs. However, converting snow to rain has the potential to significantly change SWI hydrographs. This is particularly evident in years where the basin SWE is based largely on a single, very large event, such as 1986, or a warm snow season consisting of mixed rain and snow, such as 2006.

If we compare simulation results from the 1984 and 2006 *snow seasons* (**Figures 4.5, 4.6, and 4.7**), which received similar season total precipitation and generated similar season total SWI, we see that a warm 1984 is much like the base condition in 2006, and a cold 2006 is much like the base condition in 1984. If the warming trends predicted by IPCC (2007) and indicated in Chapter 3, are correct, in the future we would expect more years similar to 2006 than 1984. As shown by this modeling experiment, under the right conditions, the effect of a small change in temperature and dew point is not gradual. If warming trends continue, the changes in the seasonal snowcover will not be gradual, but will be sudden and dramatic like those shown for the warming scenario simulation of 1986 and 2006.

This is illustrated by the detailed analysis of the ROS events in section **6.4**. Historically, like much of the western US, the largest RCEW floods have been mid-winter ROS events (Pierson et al. 2001). These have the effect of removing much if not all of the seasonal snowcover, by a combination of condensation and advective melt (Marks et al. 1998, 2001a). Climate warming will likely increase the occurrence of these events. The analysis presented in section **6.4** and **Figures 4.10 and 4.11** illustrates how a small change in temperature and dew point can shift a mixed rain/snow event to either all snow, or all rain, with significant impacts on the seasonal snowcover and the generation of SWI.

The spatial results presented in **Figures 4.6, 4.7, 4.8 and 4.9** illustrate the importance of snow redistribution to the hydrology of RME. As we can see for both the base condition and the cold scenario images, the source of late spring and early summer SWI is SWE re-deposited into drift and sheltered areas of the catchment. As snow turns to rain, re-deposition is reduced or eliminated, SWE is more uniformly distributed over the catchment, SWI is shifted to earlier in the year, and less water is available during the growing season.

The snowcover development and timing of melt water release from the RME basin is critical for sustaining the ecosystem of the RECW as in case of most of the western United States. These simulations show that if the regional climate continues to warm, snowcover over the RME basin will be reduced and timing of streamflow will shift towards earlier in the year. As most of the streamflow during the growing season comes from the snowmelt from the headwater catchments such as RME, earlier timings of streamflow can adversely affect water availability during the growing seasons when the demand for water is at its peak. Therefore future water management strategies of the region will need to be account for this alteration in the hydrologic regime.

8. References

- Aguado, E., Cayan, D. R., Riddle, L., and Roos, M. (1992). "Climate fluctuations and the timing of west coast streamflow." *J. Clim.*, 5(12), 1468-1483.
- Brutsaert, W. (1975). "On a derivable formula for long-wave radiation from clear skies." *Water Resour. Res.*, 11(5), 742-744.
- Brutsaert, W. (1982). "Evaporation into the atmosphere: Theory, history, and application." *Kluwer*, Dordrecht, Holland.

- Cayan, D. R., Kammerdiener, S.A., Dettinger, M.D., Caprio, J.M., and Peterson, D.H. (2001). "Changes in the onset of spring in the Western United States." *Bull. Am. Meteorol. Soc.*, 82(3), 399-415.
- Dettinger, M. D., and Cayan, D. R. (1995). "Large-scale atmospheric forcing of recent trends toward early snowmelt runoff in California." *J. Clim.*, 8, 606-623.
- Dettinger, M. D., Cayan, D. R., Diaz, H. F., and Meko, D. M. (1998). "North-south precipitation patterns in Western North America on interannual-to-decadal timescales." *J. Clim.*, 11(12), 3095-3111.
- Huntington, T. G., Hodgkins, G. A., Keim, B. D. and Dudley R. W. (2004). "Changes in the proportion of precipitation occurring as snow in New England (1949-2000)." *J. Clim.*, 17(13), 2626-2636.
- Hurrell, J. W. (1995). "Decadal trends in the North Atlantic Oscillation: Regional temperatures and precipitation." *Science*, 269(5224), 676-679.
- Hurrell, J. W., and Van Loon, H. (1997). "Decadal variations in climate associated with the North Atlantic Oscillation." *Clim. Change*, 36(3-4), 301-326.
- IPCC (2007). *Climate change 2007, The physical science basis*, Cambridge University Press, Cambridge, U.K.
- Knowles, N., Dettinger, M. D., and Cayan, D. R. (2006). "Trends in snowfall versus rainfall in the Western United States." *J. Clim.*, 19(18), 4545-4559.
- Link, T., and Marks, D. (1999b). "Distributed simulation of snowcover mass and energy balance in a boreal forest." *Hydrolog. Process.*, 13(13-14), 2439-2452.
- Link, T., and Marks, D. (1999a). "Point simulation of seasonal snowcover dynamics beneath a boreal forest canopies." *J. Geophys. Res.*, 104(D22), 27841-27858.
- Luce, C. H., Tarboton, D. G., and Cooley, K. R. (1998). "The influence of the spatial distribution of snow on basin-averaged snowmelt." *Hydrolog. Process.*, 12, 1671-1683.
- Marks, D., Cooley, K. R., Robertson, D. C., and Winstral, A. (2001b). "Long-term snow database, Reynolds Creek Experimental Watershed, Idaho, United States." *Water Resour. Res.*, 37(11), 2835-2838.
- Marks, D., Domingo, J., Susong, D., Link, T., and Garen, D. (1999). "A spatially distributed energy balance snowmelt model for application in mountain basins." *Hydrolog. Process.*, 13(12-13), 1935-1959.

- Marks, D., and Dozier, J. (1979). "A clear-sky longwave radiation model for remote alpine areas." *Archiv Fur Meteorologie Geophysik Und Bioklimatologie*, 27(2-3), 159-187.
- Marks, D., and Dozier, J. (1992). "Climate and energy exchange at the snow surface in the alpine region of the Sierra Nevada: 2. Snowcover energy balance." *Water Resour. Res.*, 28(11), 3043-3054.
- Marks, D., Kimball, J., Tingey, D., and Link, T. (1998). "The sensitivity of snowmelt processes to climate conditions and forest cover during rain-on-snow: A case study of the 1996 Pacific Northwest flood." *Hydrolog. Process.*, 12(10-11), 1569-1587.
- Marks, D., Link, T., Winstral, A., and Garen, D. (2001a). "Simulating snowmelt processes during rain-on-snow over a semi-arid mountain basin." *Ann. Glaciol.*, 32(1), 195-202.
- Marks, D., and Winstral, A. (2001). "Comparison of snow deposition, the snow cover energy balance, and snowmelt at two sites in a semiarid mountain basin." *J. Hydrometeorol.*, 2(3), 213-227.
- Marks, D., and Winstral, A. (2008). "Finding the rain/snow transition elevation during storm events in a mountain basin." *Hydrolog. Process.*, To appear.
- Marks, D., Winstral, A., and Seyfried, M. (2002). "Simulation of terrain and forest shelter effects on patterns of snow deposition, snowmelt and runoff over a semi-arid mountain catchment." *Hydrolog. Process.*, 16(18), 3605-3626.
- Meehl, G. A., Stocker, T. F., Collins, W. D., Friedlingstein, P., Gaye, A. T., Gregory, J. M., Kitoh, A., Knutti, R., Murphy, J. M., Noda, A., Raper, S. C. B., Watterson, I. G., Weaver, A. J., and Zhao, Z. C. (2007). "Global climate projections." *Climate change 2007: The physical science basis*. Contributions of working group I to the fourth assessment report of the Intergovernmental Panel on Climate Change, S. Solomon, D. Quin, M. Manning, Z. Chen, M. Marquis, K. B. Averyt, M. Tignor, and H. L. Miller, eds., Cambridge University Press, Cambridge, UK and New York, 747-845.
- Mote, P. W. (2003a). "Trends in snow water equivalent in the Pacific Northwest and their climatic causes." *Geophys. Res. Lett.*, 30(12), 1601, doi:10.1029/2003GL017258, 2003.
- Mote, P. W. (2003b). "Twentieth-century fluctuations and trends in temperature, precipitation, and mountain snowpack in the Georgia Basin-Puget Sound region." *Can. Water Resour. J.*, 28(4), 567-585.

- Mote, P. W. (2006). "Climate-driven variability and trends in mountain snowpack in Western North America." *J. Clim.*, 19(23), 6209-6220.
- Mote, P. W., Hamlet, A. F., Clark, M. P., and Lettenmaier, D. P. (2005). "Declining mountain snowpack in western North America." *Bull. Am. Meteorol. Soc.*, 86, 39-49.
- Nash, J. E., and Sutcliffe, I. V. (1970). "River flow forecasting through conceptual models part 1 – A discussion of principles." *J. Hydrol.*, 10, 282-290.
- Pierson, F. B., Slaughter, C. W., and Cram, Z. K. (2001). "Long-term stream discharge and suspended-sediment database, Reynolds Creek Experimental Watershed, Idaho, United States." *Water Resour. Res.*, 37(11), 2857-2861.
- Regonda, S. K., Rajgopalan, B., Clark, M., and Pitlick, J. (2005). "Seasonal cycle shifts in hydroclimatology over the Western United States." *J. Clim.*, 18, 372-384.
- Stewart, I. T., Cayan, D. R., and Dettinger, M. D. (2004). "Changes in snowmelt runoff timing in Western North America under a 'Business as usual' climate change scenario." *Clim. Change*, 62, 217-232.
- Stewart, I. T., Cayan, D. R., and Dettinger, M. D. (2005). "Changes towards earlier streamflow timing across Western North America." *J. Clim.*, 18, 1136-1155.
- Trenberth, K. E., Jones, P. D., Ambenje, P., Bojariu, R., Easterling, D., Tank, A. K., Parker, D., Rahimzadeh, F., Renwick, J. A., Rusticucci, M., Soden, B., and Zhai, P. (2007). "Observations: Surface and atmospheric climate change." *Climate change 2007: The physical science basis*. Contributions of working group I to the fourth assessment report of the Intergovernmental Panel on Climate Change, S. Solomon, D. Qin, M. Manning, Z. Chen, M. Marquis, K. B. Averyt, M. Tignor, and H. L. Miller, eds., Cambridge University Press, Cambridge, UK and New York, 235-336.
- Winstral, A., Elder, K., and Davis, B. (2002). "Modeling the effects of wind induced snow redistribution with terrain-based parameters to enhance spatial snow modeling." *J. Hydrometeorol.*, 3(5), 524-528.
- Winstral, A., and Marks, D. (2002). "Simulating wind fields and snow redistribution using terrain-based parameters to model snow accumulation and melt over a semi-arid mountain catchment." *Hydrolog. Process.*, 16(18), 3585-3603.
- Winstral, A., Marks, D., and Gurney, R. (2008a). "Modeling time-series wind fields over a semi-arid mountain catchment." *Hydrology in mountain regions: Observations, processes and dynamics*, IAHS Publication, accepted for publication, Dec., 2007.

Winstral, A., Marks, D., and Gurney, R. (2008b). "An efficient method for distributing wind speeds over heterogeneous terrain." *Hydrolog. Process.*, submitted.

CHAPTER 5

SUMMARY

1. The Automated Precipitation Correction Program

An Automated Precipitation Correction Program (APCP) was developed to remove mechanical noise signals from high frequency weighing-recording precipitation gauge data. The APCP precipitation correction utility was successfully used to process data collected during 1997 to 2006 water years at 22 dual gauge (two National Weather Service (NWS) weighing-recording gauges, one unshielded and the other shielded with Alter-type shield, located in close proximity) (Hamon 1971, 1973) stations, located in Reynolds Creek Experimental Watershed (RCEW).

Comparison of data processed by the APCP to the 'Rainfall Analyzer' (a semi-automated graphical technique previously used to process precipitation data collected at RCEW) at 11 dual gauge stations for 2002-2004 water years shows that data processed using APCP display smaller mean and standard deviation of error than RA. Being an automated technique, APCP eliminates operator biases and generate reproducible results. Time required to process raw high frequency precipitation data using the APCP is also significantly less than the graphical RA approach (few minutes against 2-3 days per station year), which is important in extensively instrumented watersheds like RCEW.

Though APCP was developed to remove mechanical noise signals from weighing-recording precipitation gauge data, the utility was also successfully used to filter soil moisture content data collected using TDR. This demonstrates that the APCP uses a

robust filtering approach and can be applied on other continuous data sources with minor adjustments.

2. Trend Analysis of Long-Term Hydro-Climatic Data

Carefully processed hydro-climate data of temperature, humidity, precipitation, snow, soil temperature, soil moisture, and streamflow, collected from 1962 to 2006 at several locations of RCEW, have been analyzed for temporal trends. Statistical significance of the observed trends has been tested using Mann-Kendall statistical test (Hirsh and Slack 1984; Lettenmaier et al. 1994; Yue et al. 2002). Significant trends of rise in temperatures have been found at all elevations of RCEW with minimum temperature increasing at a faster rate than the maximum temperature.

Though precipitation and streamflow data show no significant annual change with large year-to-year variability, seasonal shifts in streamflow has been observed with increase in winter and early spring and decrease in late spring and summer. The strongest seasonal shift in streamflow is observed at the highest elevation Reynolds Mountain East (RME) weir which is almost entirely driven by the snowmelt. The shift in streamflow becomes damped at mid and low elevation weirs.

There was no change in seasonal distribution of precipitation but the phase of precipitation has changed significantly at all elevations with more precipitation falling as rain than snow. Critical changes in precipitation regime have occurred at low and mid elevations of RCEW where precipitation regime has changed from snow dominated to rain dominated over the period of record. Snow is still the dominant form of precipitation

at high elevations of RCEW but the proportion of rain during the *snow season*¹³ has increased indicating increased frequency of rain-on-snow (ROS) events.

Analysis of snow water equivalent (SWE) data indicate decline in April 1, May 1 and Peak SWE depths as well as earlier occurrence of peak SWE. Trends are largest and most significant at low elevations while at high elevations trends are small and statistically non-significant. Soil temperature and moisture data indicate reduction in number of soil freeze days and earlier occurrence of plant-water stress.

These analyses also demonstrate that the hydrologic sensitivity to the warming climate has a strong correlation with elevation, and though greatest increase in temperatures occurred at high elevation site in RCEW, it has caused minimum change in hydrologic cycle in comparison to mid and low elevations of RCEW. Difference in hydrologic sensitivity to warming climate at different elevation range is probably due to the fact that despite increase in temperatures, average winter temperatures at high elevations still remain well below freezing point. Therefore precipitation at high elevations of RCEW is still dominated by snow. While at low and mid elevations, where average winter temperatures generally remain near to the freezing point, even smaller increase in temperature has caused a greater change in snow deposition and melt pattern.

The observed changes in climate and hydrology over RCEW are agreement with the trends of increasing temperature (IPCC 2007; Trenberth et al. 2007), declining mountain snow accumulation (Mote 2003a&b, 2006; Mote et al. 2005; Hamlet et al. 2005; Regonda et al. 2005), decreasing fraction of snow in total precipitation (Aguado et

¹³ A *snow season* is defined as the 9-month period from October 1 to June 30. Hence, the 1984 snow season represents period from October 1, 1983 to June 1, 1984

al. 1992; Dettinger and Cayan 1995; Huntington et al. 2004; Regonda et al. 2005; Knowles et al. 2006) and earlier timings of snowmelt and streamflow (Cayan et al. 2001; Stewart et al. 2004, 2005; Regonda et al. 2005) observed over most of the western USA. But results of this study not only indicate that the hydro-climate of RCEW and similar regions of the northwest USA has been substantially altered by warming climate but also that the response to warming climate varies with elevation in these mountain basins.

3. Sensitivity of Seasonal Snowcover to Warming Climate

Snowcover development and generation of melt water at headwater catchments of the RCEW are critical for basin ecosystems. Weather patterns at the RCEW are highly variable and are subjected to wet-dry precipitation cycles and warm-cold phases. This natural climate variability causes important year-to-year differences in patterns of snowcover development and melt.

The sensitivity of the seasonal snowcover at the RME basin, a headwater catchment of the RCEW, is evaluated at five snow seasons (1984, 1986, 1987, 2001, and 2006). These snow seasons represent three wet, and two dry years, with 1984 being cold and wet, 1986 cool and wet, 1987 warm and dry, 2001 cool and dry, and 2006 warm and wet. To evaluate the impact of natural climate variability, differences in simulated patterns of snow deposition, accumulation and melt between these years were assessed. To evaluate the snowcover sensitivity to changes in climate conditions, further simulations were conducted based on warm and cold scenarios. These scenarios were developed by modifying the base forcing data by +/- 2°C, keeping the precipitation mass

constant, but making associated adjustments to humidity, thermal and solar radiation, and snow redistribution.

Meteorological data from the two long-term weather stations in RME were used to define the base-condition weather and precipitation conditions and to generate distributed forcing surfaces to drive a DEM based snowcover energy and mass balance model, *Isnobal* (Marks et al. 1999a&b). Apart from obvious year-to-year variation in total volume of precipitation, snow accumulation and surface water input due to differences in precipitation, base-condition simulations showed substantial differences in key hydrologic parameters such as development of snowcover, snow distribution, timing and magnitude of peak SWE, and volume and timing of *surface water input*¹⁴ (SWI). During dry *snow seasons* (1987 and 2001) peak SWE accumulation was about a half of that of during wet *snow seasons* (1984, 1986, and 2006). Complete melt out occurred about a month earlier in dry *snow seasons* than wet *snow seasons*.

SWI shows good correlation to stream discharge once soils reach saturation during the snowmelt. Most of the SWI generated prior to the initiation of snowmelt is infiltrated into the soil and used to recharge ground water. Comparison of cumulative *snow season* SWI and measured stream discharge shows that in cold and wet snow seasons (1984 and 1986) stream discharge was a significant fraction (90% and 87%, respectively) of simulated SWI. In the warm and wet 2006 *snow season* stream discharge was only 67% of the SWI generated because it was preceded by 6 dry years and had many pre-snowmelt rain and ROS events. In dry *snow seasons* (1987 and 2001), stream discharge was only 44% and 42% of simulated SWI, respectively, because a much larger

¹⁴ Surface water input (SWI) is defined as the input of melt-water or rain at the soil surface.

fraction of SWI was required to bring the soil to saturation prior to the initiation of streamflow.

The timing of peak SWI varied between the simulated *snow seasons*. In wet and cold *snow seasons* (1984 and 1986) peak SWI occurred in late May-early June while in dry *snow seasons* (1987 and 2001) peak SWI occurred in April. The warm and wet 2006 *snow season* had two SWI peaks, one in December due to early season rain and ROS events, and the other in May.

To test the sensitivity of the snowcover development and melt to changing climate conditions, cold and warm scenarios were developed for each *snow season*, based on adjustment in air temperatures by -2°C and $+2^{\circ}\text{C}$, and associated adjustments in dew point temperatures, thermal radiation, snow redistribution and snow albedo decay. Results from cold scenario simulations indicate that colder conditions result in more snow and less rain, increase in SWE, later timing of peak SWE and later timing of peak SWI. On the other hand warm scenarios resulted in a change to less snow and more rain, a decrease in SWE, earlier timing of peak SWE and earlier timing of peak SWI.

In general, the seasonal snowcover shows smaller changes in SWE accumulation and the timing of melt under cold than warm scenarios with the exception of 2006. In all the *snow seasons* except 2006 most mid-winter precipitation fell as snow. Therefore there was little change in precipitation phase from rain to snow under the cold scenarios, which resulted only a small change in snow accumulation. Under the warm scenarios many snow events were converted to mixed rain-snow or all rain events, causing substantial changes in snow deposition. In the 2006 *snow season*, many rain and ROS events occurred under the base condition. Because of this the 2006 *snow season*

displayed about the same sensitivity in snow accumulation and melt under warm and cold scenarios.

Comparison of the base, -2°C and $+2^{\circ}\text{C}$ simulations indicate that the impact of warm or cold conditions on SWE and SWI hydrographs is small when there is no change in phase of precipitation. However a change in phase of precipitation from snow to rain or vice versa causes a significant change in SWE accumulation and SWI hydrographs. The impact of change in precipitation phase was illustrated by analysis of two mixed rain-snow and ROS events occurred near the peak SWE accumulation in 1987 and 2006 *snow seasons*. Under cold scenario both these events became snow dominated, causing increased SWE accumulation and decreased SWI when compared to base simulation. Under the warm scenario, both events showed an increase in the rain fraction of precipitation, decrease in SWE accumulation and increase in generated SWI.

Results of these simulations illustrate the sensitivity of the seasonal snowcover to changing climate conditions, and show that climate warming will substantially alter hydrologic cycle of RME and probably the entire RCEW. The frequency of ROS events will increase, with reduced snow cover and earlier timing of SWI timings if climate continues to warm as predicted. Historically, the largest floods at RCEW have occurred due to mid winter ROS events (Pierson et al. 2001). Therefore the frequency of mid-winter floods may increase due to increased ROS frequency. Earlier melt and SWI (and streamflow) will cause reduction in water availability during the dry summer period when water demand is at its peak. Results of this study will be help water managers of the region adapt to and prepare for altered hydrologic regimes that are likely under predicted climate warming.

4. References

- Aguado, E., Cayan, D. R., Riddle, L., and Roos, M. (1992). "Climate fluctuations and the timing of west coast streamflow." *J. Clim.*, 5(12), 1468-1483.
- Cayan, D. R., Kammerdiener, S. A., Dettinger, M. D., Caprio, J. M., and Peterson, D. H. (2001). "Changes in the onset of spring in the Western United States." *Bull. Am. Meteorol. Soc.*, 82(3), 399-415.
- Dettinger, M. D., and Cayan, D. R. (1995). "Large-scale atmospheric forcing of recent trends toward early snowmelt runoff in California." *J. Clim.*, 8, 606-623.
- Hamlet, A. F., Mote, P. W., Clark, M. P., and Lettenmaier, D. P. (2005). "Effects of temperature and precipitation variability on snowpack trends in the Western United States." *J. Clim.*, 18, 4545-4561.
- Hamon, W. R. (1971). "Chapter 4 – Reynolds Creek, Idaho." *Agricultural Research Service Precipitation Facilities and Related Studies*. D. M. Hershfield eds., ARS-USDA, Washington, D.C.
- Hamon, W. R. (1973). "Computing actual precipitation: Distribution of precipitation in mountainous areas." *WMO Rep. No. 362*, World Meteorological Organization, Geneva, 1, 159-173.
- Hirsch, R.M., and Slack, J.R. (1984). "Nonparametric trend test for seasonal data with serial dependence." *Water Resour. Res.*, 20(6), 727-732.
- Huntington, T. G., Hodgkins, G. A., Keim, B. D. and Dudley R. W. (2004). "Changes in the proportion of precipitation occurring as snow in New England (1949-2000)." *J. Clim.*, 17(13), 2626-2636.
- IPCC (2007). *Climate change 2007, The physical science basis*, Cambridge University Press, Cambridge, U.K.
- Knowles, N., Dettinger, M. D., and Cayan, D. R. (2006). "Trends in snowfall versus rainfall in the Western United States." *J. Clim.*, 19(18), 4545-4559.
- Lettenmaier, D. P., Wood, E. F., and Wallis J. R. (1994). "Hydro-climatological trends in the Continental United States, 1948-88." *J. Clim.*, 7(4), 586-607.
- Marks, D., Domingo, J., and Frew, J. (1999b). "Software tools for hydroclimatic modeling and analysis: Image Processing Workbench, ARS-USGS Version 2." *ARS Technical Bulletin 99-1*, USDA Northwest Watershed Research Center, Agricultural Research Service, Boise, Idaho. URL: <http://www.nwrc.ars.usda.gov/ipw>

- Marks, D., Domingo, J., Susong, D., Link, T., and Garen, D. (1999a). "A spatially distributed energy balance snowmelt model for application in mountain basins." *Hydrolog. Process.*, 13(12-13), 1935-1959.
- Mote, P. W. (2003a). "Trends in snow water equivalent in the Pacific Northwest and their climatic causes." *Geophys. Res. Lett.*, 30(12), 1601, doi:10.1029/2003GL017258, 2003.
- Mote, P. W. (2003b). "Twentieth-century fluctuations and trends in temperature, precipitation, and mountain snowpack in the Georgia Basin-Puget Sound region." *Can. Water Resour. J.*, 28(4), 567-585.
- Mote, P. W. (2006). "Climate-driven variability and trends in mountain snowpack in Western North America." *J. Clim.*, 19(23), 6209-6220.
- Mote, P. W., Hamlet, A. F., Clark, M. P., and Lettenmaier, D. P. (2005). "Declining mountain snowpack in western North America." *Bull. Am. Meteorol. Soc.*, 86, 39-49.
- Pierson, F. B., Slaughter, C. W., and Cram, Z. K. (2001). "Long-term stream discharge and suspended-sediment database, Reynolds Creek Experimental Watershed, Idaho, United States." *Water Resour. Res.*, 37(11), 2857-2861.
- Regonda, S. K., Rajgopalan, B., Clark, M., and Pitlick, J. (2005). "Seasonal cycle shifts in hydroclimatology over the Western United States." *J. Clim.*, 18, 372-384.
- Stewart, I. T., Cayan, D. R., and Dettinger, M. D. (2004). "Changes in snowmelt runoff timing in Western North America under a 'Business As Usual' Climate Change scenario." *Clim. Change*, 62, 217-232.
- Stewart, I. T., Cayan, D. R., and Dettinger, M. D. (2005). "Changes towards earlier streamflow timing across Western North America." *J. Clim.*, 18, 1136-1155.
- Trenberth, K. E., Jones, P. D., Ambenje, P., Bojariu, R., Easterling, D., Tank, A. K., Parker, D., Rahimzadeh, F., Renwick, J. A., Rusticucci, M., Soden, B., and Zhai, P. (2007). "Observations: Surface and atmospheric climate change." *Climate change 2007: The physical science basis*. Contributions of working group I to the fourth assessment report of the Intergovernmental Panel on Climate Change, S. Solomon, D. Qin, M. Manning, Z. Chen, M. Marquis, K. B. Averyt, M. Tignor, and H. L. Miller, eds., Cambridge University Press, Cambridge, UK and New York, 235-336.
- Yue, S., Pilon, P., and Cavandias, G. (2002). "Power of the Mann-Kendall and Spearman's rho tests for detecting monotonic trends in hydrological series." *J. Hydrol.*, 259(1-4), 254-271.

APPENDICES

APPENDIX A

THE AUTOMATED PRECIPITATION CORRECTION PROGRAM (APCP)

APPENDIX A

THE AUTOMATED PRECIPITATION CORRECTION PROGRAM (APCP)

The Automated Precipitation Correction Program (APCP) is a program written in Visual Basic 6.0. APCP was developed to remove mechanical noise signals (such as bucket maintenance, oscillations due to wind and temperature variation, intermittent noise, and data gaps) present in high frequency precipitation data collected using weighing-recording precipitation gauges. **Figure A.1** shows the graphical user interface of the ‘Single Gauge’ version of APCP.

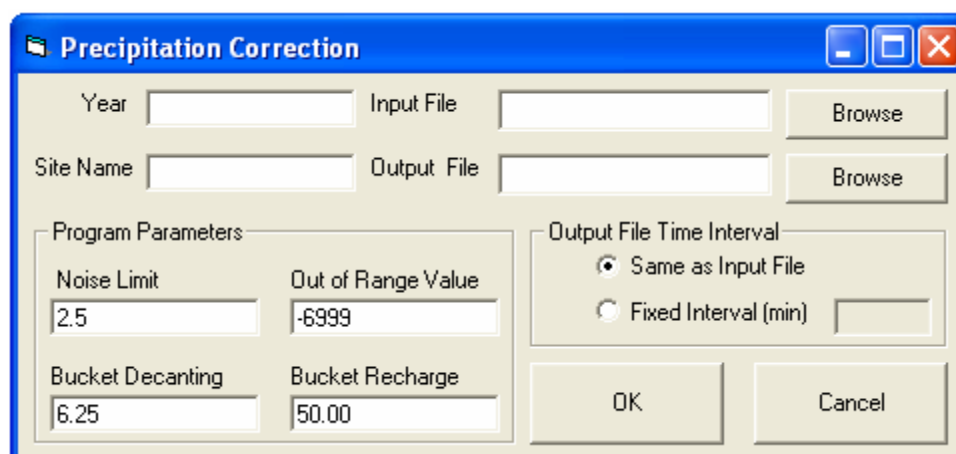


Figure A.1: Graphical user interface of ‘Single Gauge’ version of APCP

The Reynolds Creek Experimental Watershed (RCEW) operates a network of dual gauge installations for better measurement of precipitation after wind related undercatch. The ‘Dual Gauge’ version of APCP was written to correct precipitation data collected using dual gauge system from mechanical errors and repeats the similar steps to remove mechanical errors from the additional data column as in ‘Single Gauge’ version.

The graphical user interface of the ‘Dual Gauge’ version of APCP is presented in **Figure A.2**.

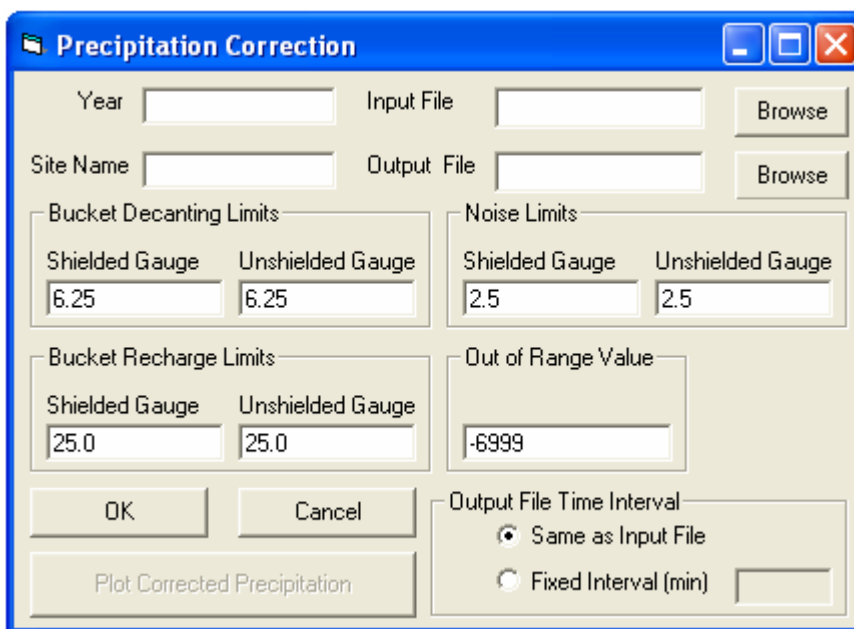


Figure A.2: Graphical user interface of the ‘Dual Gauge’ version of APCP

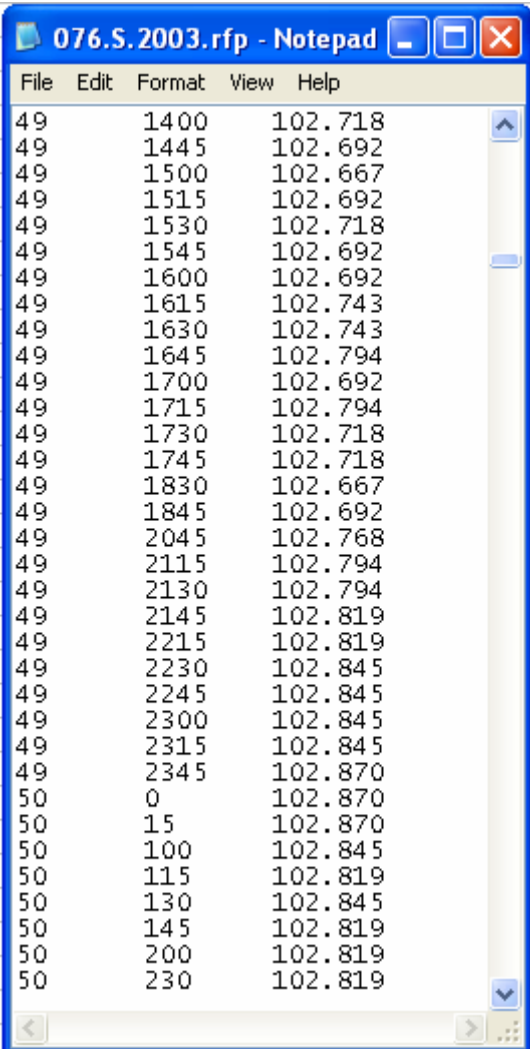
Mechanical noise signals present in precipitation data collected using weighing-recording gauges can be identified as out of range data values, intermittent noise, bucket maintenance (bucket decanting and bucket recharge), episodic noise (oscillations due to wind) and periodic noise (oscillations due to diurnal temperature variation). User defined parameters for APCP include: out of range value indicator, bucket decanting limit, bucket recharge limit, noise limit and output file time interval (optional). APCP scans the data and checks the variation in consecutive records within the user-defined limits in two separate cycles. In the first scanning cycle, APCP removes high magnitude noise signals such as out of range data values, bucket decanting, bucket recharge, and intermittent noise. In the second scanning cycle, APCP removes low magnitude noise signals such as

oscillations due to wind and diurnal temperature fluctuations. APCP uses a user defined 'Noise' limit to separate high magnitude noise signals from low magnitude noise signals.

The 'Single Gauge' version of APCP requires input data file with three data columns: Day of year, time of day (two digits of hour and two digits of minute, for example 1030 represents 10:30 AM), and measured gauge catch (**Figure A.3a**). Input file for 'Dual Gauge' version of APCP is formatted with shielded gauge catch in column three and unshielded gauge catch in column four (**Figure A.3B**).

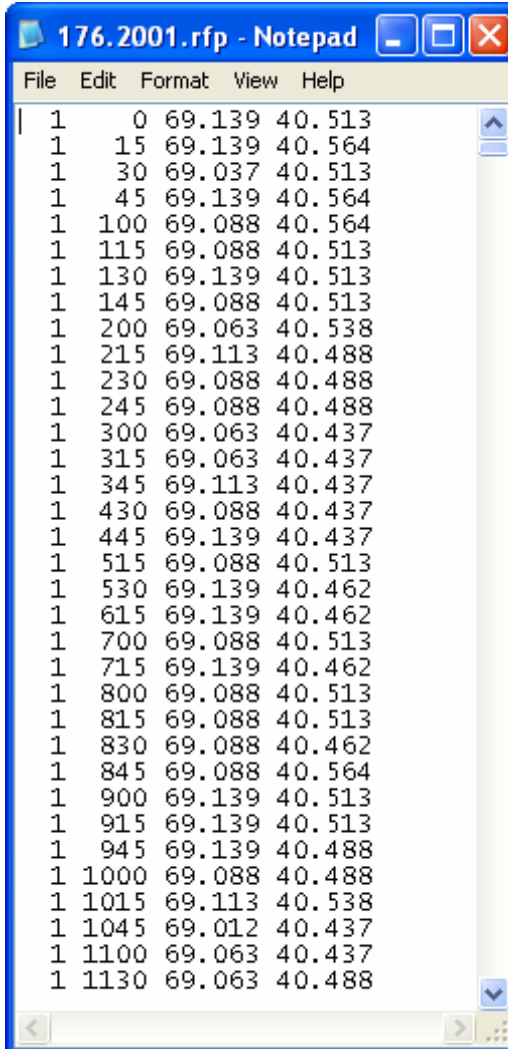
User-defined parameters for APCP should be selected based on careful observation of raw data and field notes. The parameter 'Noise' limit should be selected such that it is smaller than the minimum change caused by the high magnitude noise signals but greater than the maximum change caused by the low magnitude noise signals (for each individual gauge). The 'Bucket Decanting' and 'Bucket Recharge' limits should be selected such that they are slightly less than the minimum change in precipitation data due to 'Bucket Decanting' and 'Bucket Recharge' respectively but always greater than the 'Noise' limit (for each individual gauge). Out of range data values occur due to linkage error between gauge-data logger assembly during which data logger records very large positive or negative number (such as 9999, -6999 etc.). The 'Out of range data value' identifier should be selected based on data logger settings.

a) Single Gauge



Gauge	Precipitation
49	1400
49	1445
49	1500
49	1515
49	1530
49	1545
49	1600
49	1615
49	1630
49	1645
49	1700
49	1715
49	1730
49	1745
49	1830
49	1845
49	2045
49	2115
49	2130
49	2145
49	2215
49	2230
49	2245
49	2300
49	2315
49	2345
50	0
50	15
50	100
50	115
50	130
50	145
50	200
50	230

b) Dual Gauge



Gauge	Time Interval	Precipitation
1	0	69.139
1	15	69.139
1	30	69.037
1	45	69.139
1	100	69.088
1	115	69.088
1	130	69.139
1	145	69.088
1	200	69.063
1	215	69.113
1	230	69.088
1	245	69.088
1	300	69.063
1	315	69.063
1	345	69.113
1	430	69.088
1	445	69.139
1	515	69.088
1	530	69.139
1	615	69.139
1	700	69.088
1	715	69.139
1	800	69.088
1	815	69.088
1	830	69.088
1	845	69.088
1	900	69.139
1	915	69.139
1	945	69.139
1	1000	69.088
1	1015	69.113
1	1045	69.012
1	1100	69.063
1	1130	69.063

Figure A.3: Input files for a) Single Gauge and b) Dual Gauge version of APCP

Many hydrologic models and applications require continuous time series of precipitation data at a fixed time interval (such as hourly, 3 hourly etc.). By default APCP generates output file following the time series of input file, but precipitation data at any regular time interval can be generated by selecting the option 'Fixed Interval' and specifying the time interval in minutes in adjoining text box. **Figure A.4** presents output

file generated by the 'Dual Gauge' version of APCP at the default time interval (**Figure A.4a**) and at hourly time interval (**Figure A.4b**).

a) Default time interval

177	1415	433.5	256.0
177	1500	433.5	256.0
177	1530	433.5	256.0
177	1645	433.5	256.0
177	2015	433.5	256.0
177	2030	433.5	256.0
177	2145	433.5	256.0
177	2215	433.5	256.0
177	2300	433.5	256.0
178	0000	433.5	256.0
178	0030	433.5	256.0
178	0115	433.5	256.0
178	0345	433.5	256.0
178	0445	433.5	256.0
178	0500	433.5	256.0
178	0515	433.5	256.0
178	0530	433.5	256.0
178	0615	433.5	256.0
178	0700	433.5	256.0
178	0715	433.5	256.0
178	0730	433.5	256.0
178	0745	433.5	256.0
178	0900	433.5	256.0
178	0915	433.5	256.0
178	1100	433.5	256.0
178	1115	433.5	256.0

b) Hourly time interval

177	1300	433.5	256.0
177	1400	433.5	256.0
177	1500	433.5	256.0
177	1600	433.5	256.0
177	1700	433.5	256.0
177	1800	433.5	256.0
177	1900	433.5	256.0
177	2000	433.5	256.0
177	2100	433.5	256.0
177	2200	433.5	256.0
177	2300	433.5	256.0
178	0000	433.5	256.0
178	0100	433.5	256.0
178	0200	433.5	256.0
178	0300	433.5	256.0
178	0400	433.5	256.0
178	0500	433.5	256.0
178	0600	433.5	256.0
178	0700	433.5	256.0
178	0800	433.5	256.0
178	0900	433.5	256.0
178	1000	433.5	256.0
178	1100	433.5	256.0
178	1200	433.5	256.0
178	1300	433.5	256.0
178	1400	433.5	256.0

Figure A.4: Output file from 'Dual Gauge' version of APCP at a) Default time interval and b) Hourly time interval.

Programming code of ‘Single Gauge’ version of APCP

The program for the ‘Single Gauge’ version of APCP is presented below. In the ‘Dual Gauge’ version of APCP scanning cycles 1 and 2 are repeated for additional column of precipitation data.

Option Explicit

‘Declaration of variables

```

Dim i, j, k, n, p As Long
Dim S, MM As Integer
Dim InputYearFile As String
Dim OuputYearFile As String
Dim a As String, Myarray() As String
Dim DayOfYear() As Integer
Dim TimeOfDay() As Integer
Dim CumPPT() As Double
Dim FinalCumPPT() As Double
Dim FinalT As Long
Dim Records, RecordLength As Long
Dim StartTime As Date, TimeInterval As Double
Dim Hour, Minute As Integer
Dim NoData, MaxLimit As Double
Dim NextRecord, PreviousRecord As Long
Dim BucketDump, Recharge As Double
Dim Time() As Date
Dim Diff, ConsDiff1, ConsDiff2, ConsDiff3, ConsDiff4 As Double
Dim PPT() As Double
Dim PPT_B() As Double
Dim PPT_E() As Double
Dim CPPT() As Double, CPPTCrr() As Double
Dim FinalCPPT() As Double, FinalPPT() As Double
Dim FinalTime() As Date
Dim Final() As Double
Dim Noise As Double

Private Sub cmdCancle_Click()
    End
End Sub

Private Sub cmdOK_Click()
    On Error Resume Next
    ‘Input files/ File Name

```

```
InputYearFile = txtInputYearFile.Text
```

```
'Output files/ File Name
```

```
OuputYearFile = txtOutputYearFile.Text
```

```
i = 0
```

```
j = 0
```

```
'Assigning the bucket dump value as critical value
```

```
BucketDump = CDb1(txtBucketDump.Text)
```

```
'Note: bucket dump value should be slightly smaller then the smallest variation
```

```
'due to bucket dump. But it should be greater then critical 'Noise' limit
```

```
'Added on 10/4/05 to accommodate sudden increase due to bucket recharge
```

```
Recharge = CDb1(txtrecharge.Text)
```

```
'Critical Shielded or Unshielded gauge Noise limit
```

```
'Note: noise value should be smaller then both bucket recharge and bucket dump
```

```
Noise = CDb1(txtCritical.Text)
```

```
'Checking whether the files are in correct format
```

```
If InputYearFile = "" Then
```

```
    MsgBox "Input file is not valid"
```

```
    Exit Sub
```

```
Else
```

```
    Open InputYearFile For Input As #1
```

```
End If
```

```
If OuputYearFile = "" Then
```

```
    MsgBox "Please enter a valid output file name"
```

```
    Exit Sub
```

```
Else
```

```
    Open OuputYearFile For Output As #3
```

```
End If
```

```
'Counting the length of records in the input file
```

```
Do
```

```
    Line Input #1, a
```

```
        i = i + 1
```

```
Loop Until EOF(1)
```

Records = i 'Note: Length of records = Records-1

Seek #1, 1 'Go back to beginning of input file

i = 0

'Allocating memory to the arrays to store data records

ReDim DayOfYear(Records - 1)

ReDim TimeOfDay(Records - 1)

ReDim CumPPT(Records - 1)

ReDim CPPT(Records - 1)

ReDim CPPTCrr(Records - 1)

ReDim PPT(Records - 1)

ReDim Time(Records - 1)

'Storing data in arrays

Do

Line Input #1, a

a = " " + a

a = Replace(a, " ", ",")

a = Replace(a, " ", ",")

a = Replace(a, " ", ",")

a = Replace(a, " ", ",")

a = Replace(a, " ", ",")

a = Replace(a, " ", ",")

a = Replace(a, " ", ",")

a = Replace(a, " ", ",")

Myarray = Split(a, ",")

DayOfYear(i) = Val(Myarray(1))

'Stores Day of year

TimeOfDay(i) = Val(Myarray(2))

'Stores Time

CumPPT(i) = Val(Myarray(3))

'Stores recorded precipitation

Hour = Int(TimeOfDay(i) / 100)

Minute = TimeOfDay(i) Mod 100

Time(i) = DayOfYear(i) + Hour / 24 + Minute / (24 * 60)

i = i + 1

Loop Until EOF(1)

Close #1

'Variable to store out of range data value

NoData = CDBl(txtNoData.Text)

'Checking whether first value is out of range data value


```

If CumPPT(0) = NoData Then
  'If first (few) value(s) are out of range data value(s) then find the first acceptable data
  'value
  n = 1
  While CumPPT(n) = NoData Or CumPPT(n) < 0
    n = n + 1
  Wend
  For j = 0 To n - 1

    'And replace all the out of range data values with first acceptable data value
    CumPPT(j) = CumPPT(n)
  Next
End If

'Removing out of range data values from the records
For i = 1 To Records - 1

  If CumPPT(i) = NoData Then

    'If out of range data value(s) is found then
    'Find Previous and Next CumPPT values which are acceptable
    p = i - 1
    While CumPPT(p) < 0
      p = p - 1
    Wend

    n = i + 1
    While CumPPT(n) = NoData Or CumPPT(n) < 0
      n = n + 1
    Wend

    If CumPPT(p) - CumPPT(n) > BucketDump Or CumPPT(n) - CumPPT(p) >
    Recharge Then

      'BucketDump of BucketRecharge is associated with out of range data values
      For j = p + 1 To n - 1
        CumPPT(j) = CumPPT(p)
      Next
    Else

      'There is no BucketDump of BucketRecharge during the period of out of range
      'data values. Distribute the difference of previous and next acceptable data
      'values over the period of out of range data values.
      For j = p + 1 To n - 1
        CumPPT(j) = CumPPT(p) + (j - p) * (CumPPT(n) - CumPPT(p)) / (n - p)
      Next
    End If
  End If
End For

```

```

    Next
  End If
End If

```

```
Next
```

```
CPPT(0) = 0
```

```
PPT(0) = 0
```

‘Scanning cycle 1: Removal of High magnitude noise signals

```
For i = 1 To Records - 1
```

```
  If Abs(CumPPT(i - 1) - CumPPT(i)) > Noise Then
```

‘Change in CumPPT values greater than the ‘Noise’ limit

‘beginning of high magnitude noise signal

‘End of noise signal is assumed when at least 5 successive values show less

‘variation than the noise limit

```
  n = i
```

```
  Do
```

```
    Diff = CumPPT(i - 1) - CumPPT(n)
```

```
    ConsDiff1 = CumPPT(n) - CumPPT(n + 1)
```

```
    ConsDiff2 = CumPPT(n + 1) - CumPPT(n + 2)
```

```
    ConsDiff3 = CumPPT(n + 2) - CumPPT(n + 3)
```

```
    ConsDiff4 = CumPPT(n + 3) - CumPPT(n + 4)
```

```
    n = n + 1
```

```
  Loop Until (Abs(ConsDiff1) < Noise And Abs(ConsDiff2) < Noise And
Abs(ConsDiff3) < Noise And Abs(ConsDiff4) < Noise)
```

```
  If Diff > BucketDump Or Diff < -Recharge Then
```

‘It is a Bucket Dump or Bucket Recharge event, No precipitation during noise

```
  For j = i To n - 1
```

```
    PPT(j) = 0
```

```
  Next j
```

```
  i = n - 1
```

```
  ElseIf Abs(Diff) < Noise Or Diff > 0 Then
```

‘Noise Signal: Sudden increase or decrease then comes back approximately to

‘original. Intermittent noise: Uniformly distribute the difference in

‘precipitation before and after the noise signal over the period of noise

```
  For j = i To n - 1
```

```
    PPT(j) = (CumPPT(n - 1) - CumPPT(i - 1)) / (n - i)
```

```
  Next j
```

```

    i = n - 1

    Else
        'Sudden change may be associated with high intensity precipitation event
        For j = i To n - 1
            PPT(j) = CumPPT(j) - CumPPT(j - 1)
        Next j
        i = n - 1

    End If

    Else

        'Not a high magnitude noise
        PPT(i) = CumPPT(i) - CumPPT(i - 1)
    End If

Next i

CPPT(0) = CumPPT(0)

For i = 1 To Records - 1
    CPPT(i) = CPPT(i - 1) + PPT(i)

Next i

ReDim PPT_B(Records - 1)
ReDim PPT_E(Records - 1)

'End Scanning cycle 1

'Scanning cycle 2:Removing small noises:
'Modified on 10/5/2005
'Smoothing loop is modified form a one step procedure to a three step procedure
For i = 0 To Records - 1
    PPT_B(i) = PPT(i)
    PPT_E(i) = PPT(i)
Next

'Smoothing loop that begins with the starting of the file
If PPT_B(1) < 0 Then
    PPT_B(2) = PPT_B(1) + PPT_B(2)
    PPT_B(1) = 0
End If
If PPT_B(2) < 0 Then

```

```

If PPT_B(1) + PPT_B(2) + PPT_B(3) < 0 Then
  PPT_B(3) = PPT_B(1) + PPT_B(2) + PPT_B(3)
  PPT_B(1) = 0
  PPT_B(2) = 0
Else
  PPT_B(1) = (PPT_B(1) + PPT_B(2) + PPT_B(3)) / 3
  PPT_B(2) = PPT_B(1)
  PPT_B(3) = PPT_B(1)
End If
End If

For i = 3 To Records - 3
  If PPT_B(i) < 0 Then
    If PPT_B(i - 2) + PPT_B(i - 1) + PPT_B(i) + PPT_B(i + 1) + PPT_B(i + 2) < 0
Then
      PPT_B(i + 2) = PPT_B(i - 2) + PPT_B(i - 1) + PPT_B(i) + PPT_B(i + 1) +
PPT_B(i + 2)
      PPT_B(i - 2) = 0
      PPT_B(i - 1) = 0
      PPT_B(i) = 0
      PPT_B(i + 1) = 0
    Else
      PPT_B(i - 2) = (PPT_B(i - 2) + PPT_B(i - 1) + PPT_B(i) + PPT_B(i + 1) +
PPT_B(i + 2)) / 5
      PPT_B(i - 1) = PPT_B(i - 2)
      PPT_B(i) = PPT_B(i - 2)
      PPT_B(i + 1) = PPT_B(i - 2)
      PPT_B(i + 2) = PPT_B(i - 2)
    End If
  End If
End If

Next i

```

‘Smoothing that begins form the end of file: added 10/5/05

```

If PPT_E(Records - 1) < 0 Then
  PPT_E(Records - 2) = PPT_E(Records - 1) + PPT_E(Records - 2)
  PPT_E(Records - 1) = 0
End If
If PPT_E(Records - 2) < 0 Then
  If PPT_E(Records - 1) + PPT_E(Records - 2) + PPT_E(Records - 3) < 0 Then
    PPT_E(Records - 3) = PPT_E(Records - 1) + PPT_E(Records - 2) +
PPT_E(Records - 3)
    PPT_E(Records - 1) = 0
    PPT_E(Records - 2) = 0
  End If
End If

```

```

Else
    PPT_E(Records - 1) = (PPT_E(Records - 1) + PPT_E(Records - 2) +
PPT_E(Records - 3)) / 3
    PPT_E(Records - 2) = PPT_E(Records - 1)
    PPT_E(Records - 3) = PPT_E(Records - 1)
End If
End If

For i = Records - 3 To 3 Step -1
    If PPT_E(i) < 0 Then
        If PPT_E(i - 2) + PPT_E(i - 1) + PPT_E(i) + PPT_E(i + 1) + PPT_E(i + 2) < 0
Then
            PPT_E(i - 2) = PPT_E(i - 2) + PPT_E(i - 1) + PPT_E(i) + PPT_E(i + 1) +
PPT_E(i + 2)
            PPT_E(i + 2) = 0
            PPT_E(i - 1) = 0
            PPT_E(i) = 0
            PPT_E(i + 1) = 0
        Else
            PPT_E(i - 2) = (PPT_E(i - 2) + PPT_E(i - 1) + PPT_E(i) + PPT_E(i + 1) +
PPT_E(i + 2)) / 5
            PPT_E(i - 1) = PPT_E(i - 2)
            PPT_E(i) = PPT_E(i - 2)
            PPT_E(i + 1) = PPT_E(i - 2)
            PPT_E(i + 2) = PPT_E(i - 2)
        End If
    End If
End If

Next i

```

‘Taking average of smoothened values

```

For i = 0 To Records - 1
    PPT(i) = (PPT_B(i) + PPT_E(i)) / 2
Next

PPT(0) = 0

If PPT(1) < 0 Then PPT(1) = 0

If PPT(Records - 1) < 0 Then PPT(Records - 1) = 0

If PPT(Records - 2) < 0 Then PPT(Records - 2) = 0

```

```

CPPTCrr(0) = 0

For i = 1 To Records - 1
    CPPTCrr(i) = CPPTCrr(i - 1) + PPT(i)
Next i

n = 0
If optSame.Value = True Then

    'Printing the output File following the time format of input file
    For i = 0 To Records - 1
        Print #3, Format(DayOfYear(i), "000"); Tab(6); Format(TimeOfDay(i), "0000");
        Tab(11); Format(CPPTCrr(i), "0.00")
    Next

    'Closing the output file
    Close #3
    RecordLength = Records
Else

    'Printing the output file at the specified time interval
    TimeInterval = CDbI(txtInterval.Text)          'Specified time interval in minutes
    RecordLength = (CLng(Time(Records - 1) - Time(0)) * 24 * 60) / TimeInterval

    'Assigning arrays to store data at regular time interval
    ReDim FinalTime(RecordLength - 1)
    ReDim Final(RecordLength - 1)
    ReDim FinalCumPPT(RecordLength - 1)
    ReDim FinalCPPT(RecordLength - 1)
    ReDim FinalPPT(RecordLength - 1)

    FinalTime(0) = Time(0)

    For i = 1 To RecordLength - 1
        FinalTime(i) = FinalTime(i - 1) + TimeInterval / (60 * 24)
    Next
    j = 0
    i = 0

    Do
        If Abs(FinalTime(j) - Time(i)) < 0.000001 Then
            Final(j) = CPPTCrr(i)
            FinalCumPPT(j) = CumPPT(i)
            FinalCPPT(j) = CPPT(i)

```

```

If j = 0 Then
    FinalPPT(j) = 0
Else
    FinalPPT(j) = Final(j) – Final(j – 1)
End If

FinalT = Int((FinalTime(j) – Int(FinalTime(j))) * 24) * 100
MM = (Cint((((FinalTime(j) – Int(FinalTime(j))) * 24) – Int((FinalTime(j) –
Int(FinalTime(j))) * 24)) * 60))

If MM > 59.99 Then
    FinalT = FinalT + 100
    If FinalT = 2400 Then FinalT = 0
Else
    FinalT = FinalT + MM
End If

‘Printing output file if value is measured at regular time interval
Print #3, Format(Int(FinalTime(j) + 0.000001), ”000”); Tab(6); Format(FinalT,
”0000”); Tab(11); Format(Final(j), ”0.00”)

i = i + 1
j = j + 1

Else
    If Time(i – 1) < FinalTime(j) And FinalTime(j) < Time(i) Then

        Final(j) = CPPTCrr(i – 1) + (CPPTCrr(i) – CPPTCrr(i – 1)) * (FinalTime(j) –
Time(i – 1)) / (Time(i) – Time(i – 1))

        FinalCumPPT(j) = CumPPT(i – 1) + (CumPPT(i) – CumPPT(i – 1)) *
(FinalTime(j) – Time(i – 1)) / (Time(i) – Time(i – 1))

        FinalCPPT(j) = CPPT(i – 1) + (CPPT(i) – CPPT(i – 1)) * (FinalTime(j) –
Time(i – 1)) / (Time(i) – Time(i – 1))

    If j = 0 Then
        FinalPPT(j) = 0
    Else
        FinalPPT(j) = Final(j) – Final(j – 1)
    End If

    FinalT = Int((FinalTime(j) – Int(FinalTime(j))) * 24) * 100

```

```

MM = (Cint((((FinalTime(j) – Int(FinalTime(j))) * 24) – Int((FinalTime(j) –
Int(FinalTime(j))) * 24)) * 60))

If MM > 59.99 Then
    FinalT = FinalT + 100
    If FinalT = 2400 Then FinalT = 0
Else
    FinalT = FinalT + MM
End If
‘Printing output file by taking weighted average of value before and after the
‘time if values is not measured at time interval
Print #3, Format(Int(FinalTime(j) + 0.000001), ”000”); Tab(6);
Format(FinalT, ”0000”); Tab(11); Format(Final(j), ”0.00”)

    j = j + 1
Else
    i = i + 1
End If
End If
Loop While (i < Records)
Close #3
End If

End Sub

Private Sub cmdStartYear_Click()
dlgOpen.ShowOpen
If dlgOpen.FileTitle <> “” Then
txtInputYearFile.Text = dlgOpen.FileName
txtOutputYearFile.Text = Replace(txtInputYearFile.Text, “.rfp”, “.rfc”)
Else
MsgBox (“Not a valid file name”)
End If
End Sub

Private Sub cmdWaterYear_Click()
dlgOpen.ShowOpen
If dlgOpen.FileTitle <> “” Then
txtOutputYearFile.Text = dlgOpen.FileName
Else
MsgBox (“Not a valid file name”)
End If
End Sub

```



```
Private Sub optConstInterval_Click()  
    If optConstInterval.Value = True Then  
        txtInterval.Enabled = True  
        txtInterval.BackColor = &H80000005  
    End If  
End Sub
```

```
Private Sub optSame_Click()  
    If optSame.Value = True Then  
        txtInterval.Text = ""  
        txtInterval.Enabled = False  
        txtInterval.BackColor = &H8000000F  
    End If  
End Sub
```

APPENDIX B
THE DUAL GAUGE WIND CORRECTION PROGRAM

APPENDIX B

THE DUAL GAUGE WIND CORRECTION PROGRAM

Systematic errors, such as wind induced undercatch, wetting losses and evaporation affect all types of precipitation gauge measurements. These errors are especially significant in the case of solid precipitation. Of the systematic errors in solid precipitation measurements, wind-induced undercatch is the greatest and introduce as much as a 50-90% bias in precipitation measurement. Other systematic errors are relatively small and introduce only 2-3% bias in precipitation measurement (Goodison et al. 1998; Hamon 1971, 1973; Yang et al. 1998). To address the problem of wind induced under-catch, the dual gauge precipitation measurement system was developed in late 1960's and installed at the Reynolds Creek Experimental Watershed (RCEW) (Hamon 1971, 1973). The dual gauge system at RCEW consists of two National Weather Service (NWS) weighing-recording bucket precipitation gauges, one unshielded and the other shielded with a modified Alter shield, located in close proximity.

Hamon (1971, 73) developed instrumentation and formulation for the dual gauge system. It was based on the hypothesis that since the wind effect is reduced by the use of shield, actual precipitation can be computed if both shielded and unshielded catches are known. The analytical model developed was as follows:

$$\frac{S}{A} = e^{-aW(T_i)} \quad (1)$$

$$\frac{U}{A} = e^{-bW(T_i)} \quad (2)$$

Equation (1) and (2) result in following equation which is independent of wind speed and temperature.

$$\ln\left(\frac{U}{A}\right) = B \ln\left(\frac{U}{S}\right) \quad (3)$$

in which

$$B = \frac{b}{b-a} \quad (4)$$

where,

S = Shielded gauge catch

U = Unshielded gauge catch

A = Actual precipitation

W = Wind Speed

T_i = Temperature index

a, b, and 'B' = coefficients

Hamon (1972) set the value of coefficient 'B' at 1.8 based on studies at several dual gauge precipitation sites at RCEW which is used to obtain actual (wind corrected) precipitation.

A program in Visual Basic 6.0 is written to implement dual gauge wind correction algorithm. The program assumes that two precipitation events are distinct if separated by a 6 hour period of no precipitation, following the existing criteria used in preprocessing precipitation data collected at RCEW up to 1996 water year (Hanson 2001). The graphical user interface of the program is presented in **Figure B.2**.

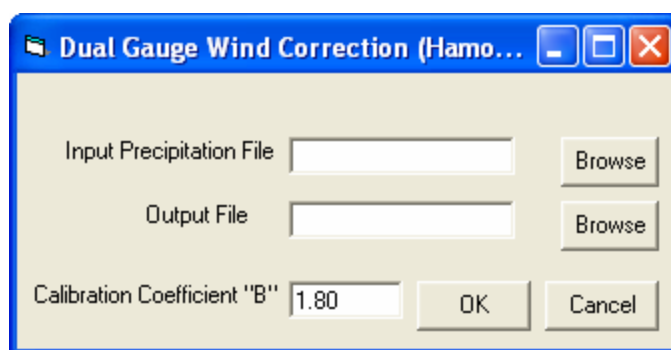


Figure B.2: Graphical user interface of the Dual Gauge Wind Correction program

The input file should contain hourly records of precipitation data, after removal of mechanical errors, with four columns containing day of year, time of day (two digits of hour and two digits of minute), shielded gauge catch and unshielded gauge catch in respective order (**Figure B.3a**). This input file can be generated using the ‘Dual Gauge’ version of the Automated Precipitation Correction Program (APCP) by selecting the option ‘Fixed Interval (min)’ and specifying ‘60’ in the adjoining text box. The output file generated by the program contain hourly records of precipitation data with columns of day of year, time of day, shielded gauge catch, unshielded gauge catch and wind corrected precipitation in respective order (**Figure B.3b**).

a) Input File

182	0300	434.7	257.2
182	0400	434.7	257.2
182	0500	434.7	257.2
182	0600	434.7	257.2
182	0700	434.7	257.2
182	0800	434.7	257.2
182	0900	434.7	257.2
182	1000	434.7	257.2
182	1100	434.7	257.2
182	1200	434.7	257.2
182	1300	438.0	259.2
182	1400	440.1	260.3
182	1500	441.3	263.0
182	1600	441.4	264.0
182	1700	441.5	264.2
182	1800	441.6	264.5
182	1900	441.6	264.9
182	2000	443.3	266.1
182	2100	443.6	266.2
182	2200	443.6	266.3
182	2300	443.6	266.4
183	0000	443.6	266.4
183	0100	443.6	266.4
183	0200	443.6	266.4
183	0300	443.6	266.4
183	0400	443.6	266.4

b) Output File

182	0300	0.0	0.0	0.0
182	0400	0.0	0.0	0.0
182	0500	0.0	0.0	0.0
182	0600	0.0	0.0	0.0
182	0700	0.0	0.0	0.0
182	0800	0.0	0.0	0.0
182	0900	0.0	0.0	0.0
182	1000	0.0	0.0	0.0
182	1100	0.0	0.0	0.0
182	1200	0.0	0.0	0.0
182	1300	3.3	2.0	1.9
182	1400	2.1	1.1	1.1
182	1500	1.2	2.7	2.7
182	1600	0.1	1.0	1.0
182	1700	0.1	0.2	0.2
182	1800	0.1	0.3	0.2
182	1900	0.0	0.4	0.4
182	2000	1.7	1.2	1.2
182	2100	0.3	0.1	0.1
182	2200	0.0	0.1	0.1
182	2300	0.0	0.1	0.1
183	0000	0.0	0.0	0.0
183	0100	0.0	0.0	0.0
183	0200	0.0	0.0	0.0
183	0300	0.0	0.0	0.0

Start

END

Figure B.3: a) Input file for (generated using 'Dual Gauge' version of APCP) and b) Output file generated by the Dual Gauge Wind Correction program.

Programming code of the 'Dual Gauge Wind Correction' program

Option Explicit

'Declaration of variables

```
Dim DualGaugeInputFile As String, DualGaugeOutputFile As String
Dim i As Long, j As Long, B As Double, Records As Long, S As Long, E As Long
Dim DayofYear() As Integer, Timeofday() As Integer
Dim CPPTS() As Double, CPPTUS() As Double, CPPTWindAdjusted() As Double
```

```

Dim CumPPTS As Double, CumPPTUS As Double
Dim PPTS() As Double, PPTUS() As Double, PPTWindAdjusted() As Double
Dim Note() As String
Dim a As String, MyArray() As String
Dim Time() As Date
Dim R As Double
Dim Hour As Integer, Minute As Integer

Private Sub cmdCancel_Click()
    frmDualGauge.Visible = False
    frmWindCorrection.Visible = True
End Sub

Private Sub cmdInputFile_Click()

    dlgOpen.ShowOpen
    If dlgOpen.FileTitle <> "" Then
        txtDualGaugeInput.Text = dlgOpen.FileName
    Else
        MsgBox ("Not a valid file name")
    End If

End Sub

Private Sub cmdOutputFile_Click()
    dlgOpen.ShowOpen
    If dlgOpen.FileTitle <> "" Then
        txtDualGaugeOutput.Text = dlgOpen.FileName
    Else
        MsgBox ("Not a valid file name")
    End If
End Sub

Private Sub cmdOK_Click()

    On Error Resume Next

    'Input files/ File Name
    DualGaugeInputFile = txtDualGaugeInput.Text

    'Output files/ File Name
    DualGaugeOutputFile = txtDualGaugeOutput.Text

    i = 0
    j = 0

```

B = CDBl(txtB.Text)

'B is the constant which was set at 1.7 by (Hamon 1971) and then based on further research studies was set at 1.8 (Hamon 1972) which is used at RCEW.

```
If DualGaugeInputFile = "" Then
  MsgBox "Input file is not valid"
  Exit Sub
Else
  Open DualGaugeInputFile For Input As #1
End If
```

```
If DualGaugeOutputFile = "" Then
  MsgBox "Please enter a valid output file name"
  Exit Sub
Else
  Open DualGaugeOutputFile For Output As #2
End If
```

'Counting the length of records in the input file

```
Do
  Line Input #1, a
  i = i + 1
Loop Until EOF(1)
```

Records = i 'Note: Length of records = Records-1

Seek #1, 1 'Go back to beginning of input file

i = 0

'Allocating space of data arrays holding records

```
ReDim DayofYear(Records - 1)
ReDim TimeofDay(Records - 1)
ReDim CPPTS(Records - 1)
ReDim CPPTUS(Records - 1)
ReDim CPPTWindAdjusted(Records - 1)
ReDim PPTS(Records - 1)
ReDim PPTUS(Records - 1)
ReDim PPTWindAdjusted(Records - 1)
ReDim Note(Records - 1)
```

```
Do
  Line Input #1, a
```



```

a = "" + a
a = Replace(a, "    ", ",")
a = Replace(a, "   ", ",")
a = Replace(a, "  ", ",")
a = Replace(a, " ", ",")
a = Replace(a, " ", ",")
a = Replace(a, " ", ",")
a = Replace(a, " ", ",")
a = Replace(a, " ", ",")
a = Replace(a, " ", ",")
a = Replace(a, " ", ",")
MyArray = Split(a, ",")

```

```

DayofYear(i) = Val(MyArray(1))
TimeofDay(i) = Val(MyArray(2))
CPPTS(i) = Format(Val(MyArray(3)), "0.0")
CPPTUS(i) = Format(Val(MyArray(4)), "0.0")

```

```

Hour = Int(TimeofDay(i) / 100)
Minute = TimeofDay(i) Mod 100
Time(i) = DayofYear(i) + Hour / 24 + Minute / (24 * 60)

```

```

i = i + 1
Loop Until EOF(1)
Close #1

```

```

PPTS(0) = 0
PPTUS(0) = 0

```

```

For i = 1 To Records - 1
  PPTS(i) = CPPTS(i) - CPPTS(i - 1)
  PPTUS(i) = CPPTUS(i) - CPPTUS(i - 1)
Next i

```

‘Implementation of Dual Gauge Correction (Hamon 1971, 1973)

‘Precipitation Events are assumed to be separated if there is no precipitation for at least 6 hrs.

```

PPTWindAdjusted(0) = 0
For i = 1 To Records - 1
  If PPTS(i) > 0.01 Or PPTUS(i) > 0.01 Then

```

```

  ‘atleast one gauge is recording precipitation
  ‘start of an precipitation event

```

Note(i) = "Start"
 S = i 'Marker to store start of event
 E = i 'Marker to store end of event

'Find the end of the event: End of precipitation event is assumed if there is no precipitation during next 6 hours

Do
 If PPTS(E + 1) + PPTUS(E + 1) > 0.01 Then
 E = E + 1
 ElseIf PPTS(E + 2) + PPTUS(E + 2) > 0.01 Then
 E = E + 2
 ElseIf PPTS(E + 3) + PPTUS(E + 3) > 0.01 Then
 E = E + 3
 ElseIf PPTS(E + 4) + PPTUS(E + 4) > 0.01 Then
 E = E + 4
 ElseIf PPTS(E + 5) + PPTUS(E + 5) > 0.01 Then
 E = E + 5

Else

 'End of precipitation event

 Note(E) = "END"

End If

Loop Until E = Records - 1 Or Note(E) = "END"

'Now calculate total shielded and unshielded gauge precipitation during the precipitation event

CumPPTS = 0

CumPPTUS = 0

For j = S To E

 CumPPTS = CumPPTS + PPTS(j)

 CumPPTUS = CumPPTUS + PPTUS(j)

Next

'Now find the ratios to compute wind corrected precipitation

'Note: 'upper limit of the Ratio $[R = (S/U)^B]$ for the event is restricted at 5.6 (based on figures presented in Hamon (1973) as in some cases due to extreme wind or malfunctioning of either gauge shielded gauge may record significantly more precipitation than unshielded gauge.

If CumPPTS >= 0.1 And CumPPTUS >= 0.1 Then

 If CumPPTS > CumPPTUS Then

```

'If storm total of shielded gauge catch is greater than unshielded gauge catch
  R = (CumPPTS / CumPPTUS) ^ B
  If R >= 5.6 Then R = 5.6
Else

'If storm total of shielded gauge catch is less than or equal to unshielded gauge
catch
  R = (CumPPTS + CumPPTUS) / (2 * CumPPTUS)
End If

For j = S To E
  PPTWindAdjusted(j) = PPTUS(j) * R
Next

Else

'One gauge is recording precipitation while other is not
'May be due to trace precipitation or melt or other reasons
'Computed precipitation is assumed as the average of the two gauges

For j = S To E
  PPTWindAdjusted(j) = (PPTS(j) + PPTUS(j)) / 2
Next
End If

i = E + 1
Else
  PPTWindAdjusted(i) = 0
End If
Next

CPPTWindAdjusted(0) = 0
For i = 1 To Records - 1
  CPPTWindAdjusted(i) = CPPTWindAdjusted(i - 1) + PPTWindAdjusted(i)
Next

For i = 1 To Records - 1
  PPTWindAdjusted(i) = Format(CPPTWindAdjusted(i), "0.0") -
    Format(CPPTWindAdjusted(i - 1), "0.0")
Next

For i = 0 To Records - 1

'Print the output file

```

Print #2, Format(DayofYear(i), "000"); Tab(6); Format(TimeofDay(i), "0000");
 Tab(11); Format(PPTS(i), "0.0"); Tab(18); Format(PPTUS(i), "0.0");
 Tab(25); Format(PPTWindAdjusted(i), "0.0"); Tab(32); Note(i)

Next
 Close #2
 End Sub

References

- Goodison, B. E., Louie, P. Y. T., and Yang, D. (1998). "WMO solid precipitation measurement intercomparison, final report." *WMO/TD-No. 872*. World Meteorological Organization, Geneva, 212pp.
- Hamon, W. R. (1971). "Chapter 4 – Reynolds Creek, Idaho." *Agricultural Research Service Precipitation Facilities and Related Studies*. D. M. Hershfield eds., ARS-USDA, Washington, D.C., 25-35.
- Hamon, W. R. (1972). "Computing precipitation." *Paper presented at ARS-SCS Snow Workshop, ARS, USDA, Boise, Idaho, March 14-16.*, 26pp.
- Hamon, W. R. (1973). "Computing actual precipitation: distribution of precipitation in mountainous areas." *WMO Rep. No. 362*, World Meteorological Organization, Geneva, 1, 159-173.
- Hanson, C. L. (2001). "Long-term precipitation database, Reynolds Creek Experimental Watershed, Idaho, United States." *Water Resour. Res.*, 37(11), 2831-2834.
- Yang, D., Goodison, B. E., Metcalfe, J. R., Golubev, V. S., Bates, R., Pangburn, T., and Hanson, C. L. (1998). "Accuracy of NWS 8" standard nonrecording precipitation gauge: results and application of WMO Intercomparison." *J. Atmos. Oceanic Technol.*, 15(1), 54-68.

APPENDIX C
PERMISSION LETTERS

April 25, 2008

Anurag Nayak
340 N 500 E Apt # 3, Logan, UT
Email: anurag.nayak@aggiemail.usu.edu

Dear Dr. Chandler,

I am in the process of preparing my Dissertation in the Biological and Irrigation Engineering Department at Utah State University. I hope to complete in spring 2008. I am requesting your permission to include the paper in which you are a co-author, titled "Objective Sub-Daily Data Correction for Weighing Bucket Type Precipitation Gauge Measurements", submitted to the Water Resources Research journal, as Chapter 2 in my dissertation.

I will include appropriate citations to your work as shown and copyright and reprint rights information in a special appendix.

Please indicate your approval of this request by signing in the space provided, and attach any other form or instructions necessary to confirm permission.

If you have any questions, please send me an email message at the above address. Thank you for your assistance

Anurag Nayak

I hereby give permission to Anurag Nayak to reprint the requested article as Chapter 2 in his dissertation.

Signed _____

Print Name _____

April 30, 2008

Anurag Nayak
340 N 500 E Apt # 3, Logan, UT
Email: anurag.nayak@aggiemail.usu.edu

Dear Dr. Marks,

I am in the process of preparing my Dissertation in the Biological and Irrigation Engineering Department at Utah State University. I hope to complete in spring 2008. I am requesting your permission to include the paper in which you are a co-author, titled "Objective Sub-Daily Data Correction for Weighing Bucket Type Precipitation Gauge Measurements", submitted to the Water Resour. Res. Journal, as Chapter 2 in my dissertation.

I will include appropriate citations to your work as shown and copyright and reprint rights information in a special appendix.

Please indicate your approval of this request by signing in the space provided, and attach any other form or instructions necessary to confirm permission.

If you have any questions, please send me an email message at the above address. Thank you for your assistance

Anurag Nayak

I hereby give permission to Anurag Nayak to reprint the requested article as Chapter 2 in his dissertation.

Signed _____

Print Name _____

April 30, 2008

Anurag Nayak
340 N 500 E Apt # 3, Logan, UT
Email: anurag.nayak@aggiemail.usu.edu

Dear Dr. McNamara,

I am in the process of preparing my Dissertation in the Biological and Irrigation Engineering Department at Utah State University. I hope to complete in spring 2008. I am requesting your permission to include the paper in which you are a co-author, titled "Objective Sub-Daily Data Correction for Weighing Bucket Type Precipitation Gauge Measurements", submitted to the Water Resour. Res. Journal, as Chapter 2 in my dissertation.

I will include appropriate citations to your work as shown and copyright and reprint rights information in a special appendix.

Please indicate your approval of this request by signing in the space provided, and attach any other form or instructions necessary to confirm permission.

If you have any questions, please send me an email message at the above address. Thank you for your assistance

Anurag Nayak

I hereby give permission to Anurag Nayak to reprint the requested article as Chapter 2 in his dissertation.

Signed _____

Print Name _____

April 30, 2008

Anurag Nayak
340 N 500 E Apt # 3, Logan, UT
Email: anurag.nayak@aggiemail.usu.edu

Dear Dr. Seyfried,

I am in the process of preparing my Dissertation in the Biological and Irrigation Engineering Department at Utah State University. I hope to complete in spring 2008. I am requesting your permission to include the paper in which you are a co-author, titled "Objective Sub-Daily Data Correction for Weighing Bucket Type Precipitation Gauge Measurements", submitted to the Water Resour. Res. Journal, as Chapter 2 in my dissertation.

I will include appropriate citations to your work as shown and copyright and reprint rights information in a special appendix.

Please indicate your approval of this request by signing in the space provided, and attach any other form or instructions necessary to confirm permission.

If you have any questions, please send me an email message at the above address. Thank you for your cooperation.

Anurag Nayak

I hereby give permission to Anurag Nayak to reprint the requested article as Chapter 2 in his dissertation.

Signed _____

Print Name _____

CURRICULUM VITAE

Anurag Nayak

Education:

Ph.D. in Irrigation Engineering, Utah State University, Logan, UT, 2008.

M. Tech. in Soil and Water Conservation Engineering, Indian Institute of Technology, Kharagpur, WB, India, 2003.

B. Tech. in Agricultural Engineering, Jawaharlal Nehru Krishi Vishwa Vidyalaya, Jabalpur, MP, India, 2001.

Experience:

Internship as support hydrologist in NWRC-ARS-USDA, and Center for Ecohydraulic Research, University of Idaho, Boise, ID, August 2007-December 2007.

Graduate Research Assistant, Utah State University, Logan, UT, January 2004- June 2007.

Research Assistant in Precision Farming Development Project, Indian Institute of Technology, Kharagpur, WB, India, February 2003-August 2003.

Research Fellowship, Indian Institute of Technology, Kharagpur, WB, India, July 2001-January 2003.

Publications:

Nayak, A., Chandler, D. G., Marks, D., McNamara, J. P., and Seyfried, M. (2008). "Objective sub-daily data correction for weighing bucket type precipitation gauge measurements." *Water Resour. Res.*, Submitted.

Bonta, J. V., and Nayak, A. (2008). "Characterizing dry times between storms in mountainous areas." *Trans. ASABE*, Submitted.

Flerchinger, G. N., Marks, D., Hardegree, S. P., Nayak, A., Winstral, A. H., Seyfried, M. S., Pierson, F. P., and Clark, P. E. (2007). "45 Years of climate and hydrologic research conducted at the Reynolds Creek Experimental Watershed." *Environmental and Water Resources: Milestones in Engineering History*. J.R. Rogers Ed., Sponsored by ASCE Environmental and Water Resources Institute (EWRI) National History & Heritage Committee. ASCE, Reston, VA, 135-143.